# Big screens with small RNAs: Loss of function genetic screens to find novel cancer genes

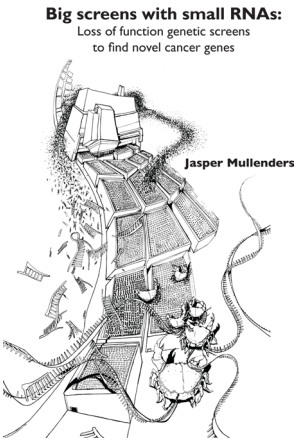


Cover: Artist impression of Big screens with small RNAs
by Rikkert Mullenders (rikkertmullenders@gmail.com)



The research described in this thesis was financially supported by the Dutch Cancer Society (KWF), the Center for Biomedical Genetics, the Cancer Genomics Center, Roche Diagnostics GmbH, Penzberg, Germany and Schering-Plough, Oss, The Netherlands.

Print: Gildeprint Drukkerijen - The Netherlands

# Big screens with small RNAs: Loss of function genetic screens to identify novel cancer genes

Grote screens met kleine RNAs: De identificatie van kanker genen door verlies van functie genetische screens

(met een samenvatting in het Nederlands)

**Proefschrift**

ter verkrijging van de graad van doctor aan de Universiteit Utrecht op gezag van de rector magnificus, prof.dr J.C. Stoof, ingevolge het besluit van het college voor promoties in het openbaar te verdedigen op maandag 26 oktober 2009 des middags te 12.45 uur

door

**Jasper Mullenders**

geboren op 17 november 1977
te Nijmegen

Promotor: Prof. dr. R Bernards

# Table of contents

# CHAPTER 1

## Introduction

## Loss of function genetic screens as a tool to improve the diagnosis and treatment of cancer

Accepted for publication by *Oncogene*

# Loss of function genetic screens as a tool to improve the diagnosis and treatment of cancer

Jasper Mullenders and René Bernards

Division of Molecular Carcinogenesis and Center for Biomedical Genetics
The Netherlands Cancer Institute, Plesmanlaan 121, 1066 CX
Amsterdam, The Netherlands

**A major impediment to the effective treatment of cancer is the molecular heterogeneity of the disease, which is also reflected in an equally diverse pattern of clinical responses to therapy. Currently, only few drugs are available that can be used safely and effectively to treat cancer. To improve this situation, the development of novel and highly specific targets for therapy is of utmost importance. Possibly even more importantly, we need better tools to predict which patients will respond to specific therapies. Such drug response biomarkers will be instrumental to individualize the therapy of patients having seemingly similar cancers. Here we discuss how RNA interference-based genetic screens can be used to address these two pressing needs in the care for cancer patients.**

### *The need for new drug targets and better biomarkers of drug response*

Traditionally, new cancer drugs have been identified mainly through empirical approaches [1]. This has led to a generation of chemotherapeutic agents that is relatively non-specific in targeting cancer cells, yielding considerable side effects. Such conventional therapies often benefit only a minority of patients, due to both intrinsic and acquired drug resistance. Another major factor limiting the effective treatment of cancer is the molecular heterogeneity of the disease. Because of this heterogeneity only few cancer types have a common "driver" mutation: a genetic alteration that is instrumental for the malignant phenotype of the cancer. One such recurrent driver mutation in chronic myelogenous leukemia is the BCR-ABL fusion gene, which is targeted by the drug imatinib mesylate [2, 3]. Imatinib mesylate is a member of a new class of anti-cancer drugs, the 'targeted-therapeutics' [4, 5]. These drugs are developed based on knowledge of which genes (often kinases) are specifically altered in cancer. Therefore such targeted

therapies are highly cancer cell-selective and have fewer side effects. Unfortunately, most cancer types do not have such frequently-occurring oncogenic driver event, making it difficult to expand on the success of this highly effective drug. Consequently, the arsenal of targeted cancer therapeutics is small, making the more conventional chemotherapy still the mainstay of treatment in today's cancer clinic. In this review we will discuss how loss-of-function genetic screens in mammalian cells using RNA interference can contribute to the identification of completely new classes of highly selective cancer drug targets.

A second major obstacle in the treatment of cancer is the unpredictable response to therapy [6]. In breast cancer, only one in thirty post-menopausal women benefit from chemotherapy. Availability of biomarkers of drug responses could greatly help in the development of a more personalized approach to cancer treatment, in which patients having seemingly similar cancers can be pre-selected for specific therapies based on their predicted responses to therapy. Here too, RNA interference-based genetic screens can be very efficient in identifying genes that control how cells respond to cancer drugs. Consequently, such genes are prime candidate biomarkers to foretell drug responsiveness in the clinic. Strategies to discover such biomarkers through RNAi-based genetic screens are discussed here also.

***Loss of function genetic screening tools***

In recent years an array of new high throughput technologies (DNA sequencing, Single Nucleotide Polymorphism (SNP) genotyping, Comparative Genomic Hybridization (CGH), proteomics, gene expression micro-arrays) have all been implemented in drug development efforts. A drawback of most of these approaches is that the data generated are mostly correlative and therefore do not directly identify the driver event among the many genetic alterations present in each cancer. Loss of function genetic screens on the other hand can also be carried out in a high throughput fashion and, as a consequence of the functional nature of the approach, leads to the identification of causal factors only.

Two complementary types of functional genetic screens can be carried out [7, 8]. Gain-of-function genetic screens involve the ectopic expression of genes. This is often brought about by expression of collections of cDNAs. For discovery of drug targets, however, loss-of-function screens are more suitable as the genetic event mimics the intended effect of the cancer drug: reduced gene product activity. In mammalian cells high throughput loss-of-function screens were not feasible for a long time. This situation changed in 2001 when it was discovered that RNA interference (RNAi) can also be used in mammalian cells to suppress gene expression [9]. Since then, many different collections of RNAi

resources have been created that cover the entire human and mouse genomes [7, 8, 10-12]. Different reagents can be used to trigger RNA interference: the original synthetic short duplex RNAs (siRNAs) and vector-encoded short hairpin RNAs (shRNAs [12]). These two RNAi reagents each come in several flavors. For example, apart from the chemically synthesized siRNAs, siRNAs have been made by nuclease cleavage of long *in vitro* transcribed double stranded RNAs: esiRNAs [13]. For plasmid-derived shRNAs different viral delivery systems are available (e.g. Moloney virus based vectors, lentiviral vectors, adenoviral vectors [14-16]. Some libraries consist of shRNA vectors that contain a shRNA embedded in a microRNA precursor for more

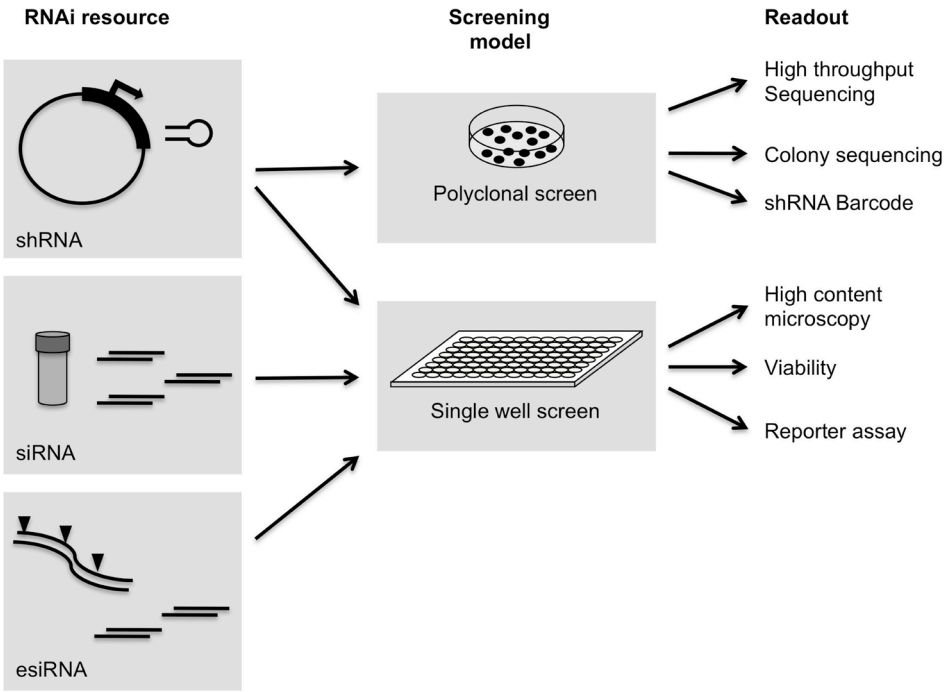


**Figure 1**
*RNAi screening modalities: RNAi can be brought about by different molecules, the vector based short hairpin RNA (shRNA) and the chemically or enzymatically generated small interference RNAs (siRNA). The choice of screening model is dependent on the species of RNAi used, shRNAs can be used in both polyclonal and single well screens, siRNAs can only be used in single well assays. This also limits the phenotypes that can be screened. Polyclonal assays are more applicable to screen growth phenotypes while single well assays can be used to screen complex phenotypes.*

efficient knockdown, but the beneficial effect of this has been disputed [17] (Fig 1).

There is no simple answer to the question which RNAi reagent is better, as each reagent has its own pros and cons. A major advantage of the use of plasmid-encoded shRNA is the possibility to perform long-term cell culture experiments, such as clonogenic assays and drug resistance assays. ShRNA-based genetic screens are particularly useful when one searches for genes whose suppression allows cells to proliferate in the presence of an anti-proliferative signal, such as a drug-induced growth arrest or a physiological growth arrest such as senescence. In this scenario, shRNA screens can be carried out in a polyclonal format, in which a single dish of cells is infected in culture with a large number of shRNA vectors, after which the cells are exposed to the anti-proliferative signal. Cells that become resistant to the growth arrest through knockdown of a specific gene will become positively selected. Since each shRNA vector contains a unique shRNA sequence to knock down a specific gene, this sequence can be used as a molecular "bar code" to identify the knockdown vector that conferred the growth advantage to the cell. This approach, known as shRNA bar code screening, has been applied successfully to find genes whose inactivation confers resistance to a p53 induced growth arrest [18, 19], the breast cancer drug Herceptin [20] and genes that allow growth under non-adherent conditions [21] (Fig 2). The screening of shRNA collections in a polyclonal fashion to identify shRNAs that are negatively selected in culture represents a more significant technical challenge. Detecting the loss of a single shRNA from a large pool is more difficult because not every cell infected with a given shRNA vector has the same degree of knockdown. Since only cells with significant knockdown of a lethal gene are negatively selected in a population, the cells that harbor a knockdown vector without having functional gene knockdown limit the signal one can obtain in this type of bar code screening approach. One solution to this problem is the use of relative small pools of ~1000 shRNAs in negative selection assays [22, 23]. More recently, this approach was optimized and also used successfully to screen larger shRNA libraries [24-27].

SiRNAs on the other hand are very suitable for high throughput single well assays, in which every well contains a siRNA reagent that targets a single transcript. An advantage of the single well screening format is that more complex biological phenotypes can be screened. Such complex phenotypes can be detected using for instance cell sorting or high throughput microscopy. Microscopic images can subsequently be analyzed by software that can be programmed to extract features like cell shape, DNA content, subcellular localization of proteins and other parameters [27-29]. This combination of single well screening and reading of complex phenotypes is referred to as "high content

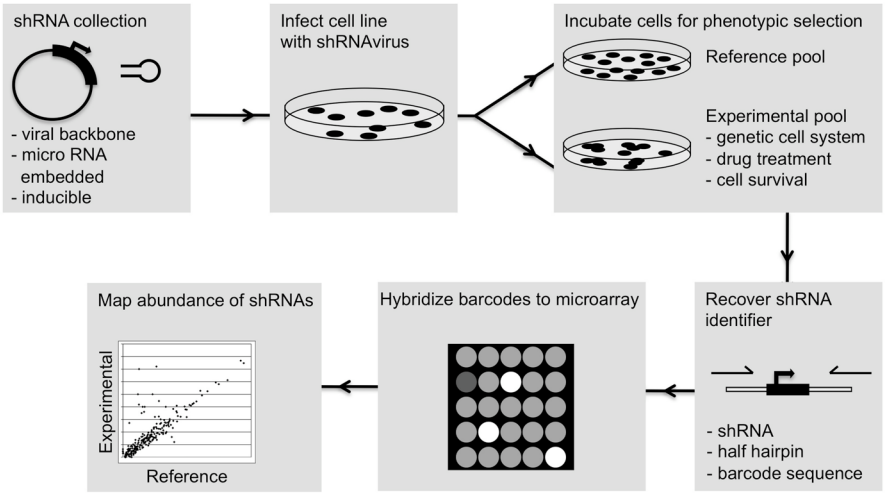


**Figure 2**

*ShRNA barcode screening: shRNA barcode screening is a very efficient technique to identify shRNAs from a large collection of vectors that give rise to a specific phenotype. Plasmids encoding shRNAs are available in various viral vectors for high-efficiency infection of target cell lines. After sufficient numbers of cells are infected (in order to have the entire library of vectors represented) two replicate cell populations are created. One population is used as reference and left untreated, while the other population is treated with the stimulus of interest. After phenotypic selection has taken place the barcode identifier can be retrieved by PCR. The barcode identifier can be a separate DNA sequence in the plasmid but also an integral part of the shRNA cassette. Hybridization of the barcode identifier to a specific microarray reveals the abundance of shRNA in both the reference and experimental population.*

screening" [30]. The cell cycle is one of the best-studied biological processes using RNAi combined with high content screening [31-34]. The parameters examined in such screens include cell number, cell cycle phase, apoptosis (sub G1) and the total number of chromosomes (ploidy). Among the hits in these screens are many genes that have previously been reported to regulate mammalian cell cycle, demonstrating the validity of the approach. High content screening also enables the identification of novel morphological phenotypes [35, 36]. Single well screens can also be performed using shRNA vectors [37, 38], but it requires significant automation to generate and handle individual shRNA vectors in single well screening format.

### *Loss of function screening strategies to identify drug targets*

Suitable targets for cancer therapy are hard to find. Most small molecule drugs today inactivate proteins by binding to the catalytic site of an enzyme. This mostly restricts the development of cancer drugs to the products of oncogenes, not tumor suppressor genes. Moreover, many of the well-known oncogenes (for example RAS and MYC) are not considered to be "druggable", i.e. proteins whose activity can be

readily inhibited by a low molecular weight compound [38]. Thus far only a small number of proteins have been identified that can be efficiently inhibited by small molecules for cancer therapy. Many of these targets belong to the family of kinases and are either specifically (over-) expressed in cancer cells (i.e. HER1 and HER2) or activated by mutation/translocation (for example HER1 and BRAF and BCR-ABL). Inhibitors of these targets can be very efficacious in blocking cancer growth with relatively mild side-effects [3, 39]. The identification of new drug targets with a similar cancer selectivity is urgently needed. There are four approaches to finding novel drug targets through RNAi-based genetic screens:

Pathway screens:

An obvious starting point to identify novel drug targets is by searching for novel components of cancer-relevant signaling pathways. While many signaling pathways have been studied for considerable time, genetic screens may identify hitherto unknown components of these pathways, which may serve as potential targets for therapy. Initial RNAi genetic screens in Drosophila using reporter gene

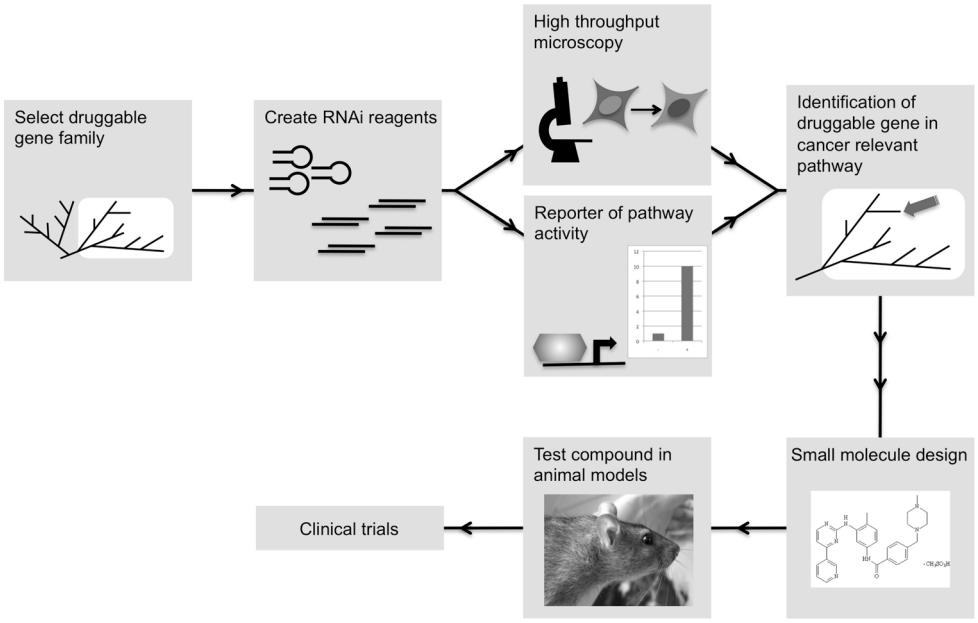


**Figure 3**

*Pathway screening using RNAi libraries targeting druggable genes: Choosing druggable genes as a starting point for RNAi screening can lead to rapid identification of a novel drug target in a cancer-relevant pathway. The first step is to select the gene family of interest. Subsequently a targeted RNAi library of either shRNAs of siRNAs must be constructed. This library can be screened in various screening models including reporters and high-content based assays. Small molecules targeting the hits identified from the screen can subsequently be used to perform in vivo experiments and finally clinical trials.*

assays established the utility of signaling pathway screens [40, 41]. More direct measurement of pathway activity was used to screen for modulators of ERK signaling, which was evaluated by immunofluorescence [42].

A particularly powerful combination is to screen subsets consisting of families of druggable genes for their ability to modulate a cancer-relevant signaling pathway. Any validated hit from such a screen would directly place a druggable gene in a cancer relevant pathway (Fig 3). As a proof of concept, we made a library of shRNA vectors targeting some 60 ubiquitin-specific proteases (DUBs) and searched for DUB enzymes that control the activity of NF-κB [43, 44]. This led to the identification of the familial cylindromatosis tumor suppressor gene *CYLD* in the NF-κB signaling pathway. This work suggested that tumors in cylindromatosis patients are caused, at least in part, by activation of NF-kB. Indeed, in a pilot clinical study, inhibitors of NF-kB were found to be useful for the treatment of patients suffering from cylindromatosis [44].

Phenotypic screens

Another screening format is to search for modulators of a specific biological phenotype, such as apoptosis, migration, invasion, senescence and responses to cytokines. One of the first genome-wide screens in mammalian cells aimed to identify genes whose suppression allowed bypass of a p53-dependent senescence-like growth arrest in human fibroblasts, which led to the identification of five novel components of the p53 pathway [18]. A screen for bypass of growth arrest caused by activation of p53 with specific small molecules allowed the identification of further components of the p53 pathway [19].

Oncogene expression can also induce a senescence-like proliferation arrest. Wajapeyee et al., identified genes whose suppression confers resistance to growth arrest induced by a BRAF oncogene [45]. Surprisingly, the authors found that suppression of *IGFBP7*, which encodes a secreted protein, was required for cells to proliferate in the presence of *BRAF*. Moreover, injection of recombinant IGFBP7 in mice carrying a BRAF mutant tumor led to inhibition of tumor growth, providing a potential new therapeutic strategy for tumors having a mutant *BRAF* oncogene.

Tumor cells often have an abrogated cell death or apoptosis pathway. Several screens have been performed to identify genes that, when knocked down, either suppress or stimulate cell death [46-48]. By screening siRNA libraries targeting kinases and phosphatases MacKeigan et al identified a surprising large number of genes that are involved in regulating apoptosis under physiological conditions [47]. In addition a number of phosphases are identified to be essential for the cytotoxic effects of certain chemotherapeutic drugs.

Synthetic lethal screens

Most targeted therapies take

advantage of the fact that certain oncoproteins are hyperactive in cancer cells, either as a consequence of activating mutations or over-expression. As was pointed out above, such targets are often not "druggable" or only expressed in a small fraction of the tumors, two factors that limit their clinical utility. In 1997, it was proposed to exploit the phenomenon of "synthetic lethality" to find completely novel classes of highly cancer-selective drug targets [49]. This strategy takes advantage of the notion, first observed in lower organisms, that some genes are only lethal to cells if a second non-lethal mutation is also present [50]. These types of genetic interactions are likely to be present in mammals also and therefore could be exploited for novel cancer treatment strategies [51, 52]. In one of the first examples, it was shown that cells with an amplified *MYC* oncogene are more sensitive to apoptosis induced by death receptor ligands [52, 53]. It is important to point out that the genes that are synthetic lethal with cancer-specific lesions are not necessarily mutated or over-expressed themselves in cancer. Consequently, large-scale cancer genome re-sequencing efforts and gene expression profiling might not identify synthetic lethality genes. As such, synthetic lethal interactions represent a potential untapped reservoir of highly cancer-selective drug targets.

Finding synthetic lethal interactions in mammalian cells is not a trivial exercise, but is greatly facilitated by large-scale RNAi genetic screens. Large-scale efforts to identify synthetic lethal interactions were initially explored in yeast [54, 55]. The advantage of performing screens in yeast is that, rather than knockdown by RNAi, knockout strains can be used. On the other hand, the increased complexity of mammalian signaling pathways may limit the value of the lessons learnt from simple model organisms. To date, synthethic lethal screens have been performed for two specific oncogenic lesions in mammalian cells: targeting the activated *KRAS* oncogene [56-59] and loss of the *VHL* tumor suppressor [59]. Most of these screens were performed using single well assays with only relatively small collections of RNAi reagents. Only one study used a genome-wide shRNA library that was screened using micro-array barcode technology [57]. Genes identified in the screens above include Polo like kinase 1 (*PLK1*), *SURVIVIN* and the *STK33* kinase. Interestingly clinical trials using small molecule inhibitors of PLK1 (BI-2536) and SURVIVIN (YM155) are already ongoing [60, 61]. Based on the results from the activated RAS RNAi synthetic lethal screens, it will be interesting to monitor the specific response of RAS mutant versus wild-type tumors in these ongoing clinical trials.

Synthetic lethal screens can also be used to find genes that are specifically toxic in two closely related cancers. For instance, Ngo et al, screened for genes that are essential for survival of activated B-cell-like Diffuse Large B cell lymphoma (DLBCL), but not for the

related germinal centre B-cell-like DLBCL cells. They identified the NF-kB pathway as essential only for survival of activated B-cell-like DLBCL, suggesting that this cancer might benefit from NF-kB inhibition [22].

*In vivo* screens

The identification of genes that regulate the process of metastasis is a very difficult and laborious task. Therefore screening in a surrogate assay for *in vivo* metastasis can be used to examine large collections of shRNAs or siRNAs. Hits from this screen can subsequently be tested *in vivo*, as the number of genes to be tested is significantly smaller. The latter approach was used to identify the *GAS1* metastasis suppressor from a complex library of shRNAs. Furthermore, when the expression level of *GAS1* in melanoma was investigated, a clear correlation between low GAS1 mRNA and metastatic potential was identified [62].

Another way to reduce the complexity of a genome wide RNAi set for *in vivo* genetic screen is to use data obtained from clinical specimen. This was elegantly shown in a study by Zender et al. [63, 64]. Using Comparative Genomic Hybridization (CGH) profiles from human liver caner samples they identified some 300 genes that were frequently lost in these tumors, making these genes candidate tumor suppressor genes for liver cancer. Based on this information, they generated a mini shRNA targeting these 300 genes. These shRNAs were introduced into immortalized, but non-oncogenic, hepatocytes that were transplanted into recipient mice. In the tumors that formed in these mice shRNAs for 16 genes were selectively enriched, demonstrating a role for these genes in hepatocyte oncogenicity. This shows that the use of selected shRNA libraries allows for the very efficient identification of genes that are functionally involved in cancer progression.

A variation on this theme is to perform these types of screens in tumor cells isolated from patients. This was shown in a recent report that described the siRNA screening of tyrosine kinases in cells derived from 30 patients suffering from leukemia [64]. In 10 out of these 30 patients at least one kinase was identified that was essential for tumor cell survival. Furthermore, the inhibition of the JAK2 kinase by a small molecule inhibitor was shown to be selectively toxic only in the tumor lines that depend on JAK2.

***Development of predictive biomarkers of therapy efficacy***

Identical treatment regimens can produce remarkably different responses in patients with seemingly indistinguishable tumors at the macromolecular level. This phenomenon reflects the heterogeneity that is seen when individual tumors are studied in more detail. Understanding the factors that predict whether patients will respond to certain treatment is very useful to create efficient therapies. Whilst different techniques can be used to identify

biomarkers of drug response, the use of RNAi to find these factors has the advantage that it will identify biomarkers based on their causal role in the response to the drug.

Two different types of drug response biomarkers can be distinguished. First, biomarkers may foretell if patients are resistant to a certain treatment and second biomarkers may predict drug sensitivity. The former biomarkers have two clinical applications: they may identify patients that fail to respond to a given therapy upfront, avoiding unnecessary toxicity. Second, understanding resistance may uncover strategies to overcome resistance. The biomarkers of drug sensitivity on the other hand may help in identifying synergistic drug combinations. RNAi can be used for the identification of both types of biomarkers through screening for modulators of drug resistance.

Biomarkers of drug resistance

The low efficacy of currently-used cancer drugs can be attributed mainly to inherent or acquired resistance of cancer cells. Multiple mechanisms have been proposed for resistance to the more conventional chemotherapy, for example the up-regulation of drug pumps and (in)-activation of pathways on which the drug works [65-67]. However, in most cases, the factors that contribute to drug resistance are not known and RNAi screens can be useful to identify genes that modulate drug responses.

When performing a functional genetic screen to find drug resistance genes it is important to use concentrations of drug that are close to levels obtained in the clinic. In long term shRNA based screens, drug concentration can be relatively low. In contrast, siRNA single well screens usually require much higher concentration of drug, as the phenotype must be measured in a much shorter time frame. For drug resistance RNAi screens, the use of shRNA vectors is therefore preferred. Drug resistance screens have been performed successfully with various anti-cancer drugs. One approach was designed to identify genes that are essential for the action of the HER2 antibody trastuzumab (Herceptin®) [20]. A single gene was identified that confers resistance to trastuzumab when it was knocked down by shRNAs. This gene encoded *PTEN*, the inhibiting phosphatase of the PI3-Kinase catalytic subunit PIK3CA. When patient samples were analyzed on their activation of the PI3-kinase pathway, a clear correlation with trastuzumab response was found. Patients with an activated PI3-Kinase pathway, loss of *PTEN* or mutation in *PIK3CA*, showed worse response to trastuzumab than patients that did not have these mutations. This example shows that results from *in vitro* RNAi screens can yield biomarkers having clinical utility to predict drug responses.

In related studies, loss of *CDK10* expression was identified as a major factor in mediating resistance to tamoxifen in breast cancer and *CDK10* levels were found to be predictive of tamoxifen response

in clinical samples [68]. Likewise, *ZNF423* was identified as a critical mediator of the response to retinoic acid in neuroblastoma and *RAD23B* was found to control responses to histone deacetylase inhibitors. In all cases, the genetic screen did not only provide potentially useful biomarkers of drug responses, but also yielded novel insights into the signaling pathways that mediate drug resistance [69, 70]. Such studies may therefore point at specific combination therapies that will be more powerful or suggest ways to overcome therapy resistance.

Enhancers of drug efficacy

Another way of finding modulators of drug responses is to search for genes whose suppression enhances the response to a given cancer drug. This is in fact a variation on the theme of synthetic lethality and is also referred to as "chemical synthetic lethality". Like most genetic screens, this principle was also pioneered in lower organisms. For instance, testing of a set of compounds that are currently used in the clinic in a heterozygous yeast strain identified strains that display a decrease in fitness in presence of the drug [71]. Performing RNAi-based drug enhancer screens in mammalian cells requires some technical adaptations to the conventional approach. To find factors that can augment the effects of a drug, the screen should be performed in presence of a low concentration of the drug, which causes only a small decrease of cell viability. In this way genes that significantly enhance loss of cell viability can be identified. Most drug screens are performed in a single-well format, which allow for effective gene knockdown due to highly efficient transfection with siRNAs.

Thus far screens have been performed aiming at the identification of sensitizers of the well-known anti-cancer drugs gemcitabine, cisplatin and paclitaxel [47, 72-76]. Although cisplatin has been approved for the treatment of human malignancies since 1978, it is still unclear why some tumors respond better to treatment than others. By screening a genome wide siRNA library to identify genes that modulate cisplatin efficacy, it was uncovered that cells that have an inactivation of both *TP53* and a member of the *BRCA* network are more sensitive to cisplatin treatment. Even though this had been reported before, this example underscores the power of large-scale loss of function genetic screens to find enhancers of drug responses.

Another example of a large RNAi based approach with the objective to find genes that, when suppressed, sensitize cells to paclitaxel treatment identified several members of the proteasome [75]. This interesting observation raises the possibility of combining treatment of taxanes with proteasome inhibitors. Intriguingly several clinical trials combing paclitaxel and the proteasome inhibitor bortezomib were already performed before the results from this study became available [77-79]. From these

Phase I/II trials it was concluded that the combination therapy is well tolerated but unfortunately not very efficacious.

***Future directions for RNAi in cancer research***

In less than a decade RNA interference has evolved into a major tool for drug discovery and even a potential therapeutic agent in its own right [80, 81]. Large RNAi collections have been made available to the scientific community enabling hundreds of RNAi screens, ranging in size from only dozens of genes to entire mammalian genomes (see Table 1 for a summary of the most noteworthy screens). Together, these screens have assigned (additional) functions to many genes in processes ranging from cancer, development, stem cell maintenance to viral replication. It should be kept in mind that many genes reported in these screens have not been validated in additional biological assays, and therefore such gene lists should be viewed with caution [81]. Of particular concern is the possible context-dependency of genetic interactions identified in RNAi screens. For instance, gene A may be synthetic lethal with the loss of gene B in lung cancer cells in which the screen was performed, but not in breast cancer. Likewise, a gene may be involved in resistance to a given drug in colon cancer, but not play a role in resistance to the same drug in prostate cancer. Understanding context dependency of genetic interactions is the major challenge for the next decade and this will be a prerequisite for a more profound understanding of how patients respond to cancer drugs. Such context dependency will ultimately be governed by cross talk between signaling pathways. Thus, if we want to fully understand how cells respond to perturbations of specific signals with targeted cancer therapies, we will need to map these interactions between signaling pathways. RNAi is exquisitely well-suited to identify functional interactions between signaling pathways. We wholeheartedly support the massive efforts that are undertaken world wide to re-sequence thousands of cancer genomes. It will without doubt provide a deep insight into the genes that are deregulated in cancer. However, we will only be able to truly appreciate the meaning of the multitude of mutations in the major signaling pathways, if we also understand how these pathways are interconnected. We therefore need in addition to the re-sequencing project a large-scale effort to map functional interactions between signaling pathways using the approaches described here. The technology is readily available and proof of concept has been delivered. All we need is a concerted funding effort to make it happen. Anyone interested?

| Reference | Type of screen | Cell lines used | Number of genes screened | RNAi method |
|---|---|---|---|---|
| | | | | |
| **Cell death screens** | | | | |
| 47 | Apoptosis | HeLa | Kinases and phosphatases | siRNA |
| 46 | TRAIL induced apoptosis | HeLa | 500 genes (mostly kinases) | siRNA |
| 48 | Necroptosis | L929 (mouse) | Genome | siRNA |
| | | | | |
| **Bypass of proliferative arrest screens** | | | | |
| 45 | B-Raf senescence | Fibroblasts | Genome | shRNA |
| 18 | Bypass p53 induced cell cycle arrest | BJ fibroblast | 8000 genes | shRNA |
| 21 | Soft agar Ras complemen-tation | HMEC | 8000 genes | shRNA |
| 82 | Soft agar Ras complemen-tation | BJ fibroblast | 4000 genes | shRNA |
| | | | | |
| **Essential genes screens** | | | | |
| 22 | Essential genes | DLBCL cell line | 2500 genes | shRNA |
| 23 | Essential genes | Multiple myeloma | 2500 genes | shRNA |
| 24 | Essential genes | DLD-1/ HCC1954/ HCT116/ HMEC | 3000 genes | shRNA |
| 25 | Essential genes | 5 human breast cancer cell lines | Various | shRNA |

**Table 1**
*An incomplete summary of some noteworthy RNAi screens performed in recent years.*

| | | | | |
|---|---|---|---|---|
| **Cell cycle screens** | | | | |
| 33 | Cell cycle | U2OS | Genome | siRNA |
| 83 | Cell cycle in presence of Taxol | HeLa | Ubiquitin associated genes | shRNA |
| 31, 32 | Cell cycle | HeLa | 17000 genes | esiRNA |
| 84 | Cell cycle and mitosis | HeLa | Genome | siRNA |
| 37 | Cell cycle | A549 | 1000 genes | shRNA |
| | | | | |
| **Pathway screens** | | | | |
| 85 | Wnt signaling | DLD-1/ HCT116 | Kinases | shRNA |
| 43 | NF-kB signaling | U2OS | Deubiquiti-nating enzymes | shRNA |
| 86 | Wnt signaling | HeLa | Genome | siRNA |
| | | | | |
| ***In vivo* screens** | | | | |
| 63 | *In vivo* hepatocellular carcinoma | p53-/- hepatoblast | 300 genes | shRNA |
| 64 | Essential tyrosine kinases | Human white blood cells | 100 tyrosine kinases | siRNA |
| 62 | Invasion in 3D cell culture | B16-F0 melanoma (mouse) | Genome | shRNA |

**Table 1 (continued)**

| | | | | |
|---|---|---|---|---|
| **Synthetic lethal screens** | | | | |
| 56 | K-Ras synthetic lethality | DLD1 k-RAS(V12) isogenic | 4000 genes | siRNA |
| 58 | K-Ras synthetic lethality | NOMO-1 vs HMEC, Fibroblast and THP-1 | 1000 genes | shRNA |
| 57 | K-Ras synthetic lethality | DLD-1 | Genome | shRNA |
| 59 | VHL synthetic lethality | 786O/RCC4 isogenic VHL knockout | Kinases | shRNA |
| | | | | |
| **Drug screens** | | | | |
| 76 | Gemcitabine | MiaPaCa-2 | Kinases | siRNA |
| 73 | Cisplatin/ Gemcitabine/ Taxol | HeLa | Genome | siRNA |
| 74 | Taxol/ Cisplatin/ Doxorubicin/5-FU | HCT116/A549/ MDA-MB-231 | Kinases | siRNA |
| 75 | Taxol | NCI-H1155 | Genome | siRNA |
| 68 | Tamoxifen | MCF-7 | Kinases | siRNA |
| 87 | PARP inhibitor | CAL51 | Kinases | siRNA |
| 72 | Taxol | A549 | 74 genes | shRNA |
| 20 | Resistance to Herceptin | BT474 | 8000 genes | shRNA |
| 69 | Resistance to Reinoic acid | F9 (mouse) | 15,000 genes | shRNA |
| 70 | Resistance to HDAC inhibitors | U2OS | 8000 genes | shRNA |

**Table 1 (continued)**

## References


1. Chabner, B.A. and T.G. Roberts, Jr., Timeline: Chemotherapy and the war on cancer. Nat Rev Cancer, 2005. 5(1): p. 65-72.
2. de Klein, A., et al., A cellular oncogene is translocated to the Philadelphia chromosome in chronic myelocytic leukaemia. Nature, 1982. 300(5894): p. 765-7.
3. Druker, B.J., et al., Effects of a selective inhibitor of the Abl tyrosine kinase on the growth of Bcr-Abl positive cells. Nat Med, 1996. 2(5): p. 561-6.
4. Sawyers, C., Targeted cancer therapy. Nature, 2004. 432(7015): p. 294-7.
5. Luo, J., N.L. Solimini, and S.J. Elledge, Principles of cancer therapy: oncogene and non-oncogene addiction. Cell, 2009. 136(5): p. 823-37.
6. EBCTCG, Effects of chemotherapy and hormonal therapy for early breast cancer on recurrence and 15-year survival: an overview of the randomised trials. Lancet, 2005. 365(9472): p. 1687-717.
7. Brummelkamp, T.R. and R. Bernards, New tools for functional mammalian cancer genetics. Nat Rev Cancer, 2003. 3(10): p. 781-9.
8. Grimm, S., The art and design of genetic screens: mammalian culture cells. Nat Rev Genet, 2004. 5(3): p. 179-89.
9. Elbashir, S.M., et al., Duplexes of 21-nucleotide RNAs mediate RNA interference in cultured mammalian cells. Nature, 2001. 411(6836): p. 494-8.
10. Moffat, J. and D.M. Sabatini, Building mammalian signalling pathways with RNAi screens. Nat Rev Mol Cell Biol, 2006. 7(3): p. 177-87.
11. Iorns, E., et al., Utilizing RNA interference to enhance cancer drug discovery. Nat Rev Drug Discov, 2007. 6(7): p. 556-68.
12. Brummelkamp, T.R., R. Bernards, and R. Agami, A system for stable expression of short interfering RNAs in mammalian cells. Science, 2002. 296(5567): p. 550-3.
13. Buchholz, F., et al., Enzymatically prepared RNAi libraries. Nat Methods, 2006. 3(9): p. 696-700.
14. Brummelkamp, T.R., R. Bernards, and R. Agami, Stable suppression of tumorigenicity by virus-mediated RNA interference. Cancer Cell, 2002. 2(3): p. 243-7.
15. Abbas-Terki, T., et al., Lentiviral-mediated RNA interference. Hum Gene Ther, 2002. 13(18): p. 2197-201.
16. Michiels, F., et al., Arrayed adenoviral expression libraries for functional screening. Nat Biotechnol, 2002. 20(11): p. 1154-7.
17. Li, L., et al., Defining the optimal parameters for hairpin-based knockdown constructs. RNA, 2007. 13(10): p. 1765-74.
18. Berns, K., et al., A large-scale RNAi screen in human cells identifies new components of the p53 pathway. Nature, 2004. 428(6981): p. 431-7.
19. Brummelkamp, T.R., et al., An shRNA barcode screen provides insight into cancer cell vulnerability to MDM2 inhibitors. Nat Chem Biol, 2006. 2(4): p. 202-6.
20. Berns, K., et al., A functional genetic approach identifies the PI3K pathway as a major determinant of trastuzumab resistance in breast cancer. Cancer Cell, 2007. 12(4): p. 395-402.
21. Westbrook, T.F., et al., A genetic screen for candidate tumor suppressors identifies REST. Cell, 2005. 121(6): p. 837-48.
22. Ngo, V.N., et al., A loss-of-function RNA interference screen for molecular targets in cancer. Nature, 2006. 441(7089): p. 106-10.
23. Shaffer, A.L., et al., IRF4 addiction in multiple myeloma. Nature, 2008. 454(7201): p. 226-31.
24. Schlabach, M.R., et al., Cancer

proliferation gene discovery through functional genomics. Science, 2008. 319(5863): p. 620-4.
25. Silva, J.M., et al., Profiling essential genes in human mammary cells by multiplex RNAi screening. Science, 2008. 319(5863): p. 617-20.
26. Luo, B., et al., Highly parallel identification of essential genes in cancer cells. Proc Natl Acad Sci U S A, 2008. 105(51): p. 20380-5.
27. Rines, D.R., et al., High-content screening of functional genomic libraries. Methods Enzymol, 2006. 414: p. 530-65.
28. Wheeler, D.B., A.E. Carpenter, and D.M. Sabatini, Cell microarrays and RNA interference chip away at gene function. Nat Genet, 2005. 37 Suppl: p. S25-30.
29. Pepperkok, R. and J. Ellenberg, High-throughput fluorescence microscopy for systems biology. Nat Rev Mol Cell Biol, 2006. 7(9): p. 690-6.
30. Neumann, B., et al., High-throughput RNAi screening by time-lapse imaging of live human cells. Nat Methods, 2006. 3(5): p. 385-90.
31. Kittler, R., et al., An endoribonuclease-prepared siRNA screen in human cells identifies genes essential for cell division. Nature, 2004. 432(7020): p. 1036-40.
32. Kittler, R., et al., Genome-scale RNAi profiling of cell division in human tissue culture cells. Nat Cell Biol, 2007. 9(12): p. 1401-12.
33. Mukherji, M., et al., Genome-wide functional analysis of human cell-cycle regulators. Proc Natl Acad Sci U S A, 2006. 103(40): p. 14819-24.
34. Bjorklund, M., et al., Identification of pathways regulating cell size and cell-cycle progression by RNAi. Nature, 2006. 439(7079): p. 1009-13.
35. Kiger, A.A., et al., A functional genomic analysis of cell morphology using RNA interference. J Biol, 2003. 2(4): p. 27.
36. Jones, T.R., et al., Scoring diverse cellular morphologies in image-based screens with iterative feedback and machine learning. Proc Natl Acad Sci U S A, 2009. 106(6): p. 1826-31.
37. Moffat, J., et al., A lentiviral RNAi library for human and mouse genes applied to an arrayed viral high-content screen. Cell, 2006. 124(6): p. 1283-98.
38. Hopkins, A.L. and C.R. Groom, The druggable genome. Nat Rev Drug Discov, 2002. 1(9): p. 727-30.
39. Carter, P., et al., Humanization of an anti-p185HER2 antibody for human cancer therapy. Proc Natl Acad Sci U S A, 1992. 89(10): p. 4285-9.
40. DasGupta, R., et al., Functional genomic analysis of the Wnt-wingless signaling pathway. Science, 2005. 308(5723): p. 826-33.
41. Baeg, G.H., R. Zhou, and N. Perrimon, Genome-wide RNAi analysis of JAK/STAT signaling components in Drosophila. Genes Dev, 2005. 19(16): p. 1861-70.
42. Friedman, A. and N. Perrimon, A functional RNAi screen for regulators of receptor tyrosine kinase and ERK signalling. Nature, 2006. 444(7116): p. 230-4.
43. Brummelkamp, T.R., et al., Loss of the cylindromatosis tumour suppressor inhibits apoptosis by activating NF-kappaB. Nature, 2003. 424(6950): p. 797-801.
44. Oosterkamp, H.M., et al., An evaluation of the efficacy of topical application of salicylic acid for the treatment of familial cylindromatosis. Br J Dermatol, 2006. 155(1): p. 182-5.
45. Wajapeyee, N., et al., Oncogenic BRAF induces senescence and apoptosis through pathways mediated by the secreted protein IGFBP7. Cell, 2008. 132(3): p. 363-74.
46. Aza-Blanc, P., et al., Identification of modulators of TRAIL-induced apoptosis via RNAi-based phenotypic screening. Mol Cell,

2003. 12(3): p. 627-37.
47. MacKeigan, J.P., L.O. Murphy, and J. Blenis, Sensitized RNAi screen of human kinases and phosphatases identifies new regulators of apoptosis and chemoresistance. Nat Cell Biol, 2005. 7(6): p. 591-600.
48. Hitomi, J., et al., Identification of a molecular signaling network that regulates a cellular necrotic cell death pathway. Cell, 2008. 135(7): p. 1311-23.
49. Hartwell, L.H., et al., Integrating genetic approaches into the discovery of anticancer drugs. Science, 1997. 278(5340): p. 1064-8.
50. Tong, A.H., et al., Systematic genetic analysis with ordered arrays of yeast deletion mutants. Science, 2001. 294(5550): p. 2364-8.
51. Kaelin, W.G., Jr., The concept of synthetic lethality in the context of anticancer therapy. Nat Rev Cancer, 2005. 5(9): p. 689-98.
52. Wang, Y., et al., Synthetic lethal targeting of MYC by activation of the DR5 death receptor pathway. Cancer Cell, 2004. 5(5): p. 501-12.
53. Rottmann, S., et al., A TRAIL receptor-dependent synthetic lethal relationship between MYC activation and GSK3beta/FBW7 loss of function. Proc Natl Acad Sci U S A, 2005. 102(42): p. 15195-200.
54. Pan, X., et al., A robust toolkit for functional profiling of the yeast genome. Mol Cell, 2004. 16(3): p. 487-96.
55. Pan, X., et al., A DNA integrity network in the yeast Saccharomyces cerevisiae. Cell, 2006. 124(5): p. 1069-81.
56. Sarthy, A.V., et al., Survivin depletion preferentially reduces the survival of activated K-Ras-transformed cells. Mol Cancer Ther, 2007. 6(1): p. 269-76.
57. Luo, J., et al., A genome-wide RNAi screen identifies multiple synthetic lethal interactions with the Ras oncogene. Cell, 2009. 137(5): p. 835-48.
58. Scholl, C., et al., Synthetic lethal interaction between oncogenic KRAS dependency and STK33 suppression in human cancer cells. Cell, 2009. 137(5): p. 821-34.
59. Bommi-Reddy, A., et al., Kinase requirements in human cells: III. Altered kinase requirements in VHL-/- cancer cells detected in a pilot synthetic lethal screen. Proc Natl Acad Sci U S A, 2008. 105(43): p. 16484-9.
60. Mross, K., et al., Phase I dose escalation and pharmacokinetic study of BI 2536, a novel Polo-like kinase 1 inhibitor, in patients with advanced solid tumors. J Clin Oncol, 2008. 26(34): p. 5511-7.
61. Satoh, T., et al., Phase I study of YM155, a novel survivin suppressant, in patients with advanced solid tumors. Clin Cancer Res, 2009. 15(11): p. 3872-80.
62. Gobeil, S., et al., A genome-wide shRNA screen identifies GAS1 as a novel melanoma metastasis suppressor gene. Genes Dev, 2008. 22(21): p. 2932-40.
63. Zender, L., et al., An oncogenomics-based in vivo RNAi screen identifies tumor suppressors in liver cancer. Cell, 2008. 135(5): p. 852-64.
64. Tyner, J.W., et al., RNAi screen for rapid therapeutic target identification in leukemia patients. Proc Natl Acad Sci U S A, 2009. 106(21): p. 8695-700.
65. Savage, P., et al., Why does cytotoxic chemotherapy cure only some cancers? Nat Clin Pract Oncol, 2009. 6(1): p. 43-52.
66. Gottesman, M.M., T. Fojo, and S.E. Bates, Multidrug resistance in cancer: role of ATP-dependent transporters. Nat Rev Cancer, 2002. 2(1): p. 48-58.
67. Rodriguez-Antona, C. and M. Ingelman-Sundberg, Cytochrome P450 pharmacogenetics and cancer. Oncogene, 2006. 25(11): p. 1679-91.
68. Iorns, E., et al., Identification of CDK10 as an important determinant of resistance to endocrine therapy

for breast cancer. Cancer Cell, 2008. 13(2): p. 91-104.
69. Huang, S., et al., ZNF423 is critically required for retinoic acid-induced differentiation and is a marker of neuroblastoma outcome. Cancer Cell, 2009. 15(4): p. 328-40.
70. Fotheringham, S., et al., Genome-wide loss-of-function screen reveals an important role for the proteasome in HDAC inhibitor-induced apoptosis. Cancer Cell, 2009. 15(1): p. 57-66.
71. Lum, P.Y., et al., Discovering modes of action for therapeutic compounds using a genome-wide screen of yeast heterozygotes. Cell, 2004. 116(1): p. 121-37.
72. Ji, D., S.L. Deeds, and E.J. Weinstein, A screen of shRNAs targeting tumor suppressor genes to identify factors involved in A549 paclitaxel sensitivity. Oncol Rep, 2007. 18(6): p. 1499-505.
73. Bartz, S.R., et al., Small interfering RNA screens reveal enhanced cisplatin cytotoxicity in tumor cells having both BRCA network and TP53 disruptions. Mol Cell Biol, 2006. 26(24): p. 9377-86.
74. Swanton, C., et al., Regulators of mitotic arrest and ceramide metabolism are determinants of sensitivity to paclitaxel and other chemotherapeutic drugs. Cancer Cell, 2007. 11(6): p. 498-512.
75. Whitehurst, A.W., et al., Synthetic lethal screen identification of chemosensitizer loci in cancer cells. Nature, 2007. 446(7137): p. 815-9.
76. Giroux, V., J. Iovanna, and J.C. Dagorn, Probing the human kinome for kinases involved in pancreatic cancer cell survival and gemcitabine resistance. Faseb J, 2006. 20(12): p. 1982-91.
77. Ma, C., et al., A phase I and pharmacologic study of sequences of the proteasome inhibitor, bortezomib (PS-341, Velcade), in combination with paclitaxel and carboplatin in patients with advanced malignancies. Cancer Chemother Pharmacol, 2007. 59(2): p. 207-15.
78. Cresta, S., et al., Phase I study of bortezomib with weekly paclitaxel in patients with advanced solid tumours. Eur J Cancer, 2008. 44(13): p. 1829-34.
79. Jatoi, A., et al., Bortezomib, paclitaxel, and carboplatin as a first-line regimen for patients with metastatic esophageal, gastric, and gastroesophageal cancer: phase II results from the North Central Cancer Treatment Group (N044B). J Thorac Oncol, 2008. 3(5): p. 516-20.
80. Castanotto, D. and J.J. Rossi, The promises and pitfalls of RNA-interference-based therapeutics. Nature, 2009. 457(7228): p. 426-33.
81. Goff, S.P., Knockdown screens to knockout HIV-1. Cell, 2008. 135(3): p. 417-20.
82. Kolfschoten, I.G., et al., A genetic screen identifies PITX1 as a suppressor of RAS activity and tumorigenicity. Cell, 2005. 121(6): p. 849-58.
83. Stegmeier, F., et al., Anaphase initiation is regulated by antagonistic ubiquitination and deubiquitination activities. Nature, 2007. 446(7138): p. 876-81.
84. Rines, D.R., et al., Whole genome functional analysis identifies novel components required for mitotic spindle integrity in human cells. Genome Biol, 2008. 9(2): p. R44.
85. Firestein, R., et al., CDK8 is a colorectal cancer oncogene that regulates beta-catenin activity. Nature, 2008. 455(7212): p. 547-51.
86. Tang, W., et al., A genome-wide RNAi screen for Wnt/beta-catenin pathway components identifies unexpected roles for TCF transcription factors in cancer. Proc Natl Acad Sci U S A, 2008. 105(28): p. 9697-702.
87. Turner, N.C., et al., A synthetic lethal siRNA screen identifying genes mediating sensitivity to a PARP inhibitor. Embo J, 2008. 27(9): p. 1368-77.

# CHAPTER II

# A large-scale RNAi screen in human cells identifies new components of the p53 pathway

Published in *Nature* 25 March 2004; 428 (6981)

# A large-scale RNAi screen in human cells identifies new components of the p53 pathway

Katrien Berns[1]*, E. Marielle Hijmans[1]*, Jasper Mullenders[1], Thijn R. Brummelkamp[1], Arno Velds[1], Mike Heimerikx[1], Ron M. Kerkhoven[1], Mandy Madiredjo[1], Wouter Nijkamp[1], Britta Weigelt[2], Reuven Agami[3], Wei Ge[4], Guy Cavet[4], Peter S. Linsley[4], Roderick L. Beijersbergen[1] & René Bernards[1]

1. Division of Molecular Carcinogenesis and Center for Biomedical Genetics, 2. Division of Experimental Therapy, and 3. Division of Tumor Biology, The Netherlands Cancer Institute, Plesmanlaan 121, 1066 CX Amsterdam, The Netherlands 4. Rosetta Inpharmatics, Inc., 12040 115th Avenue NE, Kirkland, Washington 98034, USA
* These authors contributed equally to this work

**RNA interference (RNAi) is a powerful new tool with which to perform loss-of-function genetic screens in lower organisms and can greatly facilitate the identification of components of cellular signalling pathways [1-3]. In mammalian cells, such screens have been hampered by a lack of suitable tools that can be used on a large scale. We and others have recently developed expression vectors to direct the synthesis of short hairpin RNAs (shRNAs) that act as short interfering RNA (siRNA)-like molecules to stably suppress gene expression [4, 5]. Here we report the construction of a set of retroviral vectors encoding 23,742 distinct shRNAs, which target 7,914 different human genes for suppression. We use this RNAi library in human cells to identify one known and five new modulators of *p53*-dependent proliferation arrest. Suppression of these genes confers resistance to both p53-dependent and *p19$^{ARF}$*-dependent proliferation arrest, and abolishes a DNA-damage-induced G1 cell-cycle arrest. Furthermore, we describe siRNA bar-code screens to rapidly identify individual siRNA vectors associated with a specific phenotype. These new tools will greatly facilitate large-scale loss-of-function genetic screens in mammalian cells.**

RNAi is a defence mechanism triggered by double-stranded (ds) RNAs to protect cells from parasitic nucleic acids. The dsRNAs are processed into siRNAs, which target homologous RNAs for destruction [6]. In mammalian cells, an RNAi response can be triggered by 21-base-pair siRNAs, which can cause strong, but transient, inhibition of gene expression [7]. By contrast, vector-expressed shRNAs can suppress gene expression over prolonged periods [4, 5]. In the current study, we create a large set of vectors and use them to search for components of the p53 tumour-suppressor pathway. This pathway is crucial for genome integrity as it transmits both anti-proliferative and pro-apoptotic signals in response to a variety of stress signals [8].

To construct a human RNAi library (the 'NKi library'), we selected 7,914 human genes for shRNA-mediated reduction in expression, known as knockdown. This collection of genes includes components of major cellular pathways, including the cell cycle, transcription regulation, stress signalling, signal transduction and important biological processes such as biosynthesis, proteolysis and metabolism. In addition, genes implicated in cancer and other diseases are included in the library (see Supplementary Table 1). To increase the likelihood of obtaining a significant inhibition of gene expression, we constructed three different shRNA vectors against each gene (23,742 vectors in total; Fig. 1a and Supplementary Fig. 1). The oligonucleotides specifying the shRNAs were annealed and cloned in a high-throughput fashion into pRetroSuper (pRS), a retroviral vector that contains the shRNA expression cassette [9]. Using a pool of three knockdown vectors against a single gene, we obtain on average 70% inhibition of expression for approximately 70% of the genes in the library (see [10]; data not shown). The vector-based shRNA library can be used for functional genetic screens in both short-term and long-term assays using DNA transfection or retroviral transduction.

To validate the RNAi library, we developed a cell system to screen for bypass of p53-dependent proliferation arrest. We generated primary human BJ fibroblasts, which ectopically express the murine ecotropic receptor, the telomerase catalytic subunit (TERT) and a temperature-sensitive allele of SV40 large T antigen (tsLT), yielding BJ-TERT-tsLT cells. As can be seen in Fig. 1b, these cells proliferate when grown at 32 °C, the temperature at which tsLT binds and inactivates both retinoblastoma protein (pRB) and p53, but enter into a synchronous proliferation arrest after a shift to 39 °C, at which tsLT is inactive. To determine whether this proliferation arrest is p53 dependent, we infected BJ-TERT-tsLT cells with pRS–p53 (which targets *p53* for suppression) at 32 °C, and shifted them to 39 °C after two days. Figure 1b shows that knockdown of *p53* allowed temperature-shift-induced proliferation arrest to be bypassed. Knockdown of the RB pathway component $p16^{INK4A}$ alone did not allow growth arrest

to be bypassed, but simultaneous suppression of both *p16$^{INK4A}$* and *p53* yielded a further increase in escape from growth arrest compared with knockdown of p53 alone (Fig. 1b). Thus, the conditional proliferation arrest in BJ fibroblasts depends primarily on *p53*.

We isolated polyclonal plasmid DNA from each of the 83 pools of NKi RNAi library vectors (Fig. 1a), and transfected this DNA into a packaging cell line to generate high-titre retroviral supernatants. These retroviruses were then used to infect BJ-TERT-tsLT cells at 32 °C. We co-infected cells with a shRNA vector that targets *p16$^{INK4A}$*, because suppression of this gene further enhances colony formation induced by *p53* knockdown (Fig. 1b). After two days, the cells were shifted to 39 °C and monitored for the appearance of proliferating colonies. In first-round screening, we identified six pools of infected cells that form colonies at 39 °C. To detect the biologically active shRNAs in these vector pools, we isolated several individual colonies of proliferating BJ fibroblasts and recovered the shRNA inserts of the vectors by polymerase chain reaction (PCR; see Methods). These shRNA inserts were then re-cloned, and their identity was established by DNA sequence analysis.

The majority of colonies of BJ fibroblasts that proliferated at 39 °C contained multiple shRNA inserts. Only those shRNA inserts that were present in multiple independently derived colonies were analysed in second-round selection in BJ-TERT-tsLT fibroblasts. Using this approach, we identified shRNAs against six genes that could suppress the temperature-shift-induced proliferation arrest in the BJ-TERT-tsLT cells in the second round. One of the six genes was *p53* itself, which underscores the quality of the NKi library. In addition, we found that individual shRNAs against *RPS6KA6* (ribosomal S6 kinase 4, RSK4), *HTATIP* (histone acetyl transferase TIP60), *HDAC4* (histone deacetylase 4), *KIAA0828* (a putative S-adenosyl-l-homocysteine hydrolase, SAH3) and *CCT2* (T-complex protein 1, beta-subunit) prevented the *p53*-dependent growth arrest in the BJ-TERT-tsLT fibroblasts (Fig. 1c). Knockdown of all five newly identified genes also mediated escape from proliferation arrest in BJ-TERT-tsLT cells when tested in the absence of *p16$^{INK4A}$* knockdown vector (Fig. 2b), suggesting that inhibition of these genes primarily allows the bypass of the p53 response (see below).

Some siRNAs have 'off-target' effects, which are often the result of partial homology to other transcripts [11, 12]. The shRNA library was designed to avoid off-target effects by minimizing homology of shRNAs to other transcripts (see Methods). Furthermore, it is very unlikely that two independent siRNAs against the same transcript target a common off-target transcript for suppression. For three of the five newly identified genes, we found that two of the three shRNAs present in the library mediated escape from growth arrest in the BJ-TERT-tsLT cells, suggesting that the effects

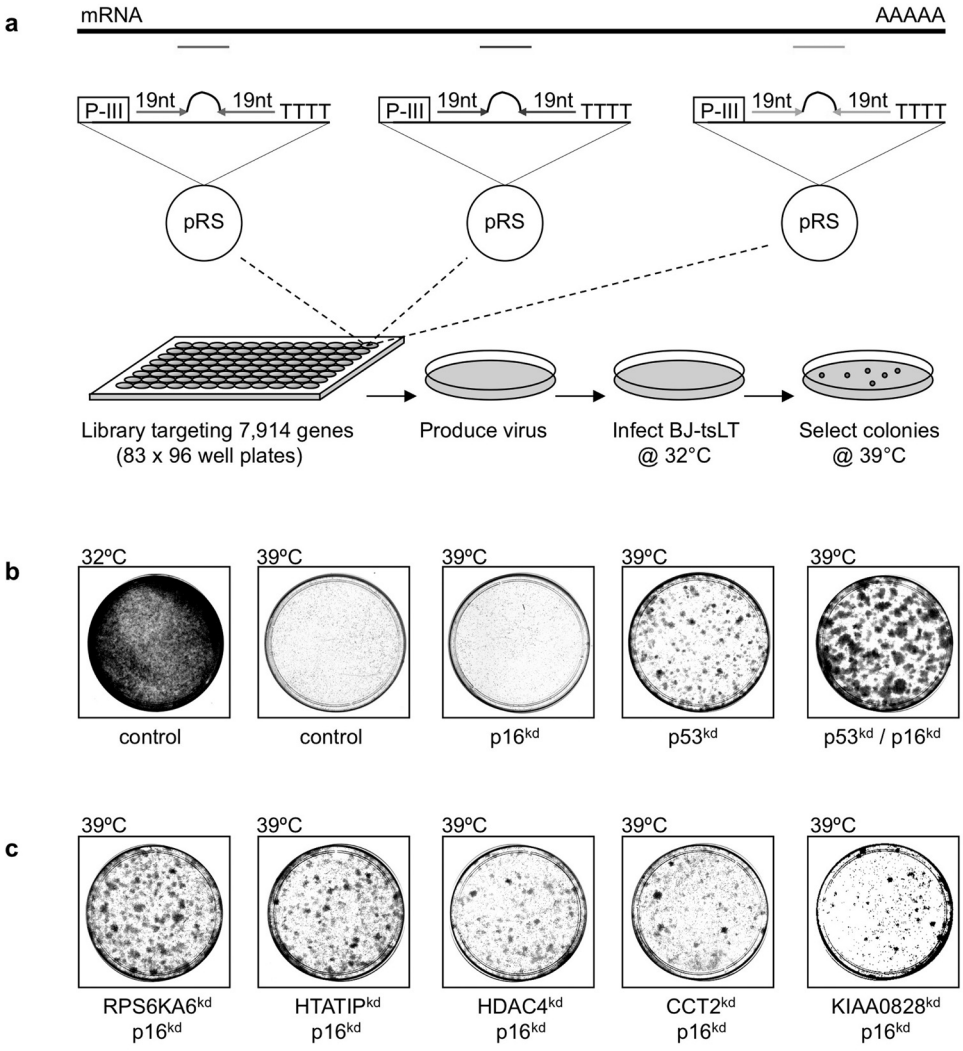


**Figure 1**

*a, Construction of the NKi RNAi library. From each gene transcript, three 19-nucleotide (nt) sequences were designed, and hairpin derivatives (59-mer oligonucleotides; see Supplementary Fig. 1) were cloned into pRS. Three vectors targeting one gene were combined in a single well of a 96-well plate. From each 96-well plate, DNA was pooled, and high-titre polyclonal virus was produced and used to infect BJ-tsLT cells at 32 °C. After two days, cells were shifted to 39 °C, and after three weeks colonies were isolated and analysed. b, The growth arrest of temperature-shifted BJ-tsLT cells is p53 dependent. Co-infection with an shRNA against $p16^{INK4A}$ enhanced colony outgrowth. Cells were infected with the indicated shRNA knockdown (kd) vectors at 32 °C. Fifty thousand cells were seeded at both 32 °C and 39 °C, and colonies were stained after three weeks. c, Knockdown of the five newly identified genes allows bypass of the p53-dependent growth arrest in BJ-tsLT cells.*

of the shRNAs were 'on-target'. For the two genes for which only one functional shRNA from the library was found, we designed a second active shRNA vector targeting the same transcript (see Supplementary Table 2). Figure 2a shows that transient co-transfection of each of the five pairs of two active shRNA vectors with the corresponding full-length complementary DNA expression vectors resulted in a substantial suppression of their cognate gene. Furthermore, we also observed a significant suppression of the corresponding endogenous transcripts (see Supplementary Fig. 2). Moreover, all five pairs of two active shRNA vectors were able to rescue the temperature-shift-induced growth arrest in the BJ-TERT-tsLT cells (Fig. 2b). Together, these data suggest that the observed escape from growth arrest is due to on-target effects of the shRNA vectors on the corresponding genes.

The tumour suppressor $p19^{ARF}$ elicits a p53-dependent proliferation arrest when ectopically expressed [13]. We argued that if the five newly identified genes act in the p53 pathway, their knockdown should confer resistance to $p19^{ARF}$-induced proliferation arrest. To test this, we used a retroviral vector encoding a p19ARF–red-fluorescent-protein (ARF–RFP) fusion protein to infect human U2-OS osteosarcoma cells. Upon infection of U2-OS cells with this virus, only very few proliferating colonies appeared. The few colonies that appeared did not express the ARF–RFP fusion protein (Fig. 2c; data not shown). By contrast, many ARF–RFP-positive colonies appeared in U2-OS cells in which *p53* was suppressed by shRNA (Fig. 2c). Importantly, each of the two independent shRNA vectors against the five newly identified genes allowed proliferation in the presence of ARF–RFP, which is shown by the presence of red fluorescence (Fig. 2c; data not shown). This result provides further support for the notion that the newly identified genes are components of the p53 pathway.

Next, we asked whether suppression of these genes allowed the p53-dependent G1 cell-cycle arrest to be bypassed after exposure to DNA damage. Figure 2d shows that exposure of U2-OS cells to ionizing radiation (IR) causes these cells to withdraw from S phase and arrest both in the G1 phase of the cell cycle (a p53-dependent process [14]) and in G2/M (a p53-independent process [14]). As expected, inactivation of p53 by shRNA completely abrogates the G1 fraction after IR, whereas introduction of a shRNA against HDM2 (the human orthologue of the mouse double minute 2 (*Mdm2*) gene), which activates p53, resulted in a marked increase in the G1 phase of the cell cycle (Fig. 2d). These results demonstrate that arrest in the G1 phase of the cell cycle after IR is determined by the activity of p53. Transfection of knockdown vectors for the five newly identified genes in each case resulted in a cell-cycle distribution identical to the cells expressing the shRNA against p53 (Fig. 2d). Thus, the knockdown of all five genes

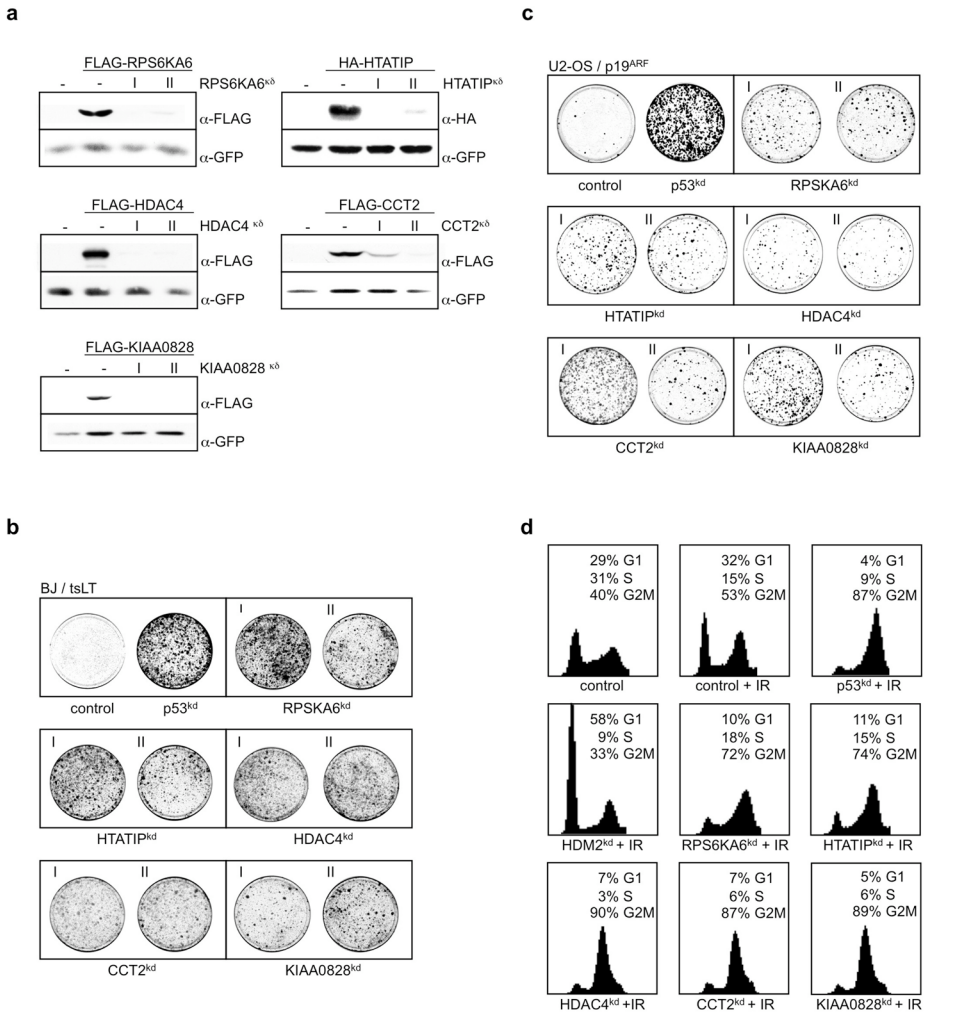


**Figure 2**

*a, Knockdown of newly identified p53 pathway components. U2-OS cells were co-transfected with the shRNA vectors (I or II) and their corresponding tagged (HA or Flag) cDNA expression vectors as indicated. Extracts were immunoblotted against Flag, HA or GFP (control). b, Knockdown of the five pairs of shRNA vectors rescue growth arrest in BJ-TERT-tsLT cells. Cells were infected with the indicated shRNA vectors (in the absence of the p16$^{INK4A}$ knockdown vector), selected at 39 °C, and colonies were stained after three weeks. c, Two independent shRNA vectors of each indicated gene rescue a p19$^{ARF}$-induced growth arrest in U2-OS cells. Cells were co-infected with the shRNA vectors and LZRS-p19$^{ARF}$–IRES–zeocin. Fifty thousand cells were seeded and zeocin/puromycin selected. Colonies were stained after two weeks. d, Rescue of a p53-dependent cell-cycle arrest following ionizing radiation. U2-OS cells were co-transfected with the indicated shRNA vectors and H2B–GFP, irradiated (+ IR, 10 Gy). GFP-positive cells were analysed by FACS.*

prevents three different forms of p53-dependent proliferation arrest (Fig. 2b–d).

A major component of the anti-proliferative response of p53 is the CDK inhibitor *p21$^{cip1}$* [15], as it is a critical downstream component of the G1 arrest in response to DNA damage [16, 17] and is required for the senescence response of human fibroblasts [18]. To test whether the five newly identified genes affect the expression of known p53 target genes, we stably expressed knockdown vectors for all five genes in U2-OS cells and determined the expression of two p53 target genes, *p21$^{cip1}$* and *BAX* [19]. In addition, p53 protein levels can be used as an indirect read-out for p53 function, as p53 protein levels are controlled by the p53 target HDM2 [20, 21]. Figure 3a shows that knocking down *RPS6KA6*, *HDAC4*, *CCT2*, *KIAA0828* or *HTATIP* causes a strong reduction in *p21$^{cip1}$* messenger RNA and protein levels, but does not affect p53 protein levels nor the levels of *BAX* mRNA and protein (Fig. 3a, b). Conversely, overexpression of *HTATIP* resulted in upregulation of *p21$^{cip1}$* expression (Fig. 3c) and further enhanced G1 cell-cycle arrest in response to DNA damage (Fig. 3d). We conclude that knockdown of all five new p53 pathway components leads to a specific downregulation of a subset of p53 target genes, which includes *p21$^{cip1}$*.

Next, we tested the significance of the inhibition of *p21$^{cip1}$* expression for the phenotypes induced by the newly identified genes. Figure 4a shows that suppression of *p21$^{cip1}$* was nearly as efficient at preventing growth arrest in BJ-TERT-tsLT cells as knockdown of *p53* itself. Furthermore, knockdown of *p21$^{cip1}$* allowed the p53-dependent growth arrest induced by *p19$^{ARF}$* (Fig. 4b) and the G1 cell-cycle arrest induced by IR in U2-OS cells (Fig. 4c) to be overridden. This suggests that suppression of *p21$^{cip1}$* is a major element in the cellular response to the effect of knocking down the newly identified p53 pathway components. However, we cannot exclude the possibility that knockdown of the newly identified genes has effects on other p53 target genes or p53-independent effects that explain (part of) their knockdown phenotype.

The RNAi screen described above is time consuming in that individual colonies of cells must be isolated and hairpin vectors recovered and tested in second-round selection. We have recently proposed an alternative strategy to rapidly screen complex shRNA vector libraries in a polyclonal format, a technique that we named 'siRNA bar-code screens' [22]. This approach, which was pioneered in yeast [23], takes advantage of the fact that each hairpin vector contains a unique gene-specific molecular identifier: the 19-mer targeting sequence. This 'molecular bar code' can be used to follow the relative abundance of individual vectors in a large population using DNA microarrays that contain the bar-code oligonucleotides [22] (Fig. 5a). To test the concept of siRNA bar-code screens, we used a subset of the shRNA library (consisting of

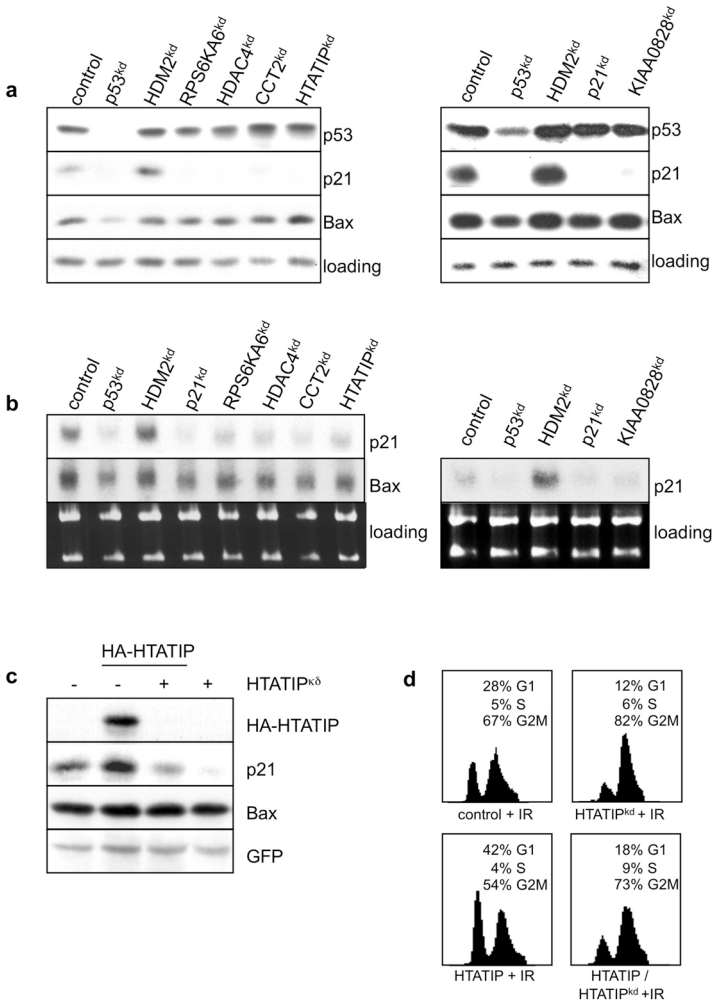


**Figure 3**
*a, U2-OS cells were stably infected with retroviruses expressing the indicated knockdown constructs. Cell extracts were immuno-blotted with antibodies against p53, p21$^{cip1}$ and BAX. b, mRNA levels of p21 and BAX in the stably infected U2-OS cells. As a loading control, RNA was stained with ethidium bromide. c, U2-OS cells were transfected with an expression vector for GFP and CMV–HA–HTATIP/pRS–HTATIP as indicated. Cell extracts were immunoblotted with antibodies against HA, p21, BAX and GFP. d, Overexpression of HTATIP in U2-OS cells increased the population of cells in the G1 phase of the cell cycle after irradiation (+ IR, 5 Gy). Co-transfection of a HTATIP shRNA vector reversed the effect of HTATIP overexpression.*

990 different vectors) to infect U2-OS cells. After one day, genomic DNA was isolated from the infected cells, and the shRNA inserts were recovered by PCR with primers flanking the shRNA expression cassette (which includes the 19-mer gene-specific 'bar codes'). The PCR fragments were then labelled with fluorescent dye, and the relative abundance of specific shRNA inserts was determined by hybridization to a DNA microarray containing the 59-mer oligonucleotides used to generate the hairpin vectors (containing the bar-code sequences). Figure 5a shows that the PCR fragments hybridize with high specificity to their complementary 59-mer oligonucleotides on the array.

To further validate the bar-code screening concept, we asked whether we could identify a mouse *p53* shRNA vector mixed in a pool of 312 human shRNA vectors in a functional screen. We infected this

set of shRNA vectors in conditionally immortalized mouse neuronal cells, which are immortal at 32 °C but enter into a synchronous p53-dependent growth arrest at 39 °C [24]. Figure 5b shows the design of the experiment and the relative abundance of all the bar codes ten days after shift to 39 °C, which activated the p53-dependent growth arrest [24]. Only the p53 knockdown vectors (indicated in red) were strongly selected in the population, whereas the set of control shRNA vectors was neither positively nor negatively selected. The positive selection of the p53 shRNA vectors occurred over time and only when the p53-dependent growth arrest was invoked (at 39 °C), and not at 32 °C, which is when p53 is inactive owing to LT binding (Fig. 5d). These data indicate that siRNA bar-code screening can be used to rapidly identify individual shRNA vectors that modulate cellular responses in large populations of vectors.

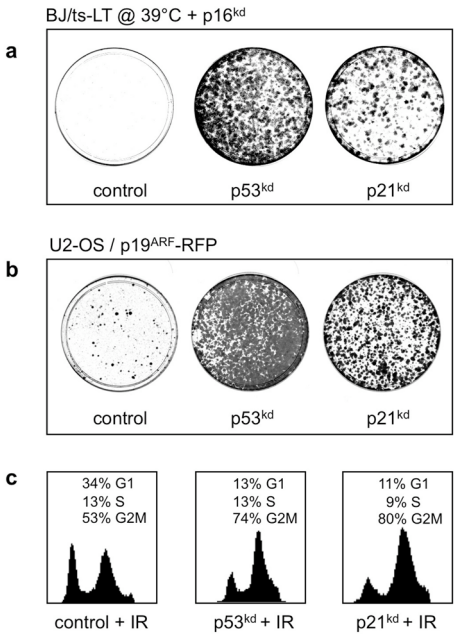


**Figure 4**

*Introduction of p53 and p21 shRNA vectors rescue a, the growth arrest of temperature-shifted BJ-tsLT cells, b, the p19$^{ARF}$-induced growth arrest in U2-OS cells and c, the p53-induced G1 arrest in U2-OS cells.*

We identify here five components of the p53 tumour-suppressor pathway through a large-scale RNAi screen in mammalian cells. Inhibition of each of these five genes confers resistance to three different aspects of p53-dependent proliferation arrest, raising the possibility that these genes are tumour-suppressor genes. p53 is a central component of the cellular response to a variety of stress signals, and the genes identified here may be part of the machinery that allow cells to respond to such signals. Our data indicate that the newly identified genes have a role, either directly or indirectly, in modulating the activity of p53 on the *p21$^{cip1}$* promoter. We did not identify the shRNA for *p21$^{cip1}$* in the genetic screen, even though it was present in the RNAi library and active in *p21$^{cip1}$* suppression. This indicates that the first screen was not saturating and that additional p53 pathway components may be identified from this library.

Our data highlight the power of large-scale RNAi screens in mammalian cells. A potentially useful application of siRNA bar-code screens is in the identification of synthetic lethal interactions (a combination of two non-lethal mutations that together result in cell

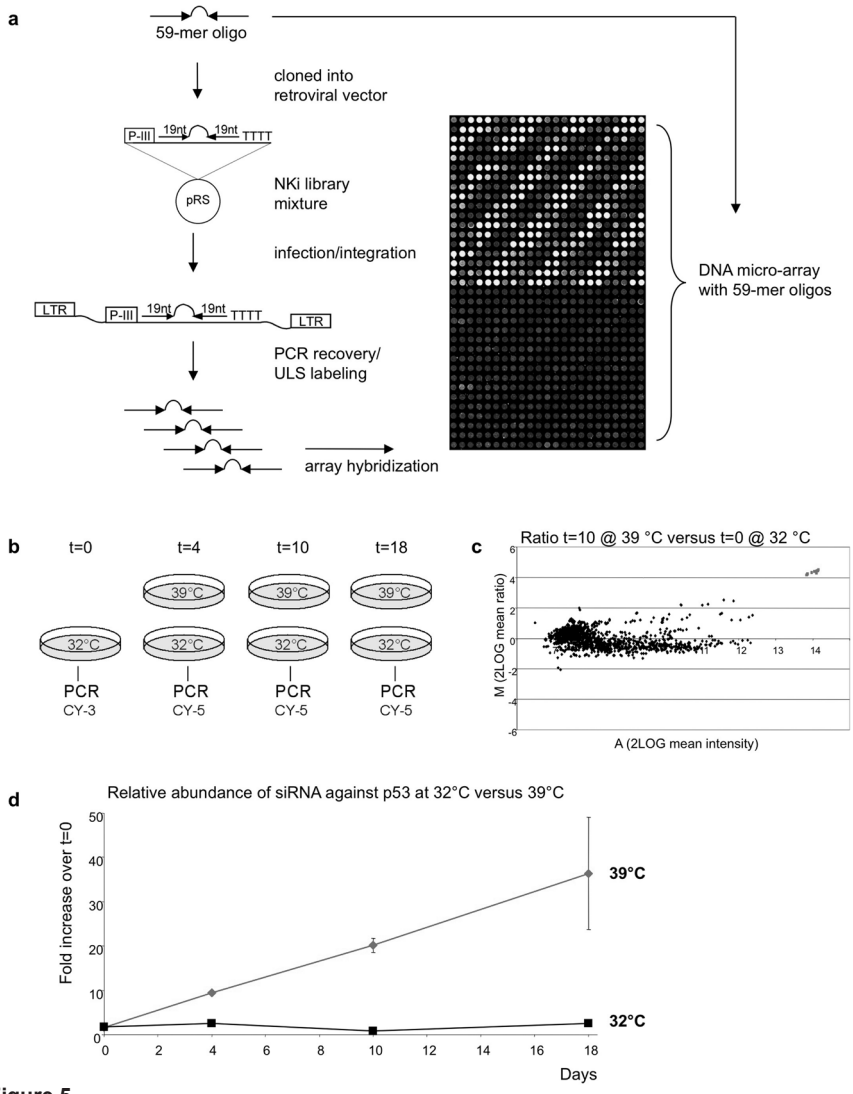


**Figure 5**

*a, DNA microarrays containing the 59-mer oligonucleotides present in a selected set of 990 different shRNA vectors were generated. Genomic DNA isolated from cells infected with these 990 shRNA vectors was used for PCR amplification. ULS-labelled bar-code fragments were hybridized on microarrays that consist of oligonucleotides that were present (upper half) or absent (lower half) in the selected set of 990 vectors. b, TsLT immortalized mouse neuronal cells [29] were infected with a retroviral supernatant containing 312 knockdown vectors directed against human genes and one against murine p53 [30]. Cells were temperature shifted to induce a senescence-like arrest and used for isolation of the bar codes at the indicated time points. c, Comparative hybridization of bar-code fragments isolated from the experiment described in b at t = 0 with bar-code fragments isolated ten days after the temperature shift. Gray spots indicate the relative abundance of the p53 shRNA. Note that only the relative abundance of the p53 knockdown vector has increased. d, Analysis of the relative abundance of p53 shRNAs in tsLT-immortalized mouse neuronal cells recovered from cells grown at 32 °C, when endogenous p53 is inactivated by the tsLT antigen, or at 39 °C, when p53 is activated owing to loss of tsLT antigen expression.*

death). The identification of such genetic interactions in mammalian cells may facilitate the development of new and more specific classes of anticancer drugs.

## Methods

### *Materials, antibodies and vectors*

IR was performed with a 2 times 415 Ci 137Cs source. Antibodies against p21 (C-19), BAX (N-20), green fluorescent protein (GFP; FL), haemagglutinin (HA; Y-11) and CDK4 (C-22) were obtained from Santa Cruz, anti-Flag M2 from Sigma and anti-p53 (ab-7) from Oncogene Research Products. HA-tagged HTATIP was PCR amplified and cloned in pRC/CMV (Invitrogen). Flag-tagged RPS6KA6, CCT2 and KIAA0828 were generated by PCR amplification and cloning into pcDNA3.1/HygroFlag. pRS, pRS–p16kd, LZRS-p19ARF-RFP–IRES–zeocin, Flag–HDAC4 and H2B–GFP have been described previously [9, 25, 26]. pEGFP-N1 was obtained from Clontech. For the generation of knockdown vectors for p53, p21 and HDM2, the following 19-nucleotide sequences were used: p53, 5′-CTA CATGTGTAACAGTTCC-3′; p21, 5′-GACCATGTGGACCTGTCAC-3′; and HDM2, 5′-GATGATGAGGTATAT CAAG-3′. Control transfections were performed with a mixture of non-functional hairpins.

### *Oligonucleotide design and library construction*

A representative mRNA sequence was selected for each target from UniGene (http://www.ncbi.nlm.nih.gov/entrez/query.fcgi?db = unigene). Sequences were masked to remove repetitive sequences using RepeatMasker (http://ftp.genome.washington.edu/cgi-bin/RepeatMasker), and vector contamination was masked by searching with NCBI BLAST (http://www.ncbi.nlm.nih.gov/BLAST/) against UniVec (http://www.ncbi.nih.gov /VecScreen/UniVec.html). Three unique 19-mers for each target were selected, where possible, (1) to contain no stretches of four or more consecutive T or A residues (to avoid premature pol III transcription termination signals); (2) to have 30–70% overall GC content; (3) to lie within the coding sequence of the target gene; (4) to begin with a G or C residue (consistent with recently established rules for strand bias [27]); (5) to begin after an AA dimer in the 5′ flanking sequence; (6) to end just prior to a TT, TG or GT doublet in the 3′ flanking sequence; (7) to not contain XhoI or EcoRI restriction-enzyme sites to facilitate subsequent shuttling of the knockdown cassette into other vector backbones; (8) to share minimal sequence identity with other genes; (9) to target all transcript variants represented by RefSeq mRNAs (http://www.ncbi.nlm.nih.gov/RefSeq/); and (10) to not overlap with other 19-mers selected from the same target sequence.

For cloning, pairs of complementary oligonucleotides were annealed and ligated into HindIII/BglII-digested pRS in 96-well plates. Ligation reactions were transformed into competent DH5alpha bacteria.

Bacterial cultures were grown overnight and plasmid DNA was isolated. All manipulations were performed using a Multimek robot.

Additional information about the NKi RNAi library can be found at http://screeninc.nki.nl/.

***Cell culture, transfection and retroviral infection***

BJ fibroblasts were cultured in a 4:1 mixture of DMEM:M199 supplemented with 15% heat-inactivated fetal calf serum. U2-OS and Phoenix cells were cultured in DMEM supplemented with 10% heat-inactivated fetal calf serum. Transfections were performed with the calcium phosphate precipitation technique. Ecotropic retoviral supernatants were produced by transfection of Phoenix packaging cells. Viral supernatants were filtered through a 0.45 μm filter, and infections were performed in the presence of 4 μg/ml polybrene (Sigma). Drug selections in U2-OS cells were performed with 2 μg/ml puromycin and 200 μg/ml zeocin (Invitrogen).

***Recovery of shRNA inserts***

Genomic DNA was isolated from expanded colonies using DNAzol (Life Technologies). PCR amplification of the shRNA inserts was performed with Expand Long Template PCR system (Roche) and the use of pRS-fw primer: '-CCCTTGAACCTCCTCGTTCGACC-3 and pRS-rev primer: 5 -GAGAC GTGCTACTTCCATTTGTC-3'. Products were digested with EcoRI/XhoI and recloned into pRS. Hairpins were sequenced with Big Dye Terminator (Perkin Elmer) using pRS-seq primer: 5'-GCTGACGTCATCAACCCGCT-3'.

***Cell-cycle analysis***

For fluorescence-activated cell sorting (FACS) analysis, U2-OS cells were co-transfected with H2B–GFP to select for transfected cells. Forty-eight hours after transfection, cells were treated with IR (5 or 10 Gy). Twenty-four hours after IR, the cells were washed and fixed in 70% ethanol at 4 °C. Before FACS analysis, cells were washed with PHN (PBS, 20 mM HEPES, 0.5% NP40) and incubated with 10 μg/ml propidium iodide and 250 μg/ml RNase A. In each assay, 8,000 GFP-positive cells were collected by FACScan and analysed using the CellQuest program (Becton Dickinson).

***Western and northern blotting***

For western blots, puromycin-selected cells were lysed in RIPA buffer (50 mM Tris pH 8; 150 mM NaCl; 1% NP40; 0.5% DOC; 0.1% SDS). Thirty micrograms of protein was separated on 8–12% SDS–polyacrylamide gel electrophoresis and transferred to polyvinylidine difluoride membranes (Millipore). Western blots were probed with antibodies. For northern analysis, 15 μg total RNA was loaded on a 1% agarose gel and blotted onto Hybond N + (Amersham). 32P-labelled probes for p21 and BAX were generated with PCR labelling.

***siRNA bar-code screens***

The shRNA inserts were amplified from genomic DNA by PCR using

the primers pRS-fw primer '-CCCTTGAACCTCCTCGTTCGACC-3' and pRS8-rev primer 5'-TAAAGC GCATGCTCCAGACT-3'. PCR products were labelled with cyanine-3 or cyanine-5 fluorescent groups using the Universal Linkage System (ULS; Kreatech Biotechnology) and purified over a KreaPure (Kreatech Biotechnology) spin column as described previously [28]. PCR products from two samples were combined and hybridized to oligonucleotide arrays in 40 µl of 25% formamide, 5 times SCC, 0.01% SDS (containing poly d(A), yeast transfer RNA and COT-1 DNA). Samples were heated to 100 °C for 1 min and applied to the array. Samples were hybridized for 18 h at 42 °C, washed and scanned using an Agilent microarray scanner. Quantification of the resulting fluorescent images was performed with Imagene 5.6 (BioDiscovery); the local background was subtracted and the data normalized and 2log transformed. Additional information on bar-code screens can be found at http://screeninc.nki.nl/.

## References


1. Lum, L., et al., Identification of Hedgehog pathway components by RNAi in Drosophila cultured cells. Science, 2003. 299(5615): p. 2039-45.
2. Kamath, R.S., et al., Systematic functional analysis of the Caenorhabditis elegans genome using RNAi. Nature, 2003. 421(6920): p. 231-7.
3. Ashrafi, K., et al., Genome-wide RNAi analysis of Caenorhabditis elegans fat regulatory genes. Nature, 2003. 421(6920): p. 268-72.
4. Brummelkamp, T.R., R. Bernards, and R. Agami, A system for stable expression of short interfering RNAs in mammalian cells. Science, 2002. 296(5567): p. 550-3.
5. Paddison, P.J., et al., Short hairpin RNAs (shRNAs) induce sequence-specific silencing in mammalian cells. Genes Dev, 2002. 16(8): p. 948-58.
6. Hannon, G.J., RNA interference. Nature, 2002. 418(6894): p. 244-51.
7. Elbashir, S.M., et al., Duplexes of 21-nucleotide RNAs mediate RNA interference in cultured mammalian cells. Nature, 2001. 411(6836): p. 494-8.
8. Sherr, C.J., The INK4a/ARF network in tumour suppression. Nat Rev Mol Cell Biol, 2001. 2(10): p. 731-7.
9. Brummelkamp, T.R., R. Bernards, and R. Agami, Stable suppression of tumorigenicity by virus-mediated RNA interference. Cancer Cell, 2002. 2(3): p. 243-7.
10. Brummelkamp, T.R., et al., Loss of the cylindromatosis tumour suppressor inhibits apoptosis by activating NF-kappaB. Nature, 2003. 424(6950): p. 797-801.
11. Semizarov, D., et al., Specificity of short interfering RNA determined through gene expression signatures. Proc Natl Acad Sci U S A, 2003. 100(11): p. 6347-52.
12. Jackson, A.L., et al., Expression profiling reveals off-target gene regulation by RNAi. Nat Biotechnol, 2003. 21(6): p. 635-7.
13. Kamijo, T., et al., Tumor suppression at the mouse INK4a locus mediated by the alternative reading frame product p19ARF. Cell, 1997. 91(5): p. 649-59.
14. Lakin, N.D. and S.P. Jackson, Regulation of p53 in response to

DNA damage. Oncogene, 1999. 18(53): p. 7644-55.
15. el-Deiry, W.S., et al., WAF1, a potential mediator of p53 tumor suppression. Cell, 1993. 75(4): p. 817-25.
16. Brugarolas, J., et al., Radiation-induced cell cycle arrest compromised by p21 deficiency. Nature, 1995. 377(6549): p. 552-7.
17. Waldman, T., K.W. Kinzler, and B. Vogelstein, p21 is necessary for the p53-mediated G1 arrest in human cancer cells. Cancer Res, 1995. 55(22): p. 5187-90.
18. Brown, J.P., W. Wei, and J.M. Sedivy, Bypass of senescence after disruption of p21CIP1/WAF1 gene in normal diploid human fibroblasts. Science, 1997. 277(5327): p. 831-4.
19. Miyashita, T. and J.C. Reed, Tumor suppressor p53 is a direct transcriptional activator of the human bax gene. Cell, 1995. 80(2): p. 293-9.
20. Barak, Y., et al., mdm2 expression is induced by wild type p53 activity. Embo J, 1993. 12(2): p. 461-8.
21. Kubbutat, M.H., S.N. Jones, and K.H. Vousden, Regulation of p53 stability by Mdm2. Nature, 1997. 387(6630): p. 299-303.
22. Brummelkamp, T.R. and R. Bernards, New tools for functional mammalian cancer genetics. Nat Rev Cancer, 2003. 3(10): p. 781-9.
23. Shoemaker, D.D., et al., Quantitative phenotypic analysis of yeast deletion mutants using a highly parallel molecular bar-coding strategy. Nat Genet, 1996. 14(4): p. 450-6.
24. Brummelkamp, T.R., et al., TBX-3, the gene mutated in Ulnar-Mammary Syndrome, is a negative regulator of p19ARF and inhibits senescence. J Biol Chem, 2002. 277(8): p. 6567-72.
25. Kanda, T., K.F. Sullivan, and G.M. Wahl, Histone-GFP fusion protein enables sensitive analysis of chromosome dynamics in living mammalian cells. Curr Biol, 1998. 8(7): p. 377-85.
26. Wang, A.H., et al., HDAC4, a human histone deacetylase related to yeast HDA1, is a transcriptional corepressor. Mol Cell Biol, 1999. 19(11): p. 7816-27.
27. Schwarz, D.S., et al., Asymmetry in the assembly of the RNAi enzyme complex. Cell, 2003. 115(2): p. 199-208.
28. Heetebrij, R.J., et al., Platinum(II)-based coordination compounds as nucleic acid labeling reagents: synthesis, reactivity, and applications in hybridization assays. Chembiochem, 2003. 4(7): p. 573-83.
29. Trettel, F., et al., Dominant phenotypes produced by the HD mutation in STHdh(Q111) striatal cells. Hum Mol Genet, 2000. 9(19): p. 2799-809.
30. Dirac, A.M. and R. Bernards, Reversal of senescence in mouse fibroblasts through lentiviral suppression of p53. J Biol Chem, 2003. 278(14): p. 11731-4.

## Acknowledgements

We thank S. Friend and J. Downward for their support of this project, M. Voorhoeve, Z. Wu, X.-j. Yang, H. Yntema and Kreatech Biotechnology for reagents, the NKI microarray facility group for assistance, A. Dirac and S. Nijman for technical help, and members of the Bernards laboratory for discussions. This work was supported by grants from the Netherlands Genomics Initiative/Netherlands Organization for Scientific Research (NWO), Cancer Research UK (CRUK), the Centre for Biomedical Genetics (CBG), the Dutch Cancer Society (KWF) and Utrecht University (ABC cluster).

# Supplementary tables and figures

**Supplementary table 1** is available at:
http://www.nature.com/nature/journal/v428/n6981/suppinfo/nature02371.html

**Supplementary table 2**
*Sequence information of identified shRNA vectors (I) and (II) refer to the two independent shRNA vector sequences that were used in the experiments outlined in Figure 2. For all other experiments, the original shRNA vector sequence (I) was used.*

| Gene symbol | | Accession | Gene name | 19-mer sequence |
|---|---|---|---|---|
| RPS6KA6 | I | NM_014496 | ribosomal protein S6 kinase, 90kDa, polypeptide 6 | GATTATCCAAAGAGGTTCT |
| RPS6KA6 | II | NM_014496 | ribosomal protein S6 kinase, 90kDa, polypeptide 6 | TGGTTGATGAGCCAATGGA |
| HTATIP | I | NM_006388 | HIV-1 Tat interactive protein, 60kDa | GTACGGCCGTAGTCTCAAG |
| HTATIP | II | NM_006388 | HIV-1 Tat interactive protein, 60kDa | CAAACGTCTGGATGAATGG |
| HDAC4 | I | NM_006037 | histone deacetylase 4 | GCCATCCAGATGGACTTTC |
| HDAC4 | II | NM_006037 | histone deacetylase 4 | GCATGTGTTTCTGCCTTGC |
| CCT2 | I | NM_006431 | chaperonin containing TCP1, subunit 2 (beta) | GCAGCAGAGGTGATTCTGC |
| CCT2 | II | NM_006431 | chaperonin containing TCP1, subunit 2 (beta) | GAGAGGCGCTGTTGAGTTC |
| KIAA0828 | I | NM_015328 | KIAA0828 protein | GAGTACATTCTGCCTTGCT |
| KIAA0828 | II | NM_015328 | KIAA0828 protein | GCTACATCAAGAACTCAGC |

**Supplementary figure 1**
*Schematic representation of the 59 nt oligonucleotides. The hairpin insert contains cloning sites, pol III transcription initiation site, 19 nt gene-specific sequence, loop, 19 nt reverse-complement sequence and polymerase III termination signal.*

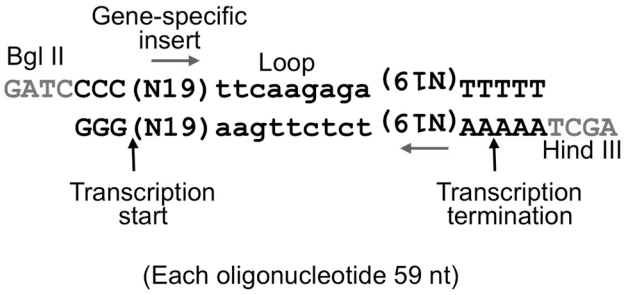


(Each oligonucleotide 59 nt)

**Supplementary figure 2**

*For the five identified genes endogenous knockdown was determined with the use of Real-Time TaqMan PCR. Total RNA was isolated from U2-OS cells stably infected with the indicated shRNA vectors. All primers were designed to be intron-spanning to preclude amplification of genomic DNA. The expression level for each of the genes tested was corrected for the input of cDNA based on the housekeeping gene glyceraldehyde-3-phosphate dehydrogenase (GAPDH) control. The quality control of the PCR reactions were assessed by standardized PCR conditions, including in each experiment a genomic DNA control and a negative non-template control. Shown is a representative experiment were the relative amount of transcripts is indicated as a percentage of transcripts detected in control RNA samples.*

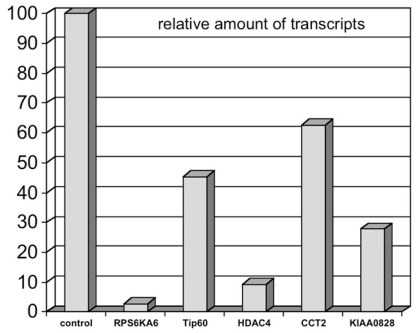

# CHAPTER III

# An shRNA barcode screen provides insight into cancer cell vulnerability to MDM2 inhibitors

Published in *Nature Chemical Biology* 13 February 2006; Vol 2

# An shRNA barcode screen provides insight into cancer cell vulnerability to MDM2 inhibitors

Thijn R Brummelkamp[1,3,4], Armida MW Fabius[1,4], Jasper Mullenders[1], Mandy Madiredjo[1], Arno Velds[1,2], Ron M Kerkhoven[1,2], René Bernards[1] & Roderick L Beijersbergen[1]

1. Division of Molecular Carcinogenesis and Center for Biomedical Genetics and 2. Central Microarray Facility, The Netherlands Cancer Institute, Plesmanlaan 121, 1066CX Amsterdam, The Netherlands. 3. Present address: Whitehead Institute for Biomedical Research, Nine Cambridge Center, Cambridge, Massachusetts 02142, USA. 4. These authors contributed equally to this work. Correspondence should be addressed to R.B. (r.bernards@nki.nl) or R.L.B. (r.beijersbergen@nki.nl).

**The identification of the cellular targets of small molecules with anticancer activity is crucial to their further development as drug candidates. Here, we present the application of a large-scale RNA interference–based short hairpin RNA (shRNA) barcode screen to gain insight in the mechanism of action of nutlin-3 (Compound [1]). Nutlin-3 is a small-molecule inhibitor of MDM2, which can activate the p53 pathway. Nutlin-3 shows strong antitumor effects in mice, with surprisingly few side effects on normal tissues [1]. Aside from p53, we here identify 53BP1 as a critical mediator of nutlin-3–induced cytotoxicity. 53BP1 is part of a signaling network induced by DNA damage that is frequently activated in cancer but not in healthy tissues [2]. Our results suggest that nutlin-3's tumor specificity may result from its ability to turn a cancer cell–specific property (activated DNA damage signaling [3]) into a weakness that can be exploited therapeutically.**

The tumor-suppressor gene *TP53* (also called *p53* and encoding the protein p53) is the gene most frequently mutated in human cancer. However, approximately 50% of all human tumors retain normal p53 [4]. Direct activation of p53 in these tumors could in principle be used as a means to eradicate tumor cells. The activity of p53 is tightly regulated. p53 is activated in response to a variety of stresses, such as DNA damage, nutrient deprivation or oncogene activation, resulting in the transcriptional activation of target genes involved in growth arrest and apoptosis [5]. To protect healthy cells from the deleterious effects of uncontrolled p53 activation, p53 is subject to a negative feedback loop activated by the protein product of

one of its target genes, MDM2. The protein MDM2 binds to p53, inhibits transcriptional activation, causes nuclear export and acts as an E3 ligase to target p53 for proteasomal degradation [6, 7].

One potential approach for activating p53 in tumor cells is to disrupt the interaction between MDM2 and p53 with the small molecule nutlin-3 [1, 8]. Nutlin-3 binds to MDM2, thereby preventing the interaction with p53 and causing p53 to be stabilized. Nutlin-3 has strong antitumor effects *in vivo* but, notably, few toxic effects in normal mice [1]. In theory, activation of p53 could be at least as deleterious to normal cells as to tumor cells, because the former are not attenuated in their ability to undergo apoptosis and are more obedient to growth-inhibitory signals than are cancer cells. However, tumor cells that have lost the *p53* gene through mutation seem to be exquisitely sensitive to reintroduction of the wild-type gene [9]. This phenomenon has never been understood in detail, and has often been attributed to the presence of other oncogenic mutations or to a differential wiring of the p53 network in tumor cells as compared to normal cells [9]. We report here a loss-of-function genetic screen designed to identify important components of the p53 network mediating the cytotoxic effect of nutlin-3 in human tumor cells.

A variety of approaches can be used for the identification of genes essential for a drug-induced phenotype [9-16], including the recently developed RNAi barcode screening technology [10-13]. Barcode screens use DNA microarrays to follow the relative abundance, under particular conditions, of each shRNA vector in a large population of cells infected with an shRNA vector library (Fig. 1a). Using retroviral infection, we introduced a collection of 23,742 different pRETRO-SUPER vectors designed to target 7,914 human genes for suppression by RNA interference (RNAi) into MCF-7 cells (which have wild-type p53 [10]). The infected cells were split into two pools, one of which was left untreated and was used as a reference while the other was exposed to 4 μM nutlin-3. MCF-7 cells respond to this concentration of nutlin-3 predominantly by undergoing cell-cycle arrest rather than apoptosis (data not shown and Fig. 2c), possibly because the cells have a deficiency in caspase-3 [14]. After 14 d of selection with nutlin-3, we recovered shRNA cassettes by PCR amplification and analyzed them by hybridization to DNA microarrays as described [10, 15]. A small number of shRNA vectors were consistently enriched in the population treated with nutlin-3 (Fig. 1b). As expected, one of these vectors that was positively selected in the presence of nutlin-3 as compared to untreated control cells is directed against p53 which validates the shRNA barcode approach used here. Loss of p53 confers resistance to nutlin-3 by removing the effector of MDM2 [1]. In addition, several of the shRNA vectors we identified target proteins with known or predicted functions in

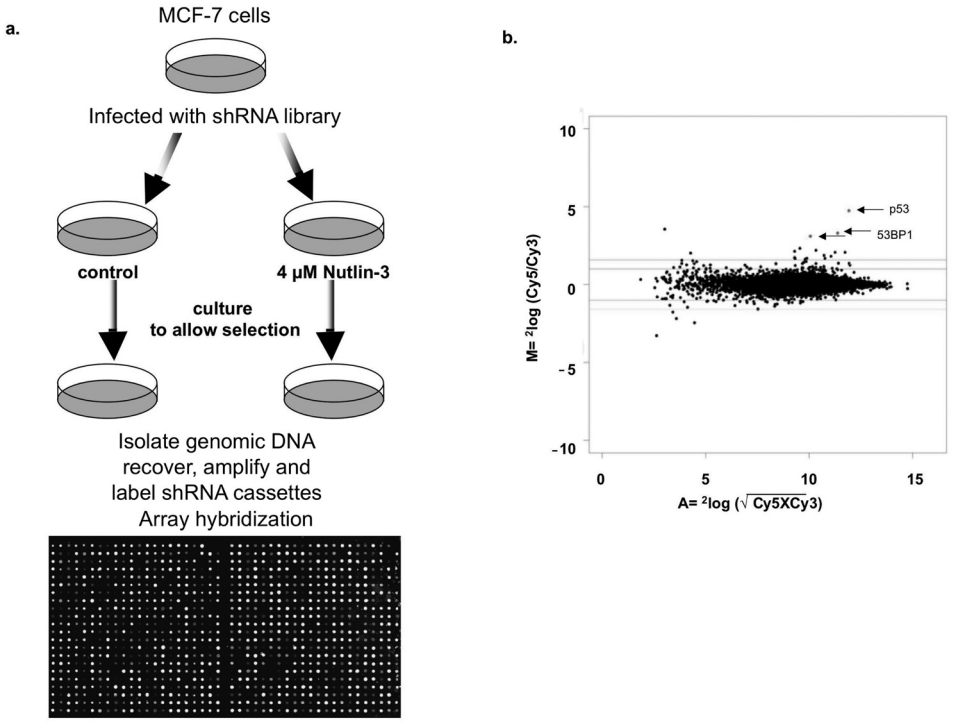


**Figure 1**

**shRNA barcode screen identifies 53BP1 as a mediator of the antiproliferative effects of nutlin-3.**

*(a) Schematic outline of the nutlin-3 barcode experiment in MCF-7 cells. Identical populations of MCF-7 cells infected with the NKI shRNA library were either left untreated or treated with 4 μM nutlin-3. After 14 d the shRNA cassettes were recovered and labeled10, 11. The labeled shRNA probes were hybridized to DNA microarrays containing the sequences complementary to the hairpin oligos. (b) Analysis of the relative abundance of shRNAs recovered from the nutlin-3 barcode experiment. Data are normalized and depicted as M, the 2log (ratio Cy5/Cy3), versus A (2log (radicintensity Cy3 times Cy5)). The data are the average of two independent hybridization experiments performed in duplicate with reversed color. (c) List of genes targeted by the shRNA vectors from b that were significantly enriched (P < 0.01) in nutlin-3–treated cells. The vectors for TP53 and both vectors for 53BP1 have been validated for knockdown and rescue of nutlin-3–induced cell-cycle arrest. Column M depicts the 2log ratio of the abundance of barcodes present in cells treated with nutlin-3 (Cy5) as compared to untreated cells (Cy3).*

p53-mediated pathways (Fig. 1c). Two of these shRNA vectors target p53-binding protein-1 (*53BP1*), through independent sequences. 53BP1 has been implicated in DNA damage sensing leading to p53 activation. In addition, we found an shRNA vector targeted against protein heterogeneous nuclear ribonucleoprotein K (*hnRNPK*), which has recently been identified as an MDM2 target and transcriptional coactivator of p53 in response to DNA damage [16]. The observation that depletion of *hnRNPK* abrogates the transcriptional induction of p53 target genes is consistent with an override of a nutlin-3–mediated cell-cycle arrest upon hnRNPK inactivation. We also identified three vectors targeting genes encoding known p53 transcriptional targets:

BCL2-antagonist of cell death (*BAD*), placental bone morphogenic protein (*PLAB*) and immediate-early response 3 (*IER3*, also called IEX-1). Both BAD and IEX-1 have roles in the regulation of apoptosis. IEX-1 can block the PI3K/AKT pathway, resulting in increased sensitivity to apoptosis [17]. *PLAB* is also implicated as an important downstream mediator of DNA damage signaling [18]. Other shRNA vectors we identified in our screen target genes that are not implicated in the regulation of p53 or p53-dependent pathways. The presence of the genes encoding TGFbeta-inducible early growth response-1 (*TIEG1*, also called *KLF10*) and *PLAB* among the targets of the vectors identified suggests that the TGFbeta pathway is involved in the cell-cycle arrest induced through the activation of the p53 pathway by nutlin-3 treatment. Notably, *TIEG1* expression is reduced in invasive breast cancer cells [19]. The shRNA barcode screen did not identify genes that enhance the cytotoxic effects of nutlin-3 in MCF-7 cells—that is, there were no shRNA vectors that were significantly depleted from the population as a result of nutlin-3 treatment. This may either be a consequence of the biological system or reflect a technical limitation of the current barcode protocol. In addition, we cannot exclude the possibility that some vectors are selected in this screen as a result of effects on cellular components other than the intended targets.

Our identification of two independent shRNA vectors targeted against 53BP1 in our screen greatly reduces the possibility that the observed effects are due to 'off-target' effects of the RNAi vectors. Moreover, this indicates that the observed phenotype is due to the reduced expression of the intended target. We therefore focused our subsequent validation on the effect of 53BP1 on nutlin-3 cytotoxicity. To validate the selection of shRNAs against *53BP1* in our barcode experiment, we performed a long-term growth assay with MCF-7 cells expressing the two different shRNA vectors against *53BP1*. MCF-7 cells exposed to nutlin-3 undergo a proliferation arrest and acquire a flattened phenotype (Fig. 2a,b, left). In contrast, MCF-7 cells transduced with shRNA encoding retroviruses against *p53* or *53BP1* and exposed to nutlin-3 show a cellular morphology resembling that of untreated MCF-7 cells. This effect is not unique to MCF-7 breast cancer cells, as inhibition of *53BP1* also alleviates the cytotoxic effects of nutlin-3 in A549 (human lung cancer) cells (Fig. 2b, right). We tested the effect of the inactivation of either *p53* or *53BP1* on the cell-cycle progression of MCF-7 cells exposed to 4 μM nutlin-3 for 48 h. The percentage of MCF-7 cells in S-phase, as determined by BrdU incorporation, was reduced from 44% for control cells to 2% in cells exposed to nutlin-3, whereas knockdown of *p53* or *53BP1* largely prevented this reduction, resulting in S-phase percentages of 29% and 17%, respectively (Fig. 2c). To further validate the efficacy of the shRNA vectors against 53BP1, we tested their effects on the expression

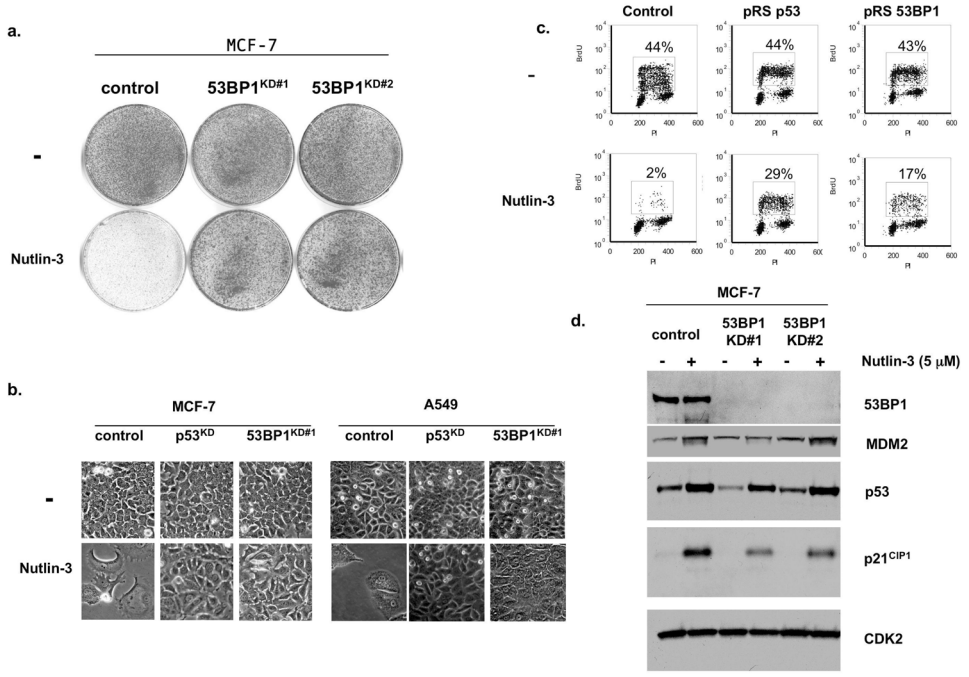


**Figure 2**

**53BP1 modulates the cellular cytotoxicity induced by nutlin-3 in MCF-7 cells.**

*(a) MCF-7 cells infected with shRNAs against GFP or two independent shRNAs directed against 53BP1 (knockdown vector is labeled KD), untreated or treated with 4 μM nutlin-3 for 14 days. Cell density is visualized by Coomassie staining of the cells. (b) MCF-7 cells and A549 cells infected with shRNAs directed against GFP, p53 or 53BP1, untreated or treated with nutlin-3.(c) Cell-cycle profile and BrdU incorporation of MCF-7 infected with shRNAs against GFP (control), p53 or 53BP1. Percentages of BrdU-positive cells are shown. (d) Western blot analysis of the MCF-7 cells expressing either shRNA against GFP (control) or one of the two shRNAs against 53BP1, 53BP1#1 or 53BP1#2. The cells were analyzed for the expression levels of 53BP1, the stabilization of p53 and the induction of p21 and MDM2.*

of 53BP1, the stabilization of p53 by nutlin-3, and the activation of a p53 target gene, *CDKN1A* (also called p21 and encoding $p21^{cip1}$). Both shRNA vectors targeting *53BP1* were active in inhibiting *53BP1* expression (Fig. 2d). The induction of p53 by nutlin-3 treatment is not altered in the presence or absence of 53BP1 expression. Notably, the shRNA-mediated knockdown of *53BP1* impairs the activation of the p53 target gene CDKN1A by nutlin-3. These results demonstrate that, beside p53, 53BP1 also has an essential role in mediating the cytotoxic effects of nutlin-3 in MCF-7 cells.

53BP1 is a component of the ATM-CHK-53BP1 pathway that is activated by double-stranded DNA breaks or shortened telomeres, resulting in the induction of p53 [20]. Notably, this ATM-CHK-53BP1 DNA damage checkpoint-signaling

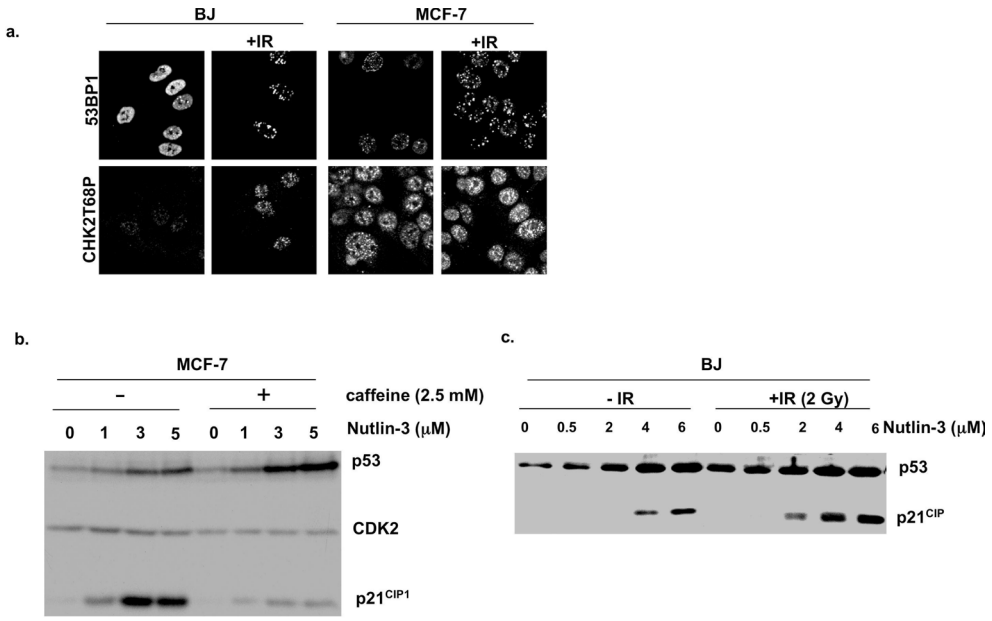


**Figure 3**

**Intrinsic DNA damage signaling contributes to the cytotoxic effect of nutlin-3 in MCF-7 cells.**

*(a) Immunolocalization of p53BP1 (above) and CHK2 (below) in human primary fibroblasts (left) and MCF-7 cells (right) before and after irradiation. (b) Western blot analysis of the stabilization of p53 and induction of p21 in MCF-7 cells treated with increasing concentrations nutlin-3 for 18 h in the absence or presence of 2.5 mM caffeine. The cells were pretreated with 2.5 mM caffeine for 12 h.(c) Western blot analysis of the stabilization of p53 and the induction of p21 in normal BJ fibroblasts treated with increasing concentrations nutlin-3 without or with exposure to 2Gy irradiation.*

pathway is often constitutively activated in human cancers and premalignant lesions, but not in normal, healthy tissues [2, 3, 21]. Based on the role of 53BP1 in mediating the antiproliferative effect of nutlin-3 identified here, we hypothesized that intrinsic DNA damage signaling in MCF-7 cells is required for nutlin-3 cytotoxicity. The presence of activated DNA damage signaling in MCF-7 cells was demonstrated by the detection of nuclear foci containing 53BP1, a characteristic of DNA damage–induced activation of 53BP1 [22]. Indeed, a substantial fraction of MCF-7 cells show localization of 53BP1 in nuclear foci. Normal BJ fibroblasts have diffuse nuclear staining, although some 53BP1 foci are present (Fig. 3a, above). The presence of DNA damage foci in normal human fibroblasts in culture is in agreement with previous studies describing the presence of H2AX DNA damage foci and p53 activation in primary cells cultured *in vitro* [23]. MCF-7 cells also show strong nuclear staining with an antibody directed against phosphorylated CHK-2, even in the absence of ionizing radiation (Fig. 3a, below). In contrast, normal BJ fibroblasts show very little immunoreactivity, whereas BJ fibroblasts treated

with ionizing radiation show strong nuclear staining (Fig. 3a, below). Together these data indicate that in MCF-7 cells, in the absence of ionizing irradiation, activation of DNA damage checkpoint signaling involving 53BP1 occurs, reflecting DNA damage signaling seen in many human tumors [2].

The presence of activated DNA damage checkpoints in MCF7 cells suggests that DNA damage–induced 'stress signals' could be important in sensitizing MCF-7 cells to MDM2 inhibition. To test this, we inhibited DNA damage signaling in MCF-7 cells through inhibition of ATM/ATR-dependent checkpoints by caffeine (Compound 2) treatment [24-26]. The inhibition of ATM/ATR kinases in MCF-7 cells resulted in a decrease in the transcriptional activation by p53 in response to nutlin-3 exposure, as evidenced by induction of *p21*$^{cip1}$ (Fig. 3b). The inhibition of ATM/ATR kinases does not prevent p53 accumulation in response to nutlin-3 exposure, indicating that p53 stabilization and transactivation are separate events (Fig. 3b). To further test whether DNA damage signaling enhances the effects of nutlin-3, we treated normal BJ fibroblasts with increasing concentrations of nutlin-3 in the absence or presence of a low level of DNA damage induced by ionizing radiation. A more robust activation of the p53 target gene *p21*$^{cip1}$ was seen in response to nutlin-3 treatment in the presence of DNA damage (Fig. 3c). From these results we conclude that inhibition of intrinsic DNA damage signaling by *53BP1* knockdown prevents full activation of p53 after stabilization in response to MDM2 inhibition.

Genomic instability is a well-recognized property of the vast majority of human cancers. This labels cancer tissues with

a.

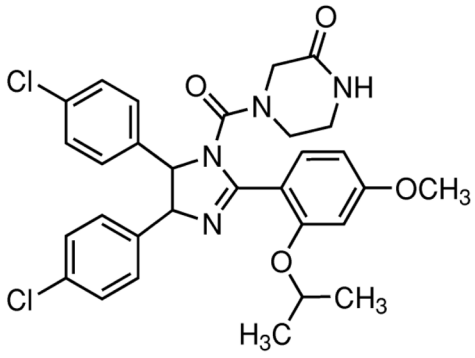


b.

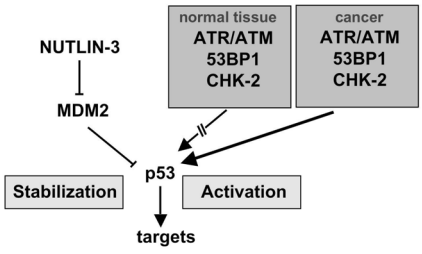


**Figure 4**

**The cytotoxic effect of nutlin-3 in tumor cells is enhanced by intrinsic DNA damage signaling.**

*(a) Chemical structure of nutlin-3.(b) Schematic representation of a putative model reflecting the intrinsic DNA damage signaling (involving 53BP1) present in tumor cells (but absent in normal cells) increasing the cytotoxicity associated with nutlin-3 treatment.*

a feature not seen in normal tissues, and it has therefore been suggested that genetic instability is an Achilles heel of tumor cells that could be exploited by future anticancer therapeutics [27]. Recent experiments have indicated that activation of DNA damage signaling (involving H2AX, 53BP1, ATR and ATM) occurs very early during tumorigenesis [3, 21]. Our data indicate that this DNA damage signaling enhances the effects of the MDM2 inhibitor nutlin-3 (Fig. 4). The absence of such signals in normal cells *in vivo* may well explain their reduced sensitivity to nutlin-3 [2]. The consequences of partial inactivation of MDM2 by small-molecule inhibitors resemble the phenotype seen in mice carrying a hypomorphic allele of *MDM2*. These mice are viable but show severe radiosensitivity [28].

Our data suggest that MDM2 inhibitors would be most effective for tumors that have both wild-type p53 and activated DNA damage signaling, which is a substantial fraction of all human tumors. However, a combination of MDM2 inhibitors with DNA-damaging treatments may be harmful to normal cells and would cause undesired side effects in patients. In conclusion, the present study illustrates that shRNA barcode screens can be used to reveal cellular components that mediate drug cytotoxicity, resulting in a more complete understanding of drug action and enabling more rational decisions to be made in regard to drug application.

## Methods

### *Cell culture*

MCF-7 breast cancer cells and BJ primary human fibroblasts, both expressing the ecotropic receptor, were cultured in DMEM supplemented with 10% fetal calf serum and penicillin and streptomycin. Cells were grown at 37 °C in 5% CO2. Phoenix cells were used to produce ecotropic retroviruses as described previously [11]. Nutlin-3 ((+/-)-4-[4,5-bis(4-chlorophenyl)-2-(2-isopropoxy-4-methoxyphenyl)-4,5-dihydroimidazol-1-carbonyl] piperazin-2-one) was obtained from Cayman Chemical. Caffeine pretreatment of MCF-7 cells was performed by incubation with 2.5 mM caffeine (Sigma-Aldrich) for 12 h.

### *Barcode screen*

MCF-7 cells were infected with retroviruses representing the complete Netherlands Cancer Institute (NKI) shRNA library described previously [10]. Infected cells were selected on puromycin (2.0 µg/ml) for 4 d and split into two populations. One population was left untreated, while the other population was exposed to 4 µM nutlin-3. After 14 d, genomic DNA was isolated with DNAzol (Invitrogen) and shRNA inserts were amplified from genomic DNA by

PCR using the primers pRS-T7-fw, 5'-GGCCAGTGAATTGTAATACGAC-TCACTATAGGGAGGCGGCCCT TGAACCTCCTCGTTCGACC-3', containing a T7 RNA polymerase promoter sequence, and pRS8-rev, 5'-TAAAGCGCATGCTCCAGACT-3'. After purification (QIAquick PCR purification kit, Qiagen), PCR products were used for linear RNA amplification using the Megascript T7 kit (Ambion), and purified RNA probes (RNeasy, Qiagen) were labeled with cyanine-3 (Cy3) or cyanine-5 (Cy5) fluorescent groups using ULS (Kreatech) and purified over a KreaPure (Kreatech) spin column as described [29]. Labeled RNA probes from untreated and nutlin-3–treated cells were combined and hybridized to oligonucleotide arrays in 40 µl of hybridization mixture (25% formamide, 5times SCC, 0.01% SDS, 25% Kreablock (Kreatech)). Samples were heated to 100 °C for 5 min and applied to the array. Microarrays were hybridized for 18 h at 42 °C, washed and scanned using an Agilent microarray scanner. Quantification of the resulting fluorescent images was performed with Imagene 5.6 (BioDiscovery), local background was subtracted, and the data were normalized [30] and 2log transformed.

***Plasmids***

The shRNA sequences used to target p53 and p53BP1 were as follows: p53 5'-GACTCCAGTGGTAATCTAC-3'; 53BP1#1 5'-GATACTGCCTCATCACA GT-3'; 53BP1#2 5'-GAACGAGGAG ACGGTAATA-3' The shRNA sequences were cloned into pRETROSUPER as described previously [10].

***Cell-cycle analysis***

MCF-7 cells infected with shRNA vectors against GFP (control), p53 and 53BP1 were treated for 48 h with nutlin-3 or left untreated. The cells were labeled with 10 µM BrdU for 30 min before harvesting. Cells were fixed in 70% ethanol and permeabilized in HCl-Triton solution (2 M HCl, 0.5% Triton X-100). The samples were neutralized in borate solution (0.1 M Na2B4O7.10H2O) and labeled with antibody to BrdU (Dako; 1% BSA in PBS containing 0.5% Tween-20) in combination with FITC-conjugated secondary antibody (Dako; goat anti–mouse IGM–FITC). Samples were incubated with 10 µg/ml propidium iodine and 250 µg/ml RNase. In each assay 10,000 cells were collected by FACScan (Becton Dickinson) and analyzed using the FCS Express program (De Novo Software).

***Western blotting***

Protein lysates were separated on SDS-PAGE gels, blotted onto nitrocellulose membranes and incubated with antibodies directed against MDM2 (2A10 and SMP14, Santa Cruz), 53BP1 (Novus Biologicals), p53 (DO-1), p21 (C19, Santa Cruz), CDK4 (C-22, Santa Cruz) and CDK2 (M2, Santa Cruz).

***Immunofluorescence***

Cells grown on coverslips were washed with PBS, fixed and permeabilized in 3% paraformaldehyde and 0.1% Triton X-100, and washed three times with PBS containing 0.05% saponin. Slides were blocked with

10% normal goat serum in PBS with 0.05% saponin. Cells were stained with antibodies directed against 53BP1 (1:100, Novus Biologicals) and against phosphorylated CHK-2 (p-T68-CHK2; 1:100, Cell Signaling Technologies); FITC-conjugated goat anti-rabbit antibodies were used as secondary antibodies. All antibodies were diluted in PBS containing 10% normal goat serum and 0.05% saponin.

***Microarray data***

Microarray datasets for the barcode experiments can found at the authors' supporting website (http://www.screeninc.nl).

## References


1. Vassilev, L.T., et al., In vivo activation of the p53 pathway by small-molecule antagonists of MDM2. Science, 2004. 303(5659): p. 844-8.
2. DiTullio, R.A., Jr., et al., 53BP1 functions in an ATM-dependent checkpoint pathway that is constitutively activated in human cancer. Nat Cell Biol, 2002. 4(12): p. 998-1002.
3. Gorgoulis, V.G., et al., Activation of the DNA damage checkpoint and genomic instability in human precancerous lesions. Nature, 2005. 434(7035): p. 907-13.
4. Lane, D.P. and P.M. Fischer, Turning the key on p53. Nature, 2004. 427(6977): p. 789-90.
5. Vogelstein, B., D. Lane, and A.J. Levine, Surfing the p53 network. Nature, 2000. 408(6810): p. 307-10.
6. Kubbutat, M.H., S.N. Jones, and K.H. Vousden, Regulation of p53 stability by Mdm2. Nature, 1997. 387(6630): p. 299-303.
7. Kussie, P.H., et al., Structure of the MDM2 oncoprotein bound to the p53 tumor suppressor transactivation domain. Science, 1996. 274(5289): p. 948-53.
8. Zheng, X.S., T.F. Chan, and H.H. Zhou, Genetic and genomic approaches to identify and study the targets of bioactive small molecules. Chem Biol, 2004. 11(5):p. 609-18.
9. Harris, M.P., et al., Adenovirus-mediated p53 gene transfer inhibits growth of human tumor cells expressing mutant p53 protein. Cancer Gene Ther, 1996. 3(2): p. 121-30.
10. Berns, K., et al., A large-scale RNAi screen in human cells identifies new components of the p53 pathway. Nature, 2004. 428(6981): p. 431-7.
11. Brummelkamp, T.R. and R. Bernards, New tools for functional mammalian cancer genetics. Nat Rev Cancer, 2003. 3(10): p. 781-9.
12. Paddison, P.J., et al., A resource for large-scale RNA-interference-based screens in mammals. Nature, 2004. 428(6981): p. 427-31.
13. Westbrook, T.F., et al., A genetic screen for candidate tumor suppressors identifies REST. Cell, 2005. 121(6): p. 837-48.
14. Janicke, R.U., et al., Caspase-3 is required for DNA fragmentation and morphological changes associated with apoptosis. J Biol Chem, 1998. 273(16): p. 9357-60.
15. Brummelkamp, T.R., et al., Functional identification of cancer-relevant genes through large-scale RNA interference screens in mammalian cells. Cold Spring Harb Symp Quant Biol, 2004. 69: p. 439-45.
16. Moumen, A., et al., hnRNP K: an HDM2 target and transcriptional coactivator of p53 in response to DNA damage. Cell, 2005. 123(6): p. 1065-78.
17. Wu, M.X., Roles of the stress-

induced gene IEX-1 in regulation of cell death and oncogenesis. Apoptosis, 2003. 8(1): p. 11-8.
18. Wong, J., P.X. Li, and H.J. Klamut, A novel p53 transcriptional repressor element (p53TRE) and the asymmetrical contribution of two p53 binding sites modulate the response of the placental transforming growth factor-beta promoter to p53. J Biol Chem, 2002. 277(29): p. 26699-707.
19. Reinholz, M.M., et al., Differential gene expression of TGF beta inducible early gene (TIEG), Smad7, Smad2 and Bard1 in normal and malignant breast tissue. Breast Cancer Res Treat, 2004. 86(1): p. 75-88.
20. Wang, B., et al., 53BP1, a mediator of the DNA damage checkpoint. Science, 2002. 298(5597): p. 1435-8.
21. Bartkova, J., et al., DNA damage response as a candidate anti-cancer barrier in early human tumorigenesis. Nature, 2005. 434(7035): p. 864-70.
22. Rappold, I., et al., Tumor suppressor p53 binding protein 1 (53BP1) is involved in DNA damage-signaling pathways. J Cell Biol, 2001. 153(3): p. 613-20.
23. Sedelnikova, O.A., et al., Senescing human cells and ageing mice accumulate DNA lesions with unrepairable double-strand breaks. Nat Cell Biol, 2004. 6(2): p. 168-70.
24. Blasina, A., et al., Caffeine inhibits the checkpoint kinase ATM. Curr Biol, 1999. 9(19): p. 1135-8.
25. Zhou, B.B., et al., Caffeine abolishes the mammalian G(2)/M DNA damage checkpoint by inhibiting ataxia-telangiectasia-mutated kinase activity. J Biol Chem, 2000. 275(14): p. 10342-8.
26. Sarkaria, J.N., et al., Inhibition of ATM and ATR kinase activities by the radiosensitizing agent, caffeine. Cancer Res, 1999. 59(17): p. 4375-82.
27. Lengauer, C., K.W. Kinzler, and B. Vogelstein, Genetic instabilities in human cancers. Nature, 1998. 396(6712): p. 643-9.
28. Mendrysa, S.M., et al., mdm2 Is critical for inhibition of p53 during lymphopoiesis and the response to ionizing irradiation. Mol Cell Biol, 2003. 23(2): p. 462-72.
29. Heetebrij, R.J., et al., Platinum(II)-based coordination compounds as nucleic acid labeling reagents: synthesis, reactivity, and applications in hybridization assays. Chembiochem, 2003. 4(7): p. 573-83.
30. Quackenbush, J., Microarray data normalization and transformation. Nat Genet, 2002. 32 Suppl: p. 496-501.

## Acknowledgments

We thank the Netherlands Cancer Institute microarray facility group for assistance; K. Berns, S. Nijman, H. Ovaa and members of the Bernards and Beijersbergen laboratories for help and discussions; L. Oomen for help with confocal microscopy; and R. Kortlever for critically reading the manuscript. This work was supported by grants from the Dutch Cancer Society (KWF) and the European Union integrated project INTACT.

# CHAPTER IV

# A large scale shRNA barcode screen identifies the circadian clock component ARNTL as putative regulator of the p53 tumor suppressor pathway

Published in *PLOS One* 11 March 2009; Vol 4

# A large scale shRNA barcode screen identifies the circadian clock component ARNTL as putative regulator of the p53 tumor suppressor pathway.

Jasper Mullenders[1], Armida WM Fabius[1], Mandy Madiredjo, René Bernards and Roderick L Beijersbergen

Division of Molecular Carcinogenesis, Centre for Biomedical Genetics and Cancer Genomics Centre, Netherlands Cancer Institute, Amsterdam, The Netherlands
1. These authors contributed equally to this work.

**Background:** The p53 tumor suppressor gene is mutated in about half of human cancers, but the p53 pathway is thought to be functionally inactivated in the vast majority of cancer. Understanding how tumor cells can become insensitive to p53 activation is therefore of major importance. Using an RNAi-based genetic screen, we have identified three novel genes that regulate p53 function.

**Results:** We have screened the NKI shRNA library targeting 8,000 human genes to identify modulators of p53 function. Using the shRNA barcode technique we were able to quickly identify active shRNA vectors from a complex mixture. Validation of the screening results indicates that the shRNA barcode technique can reliable identify active shRNA vectors from a complex pool. Using this approach we have identified three genes, ARNTL, RBCK1 and TNIP1, previously unknown to regulate p53 function. Importantly, ARNTL (BMAL1) is an established component of the circadian regulatory network. The latter finding adds to recent observations that link circadian rhythm to the cell cycle and cancer. We show that cells having suppressed ARNTL are unable to arrest upon p53 activation associated with an inability to activate the p53 target gene $p21^{CIP1}$.

**Conclusions:** We identified three new regulators of the p53 pathway through a functional genetic screen. The identification of the circadian core component ARNTL strengthens the link between circadian rhythm and cancer.

## Introduction

The TP53 gene product is important in the cellular response to different types of stress [1,2]. A major physiological stress is DNA damage. DNA damage leads to activation of the ATM/ATR, CHK1/2 cascade, which in turn activates p53. Activation of p53 is achieved by increased stability and post translational modifications of the p53 protein. These modifications include phosphorylation, methylation [3], ubiquitination [4,5] and acetylation [6] leading to enhanced transcriptional activity of p53. Furthermore, oncogene activation can also lead to p53 activation through activation of the $p19^{ARF}$ protein. $p19^{ARF}$ inhibits MDM2, the major E3 ubiquitin ligase for p53 [7] leading to stabilization and activation of p53. Activation of p53 leads to transcriptional activation of a large set of p53 target genes, which in turn causes cell cycle arrest or apoptosis [8].
The p53 pathway is inactivated in almost all human cancers [9]. In about half of human cancers this is due to mutation or deletion of the *TP53* gene itself. However in a significant fraction of human tumors, the p53 pathway is inactivated through alteration in cellular components acting up- or down-stream of p53. For example, amplification of the negative regulator of p53, MDM2, leads to accelerated degradation and inactivation of p53 [2,10].

As a model to screen for genes that modulate p53 function, we previously developed a human fibroblast cell line named BJtsLT [11]. These cells express a temperature-sensitive mutant of the SV40 large T antigen, which allows the cells to proliferate at the permissive temperature (32ºC). However, when the cells are shifted to 39ºC, the large T antigen is degraded and the cells enter a stable p53-dependent cell cycle arrest.

We and others have previously described the construction and initial screening of shRNA libraries using the barcode technique [11-17]. The barcode technique allows the rapid identification of individual shRNA vectors from a large pool of shRNA vectors that produce a specific phenotype. This approach takes advantage of the fact that each shRNA vector contains a unique 19-mer sequence as part of the shRNA cassette, which can serve as a molecular "barcode" identifier. Briefly, cells are infected with the pooled shRNA library of some 24,000 vectors. The population of cells is then split into two separate populations. One population is used as a reference sample while the other sample is subjected to a selective treatment. Knockdown of a specific gene by the shRNA vector can lead to three possible cellular responses to this treatment. First the cells can remain unaffected identical to control cells, second the cells can become more sensitive to the treatment and third the cells can acquire resistance to the treatment. As a consequence of the differential response to the treatment, the

relative number of cells that harbor a specific shRNA can increase, decrease or remain the same. The relative abundance of each shRNA cassette can be determined by the isolation of the shRNA cassettes from the population, labeling of the barcode identifiers with different fluorescent dyes and subsequent hybridization to DNA microarrays representing all shRNA sequences. By comparing the relative abundance of all shRNAs against the reference population, shRNAs responsible for the three possible phenotypes can be identified.

The shRNA barcode technique can be used for different screening approaches, most notably the identification of genes that are involved in drug resistance. For instance, we have used the barcoding approach to identify genes that are involved in the resistance to the cytotoxic effects of Nutlin-3, a drug that activates p53 by acting as an inhibitor of MDM2 [13]. This led to the identification of 53BP1, a p53 binding protein, as a critical modulator of the effect of Nutlin-3. More recently, we found the tumor suppressor *PTEN* as a gene, which upon decreased expression confers resistance to trastuzumab in breast cancer [12]. Significantly, the PI3K pathway, which is negatively regulated by PTEN, was also shown to be a major regulator of trastuzumab sensitivity in the clinic, underscoring the utility of the *in vitro* genetic screens to identify drug modulators.

In the first screen applying the NKI shRNA library, Berns et al. used BJtsLT cells to identify 5 new players in the p53 pathway [11]. This screen did not take advantage of the barcode technology. Rather, it was performed by the conventional method of isolating and expanding colonies that are resistant to p53-mediated growth arrest. Subsequent isolation of the shRNA inserts and sequence analysis was required to identify the shRNA responsible for the bypass of the p53 mediated cell cycle arrest. This method is rather laborious and such an approach may not uncover all active shRNAs in a library. Moreover, due to the labour-intensive nature of the screen, only part of the 24,000 vector NKI shRNA library was covered in this initial approach. Here we describe the screening of the entire NKI shRNA library for modulators of p53 activity using the barcode technology. We find three additional genes whose suppression causes resistance to p53-dependent proliferation arrest.

## Results

### *Screening of the BJtsLT cells*

To identify shRNA vectors that can modulate the activity of the p53 pathway, we performed a shRNA bar code screen in BJtsLT cells infected with the NKI shRNA library (See Figure 1a). These cells proliferate at 32°C but enter into a p53-dependent proliferation arrest at 39°C [11]. The infected cells were cultured for three days at 32°C to allow retroviral integration and for gene knockdown to become effective. At day 4 the cells were

split into two populations; one was kept at 32°C and the other was shifted to 39°C. The BJtsLT at 32°C were cultured until the population reached confluency and genomic DNA was isolated. The BJtsLT cells grown at 39°C cease proliferation unless a shRNA is expressed that inactivates the p53-dependent anti-proliferative response. Such cells will continue to proliferate and give rise to a colony. In addition to infection with the NKI shRNA library, we also used a shRNA vector targeting p53 as a positive control for colony outgrowth of the BJtsLT cells at 39°C. After 3 weeks of culturing at 39°C, the control plates infected with p53 shRNA vector contained large numbers of colonies consisting of rapidly proliferating cells (data not shown). The plates infected with the shRNA library also contained several colonies. Colonies from the library-infected plates were pooled and genomic DNA was isolated. The shRNA cassettes were recovered from the genomic DNA using PCR. The recovered shRNA inserts from both the control population and the colonies that continued proliferation at 39°C following infection with the shRNA library, were used to hybridize DNA microarrays containing all 24,000 19-mer sequences of the NKI shRNA library. The hybridization was performed for each of the replicate experiments, after which the results were combined to increase the statistical significance of the enriched shRNA vectors identified. Those shRNA vectors that confer resistance to the p53 mediated cell cycle arrest are enriched in the population cultured at 39°C and can be detected as outliers in a MA-plot representation of the barcode microarray experiment (figure 1b).

From this MA-plot we generated a "hit list" of shRNA vectors that are specifically enriched in cell cultured at 39°C. The following considerations were used to produce this hit list (summarized in figure 1c). We excluded all shRNAs that had an intensity (A-value) lower than 10, as spots with a relative low intensity are likely to be "noise" and as a consequence can have aberrantly high "M" ratios. In addition we only included shRNAs if their ratio ($M=^2$log ratio cy5/cy3) was >0.75, this effectively means the top 100 most enriched shRNAs on the micro-array.

To shorten the list of shRNA vectors to be validated, we first asked where shRNA vectors targeting known components of the p53 pathway were positioned in the top 100. In total, five shRNA vectors targeting known components of the p53 pathway were present in the top 100 and their distribution was as follows (Table 1): one shRNA vector targeting *p53* (position #8), two shRNA vectors targeting $p21^{cip1}$ (#7 & #37) and two shRNA vectors targeting *53BP1* (#5 & #36). As we identified shRNA vectors targeting *53BP1* and $p21^{cip1}$ at positions 36 and 37 on the hit list, we decided to individually test all shRNA vectors on positions 1-37 in a second round selection. Included in this set are vectors targeting 3 out of 5 genes that were previously identified and validated by Berns et al., (2004): *HDAC4* (#2) *KIA0828* (#13),

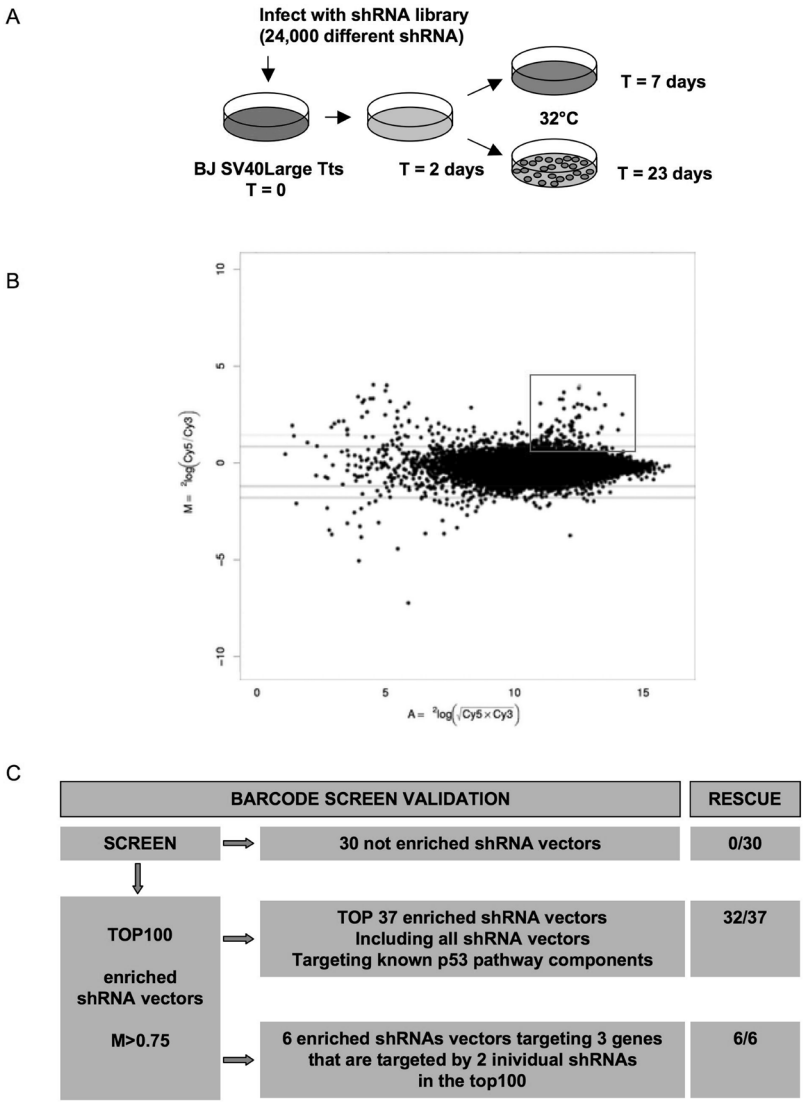


**Figure 1**

**shRNA barcode screen identifies mediators of the p53 dependent cell cycle arrest.**

*a) Schematic outline of the BJtsLT genetic screen. BJtsLT cells were infected with the NKI shRNA library and were either left at 32°C or shifted to 39°C. After 7 days the cells at 32°C had reached confluency and were harvested. Cells at 39°C were harvested after 23 days after which they had formed visible colonies.*

*b) Analysis of the relative abundance of shRNAs recovered from the BJtsLT barcode experiment. Data are normalized and plotted as M, the ²log (ratio Cy5/Cy3), versus A (²log(√intensity Cy3 × Cy5)). The data are the average of two independent hybridization experiments performed in duplicate with reversed colour. A box is drawn around the top 100 enriched shRNAs at 39°C.*

*c) Schematic overview of selection criteria used to select hits from the shRNA barcode screen for further validation.*

| Rank | M | A | Rescue | HUGO | RefSeq | 19mer_start | 19mer_sequence | Remarks |
|---|---|---|---|---|---|---|---|---|
| 1 | 4.07 | 12.24 | + | KCNK9 | NM_016601 | 217 | GTACAACATCAGCAGCGAG | |
| 2 | 3.95 | 12.22 | + | HDAC4 | NM_006037 | 3751 | GCATGTGTTTCTGCCTTGC | Berns et al |
| 3 | 3.73 | 11.65 | + | ABHD6 | NM_020676 | 374 | GGATATGTGGCTCAGTGTG | |
| 4 | 3.67 | 12.98 | + | MYCL1 | NM_005376 | 933 | GAGACACTCCAAACCTGAA | |
| 5 | 3.39 | 11.49 | + | TP53BP1 | NM_005657 | 657 | GATACTGCCTCATCACAGT | Known p53 pathway |
| 6 | 3.39 | 11.60 | + | XRCC1 | NM_006297 | 258 | GGAGGAGCAGATACACAGT | |
| 7 | 3.18 | 10.76 | + | CDKN1A | NM_078467 | 919 | CTAGGCGGTTGAATGAGAG | Known p53 pathway |
| 8 | 3.14 | 12.17 | + | TP53 | NM_000546 | 1026 | GACTCCAGTGGTAATCTAC | Known p53 pathway |
| 9 | 3.09 | 13.20 | + | CALCA | NM_001741 | 428 | AGGGATATGTCCAGCGACT | |
| 10 | 3.00 | 12.03 | + | RBCK1 | NM_031229 | 1389 | GTCAGTACCAGCAGCGGAA | this manuscript |
| 11 | 2.99 | 12.52 | + | INSRR | J05046 | 2402 | GAACAGTGTCCTTCTGCGC | |
| 12 | 2.92 | 11.65 | + | SSR4 | NM_006280 | 377 | GAGTCCTACAGCCTCCTCA | |
| 13 | 2.91 | 12.60 | + | KIAA0828 | NM_015328 | 3945 | GAGTACATTCTGCCTTGCT | Berns et al |
| 14 | 2.91 | 12.83 | + | PTPRN2 | NM_002847 | 2968 | GAGATTGATATCGCAGCGA | |
| 15 | 2.63 | 13.86 | + | TCEAL1 | NM_004780 | 386 | GGACCTGTTTGAGGTTCGC | |
| 16 | 2.56 | 12.22 | + | LHX3 | AF156888 | 266 | GTGTCTCAAGTGCAGCGAC | |
| 17 | 2.47 | 12.12 | + | NR2E3 | AF148128 | 852 | GTGGGCCAAGAACCTGCCT | |
| 18 | 2.35 | 11.37 | + | LOC90925 | BC002792 | 226 | AGAACTGGAGTGGATGGGG | |
| 19 | 2.28 | 11.94 | + | MPZ | NM_000530 | 793 | GGATAAGAAATAGCGGTTA | |
| 20 | 2.26 | 11.49 | + | NR2E3 | NM_014249 | 889 | GTGGGCCAAGAACCTGCCT | |
| 21 | 2.21 | 11.98 | + | PENK | NM_006211 | 779 | GATACGGAGGATTTATGAG | |
| 22 | 2.12 | 10.78 | + | SLIT2 | NM_004787 | 490 | AGAGGAGCATTCCAGGATC | |
| 23 | 2.09 | 11.87 | + | TRAR3 | NM_175057 | 52 | GTGAACGAATCCTGCATTA | |
| 24 | 2.04 | 11.66 | − | CDKN2A | NM_000077 | 745 | GAACCAGAGAGGCTCTGAG | |
| 25 | 2.04 | 11.96 | + | HTATIP | NM_006388 | 1045 | GTACGGCCGTAGTCTCAAG | Berns et al |
| 26 | 2.02 | 11.21 | + | PRPF18 | NM_003675 | 228 | AGAGGAGGACCAGAAACCA | |
| 27 | 2.02 | 11.93 | − | GOLGA5 | NM_005113 | 2209 | GATACCCCATAGCGCGAGT | |
| 28 | 2.01 | 13.08 | − | TIEG | NM_005655 | 2179 | GAATTGGAATCCTCCTTAA | |
| 29 | 1.97 | 11.92 | − | COL12A1 | NM_004370 | 1844 | GGATGCCGTTCGCTCAGAA | |
| 30 | 1.94 | 13.07 | + | RAD51C | NM_058216 | 263 | GATATGCTGGTACATCTGA | |
| 31 | 1.85 | 13.70 | − | TLR4 | NM_003266 | 2180 | GACCATCATTGGTGTGTCG | |
| 32 | 1.83 | 11.43 | + | RAB2 | NM_002865 | 725 | GAAGGAGTCTTTGACATTA | |
| 33 | 1.83 | 11.05 | + | ZNF347 | NM_032584 | 387 | GAGTAATACAGGAGAAGTA | |
| 34 | 1.82 | 12.01 | + | HSD17B4 | NM_000414 | 142 | AGAGGAGCGTTAGTTGTTG | |
| 35 | 1.80 | 11.91 | − | GCGR | NM_000160 | 547 | AGTGCAACACCGCTTCGTG | |
| 36 | 1.75 | 11.19 | + | TP53BP1 | NM_005657 | 387 | GAACGAGGAGACGGTAATA | Known p53 pathway |
| 37 | 1.72 | 11.09 | + | CDKN1A | NM_078467 | 560 | GACCATGTGGACCTGTCAC | Known p53 pathway |
| 40 | 1.67 | 11.13 | + | RPS6KA6 | NM_014496 | | GATTATCCAAAGAGGTTCT | Berns et al |
| 46 | 1.49 | 10.96 | + | RBCK1 | NM_031229 | 710 | GGGGATGAACAGGTGGCAA | this manuscript |
| 51 | 1.31 | 10.57 | + | TNIP1 | NM_006058 | 1718 | GGAAGAGCTGAAGAAGCAA | this manuscript |
| 59 | 1.23 | 11.67 | + | TNIP1 | NM_006058 | 408 | GAGTCCCAGATGGAAGCGA | this mansucript |
| 74 | 1.00 | 10.42 | + | ARNTL | NM_001178 | 1468 | GAACTTCTAGGCACATCGT | this manuscript |
| 99 | 0.76 | 11.55 | + | ARNTL | NM_001178 | 590 | GGGAAGCTCACAGTCAGAT | this manuscript |

Under rescue; + means a validated shRNA, − means not validated. *M* indicates the $^2$log (ratio Cy5/Cy3), A the $^2$log(√intensity Cy3×Cy5).
doi:10.1371/journal.pone.0004798.t001

**Table 1**
*List of genes targeted by shRNA vectors that were selected by the criteria as in figure 1c.*

*HTATIP* (#25). The identification of these shRNA vectors provides further support for the notion that the barcode method enables both fast and reliable screening of shRNA libraries.

In addition, we selected 3 genes that were represented by two independent shRNAs in the top 100 (of which one is present in the 37 already selected shRNAs), bringing the total number of shRNAs to be tested to 42. We included these 3

additional genes in the validation, because if two independent shRNAs targeting the same transcript are enriched in the shRNA screen, this gives higher level of confidence to that specific hit. This is because it is less likely to be "off target" when two independent shRNAs yield the same phenotype and such off target effects of shRNAs are a common problem in these types of genetic screens [18,19]. The other three genes, *ARNTL* [20], *RBCK1* [21] and *TNIP1* [22] have not been linked to p53 before.

To prove that the shRNA barcode technique specifically identifies shRNAs that are enriched in the experiment we also tested 30 randomly-selected shRNAs not enriched in the experiment. All shRNAs were re-tested in the BJtsLT cells. Cells were infected with individual shRNAs, shifted to 39°C and incubated for 3 weeks. When colonies were observed the cells were fixed and stained. As expected, none of the 30 randomly-selected shRNAs was able to produce colonies at 39°C (data not shown). However, for 37 of the 42 enriched shRNA vectors, we could clearly demonstrate that they allowed the cells to proliferate at 39°C. Among the genes targeted by these 37 shRNA vectors were all known p53 pathway components. In addition, we also observed rescue of growth arrest by all three genes that were targeted by two individual shRNAs: *ARNTL*, *RBCK1* and *TNIP1* (Figure 2). Therefore we decided to focus on these three newly identified genes for which we identified two independent shRNAs.

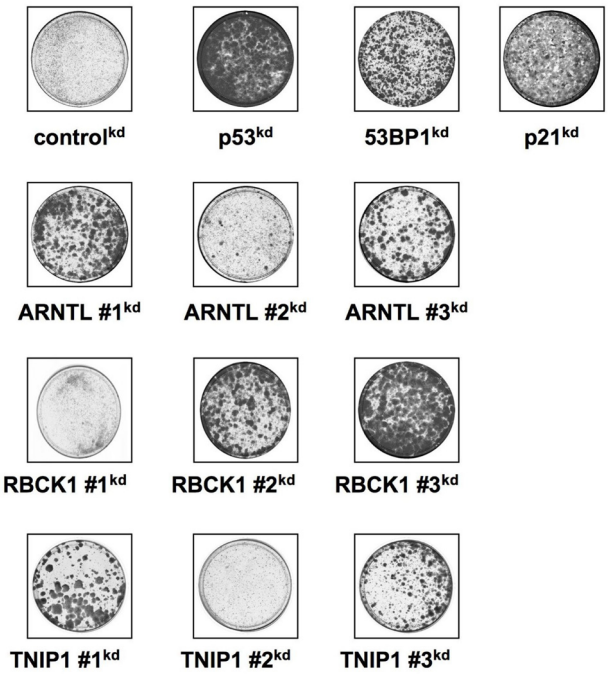


**Figure 2**
**Colony formation ARNTL, RBCK1 and TNIP1 shRNA vectors.**
*Cells were infected with shRNA vectors targeting ARNTL, RBCK1 and TNIP1 and control shRNA vectors targeting GFP, p53, 53BP1 and p21. Cells were infected at 32°C and shifted to 39°C 2 days after infection. After three weeks culture at 39°C, the cells were fixed and stained.*

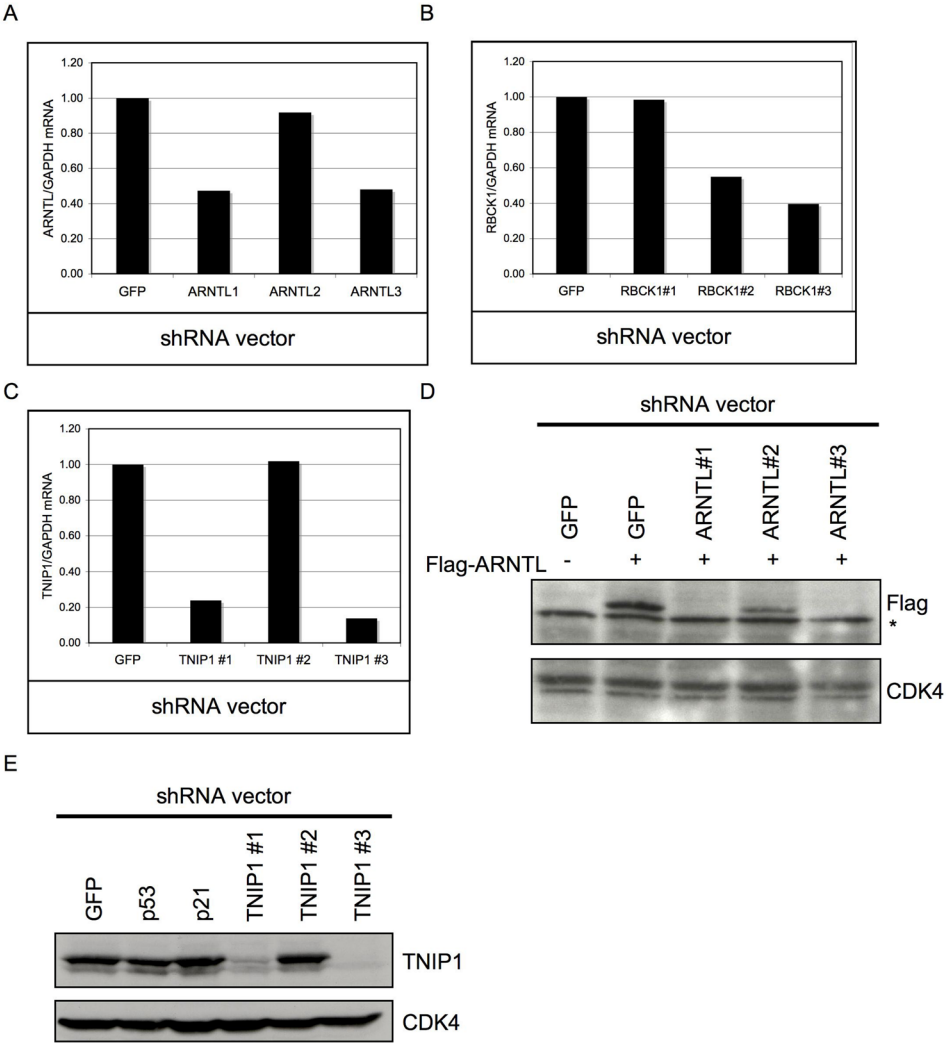


**Figure 3**

**Barcode identified shRNA vectors suppress protein and mRNA levels of their targets.**

- *a) QRT-PCR for ARNTL in BJtsLT cells. BJtsLT cells were infected with indicated shRNA vectors. Samples for RNA isolation were taken 8 days after shift to 39°C.*
- *b) QRT-PCR for RBCK1 in BJtsLT cells. BJtsLT cells were infected with indicated shRNA vectors. Samples for RNA isolation were taken 8 days after shift to 39°C.*
- *c) QRT-PCR for TNIP1 in BJtsLT cells. BJtsLT cells were infected with indicated shRNA vectors. Samples for RNA isolation were taken 8 days after shift to 39°C.*
- *d) Flag-ARNTL together with the shRNA vectors targeting ARNTL were transiently transfected in Phoenix cells. Extracts were immunoblotted using Flag and CDK4 (control) antibodies.*
- *e) BJ cells were infected with the indicated shRNA vectors and Extracts were immunoblotted using TNIP and CDK4 (control) antibodies.*

To show the sensitivity and selectivity of the shRNA barcode technique, we decided to test all three shRNA vectors targeting *ARNTL*, *RBCK1* and *TNIP1* that are present in the library. As mentioned before, for these three genes we found only two of the three shRNAs to be enriched in the screen, whereas one shRNA vector was not enriched. When we infected all three shRNA vectors independently into BJtsLT cells we found that only shRNAs enriched in the shRNA barcode screen gave rise to colonies (Figure 2).

***Knockdown of target genes by shRNA vectors***

Next, we investigated if the shRNA vectors targeting *ARNTL*, *TNIP1* and *RBCK1* also reduced mRNA levels of their cognate target genes. BJtsLT cells were infected at 32°C and shifted to 39°C 3 days after infection. When colonies appeared, RNA was isolated and subjected to quantification by QRT-PCR. The result from the QRT-PCR showed that enriched shRNA vectors targeting *ARNTL*, *RBCK1* and *TNIP1* were more potent in decreasing target mRNA than the shRNA vectors that were not enriched (Figure 3a, 3b, 3c). In addition, we tested for both ARNTL and TNIP1 if protein levels were also affected by the shRNA vectors. For ARNTL we co-expressed the three shRNA vectors together with a cDNA encoding hARNTL in Phoenix cells. From the western blot analysis it was clear that only the vectors that could produce colonies also induced potent knockdown of protein expression, thus linking gene knockdown to the p53 growth arrest bypass phenotype (Figure 3d). Knockdown of TNIP1 was determined by analyzing endogenous protein levels in BJtsLT cells (Figure 3e). As can be seen only the vectors that are enriched in the barcode screen and validated to enable colony growth at 39°C were able to reduce endogenous TNIP1 protein levels. We conclude that by limiting the hit selection to genes that are targeted by two independent shRNAs we have only selected 'on-target' hits from a complex library.

***Knockdown of ARNTL, RBCK1 and TNIP1 in BJtsLT cells leads to reduced p21$^{CIP1}$ levels***

p21$^{CIP1}$ is one of the critical effectors of p53 to induce a cell cycle arrest [23]. This is further supported by our identification of two shRNAs targeting *p21$^{CIP1}$* in the list of outliers of the BJtsLT screen. We therefore examined the effect of knockdown of *ARNTL*, *RBCK1* and *TNIP1* on *p21$^{CIP1}$* induction. We tested the effects on p21$^{CIP1}$ in the BJtsLT system that we used for the initial screen. When BJtsLT cells are shifted to 39°C, a rapid increase in p21$^{CIP1}$ protein levels is observed (Figure 4a). As expected, this p21$^{CIP1}$ induction is attenuated in cells infected with shRNA vectors targeting *p53*, *p21$^{CIP1}$* or *53BP1* (Figure 4a). When we used shRNA vectors targeting *ARNTL*, *RBCK1* and *TNIP1* we observed a decrease in p21$^{CIP1}$ levels for those shRNA vectors that produced colonies at 39°C, but not for shRNA vectors that failed to produce colonies (Figure 4a-c).

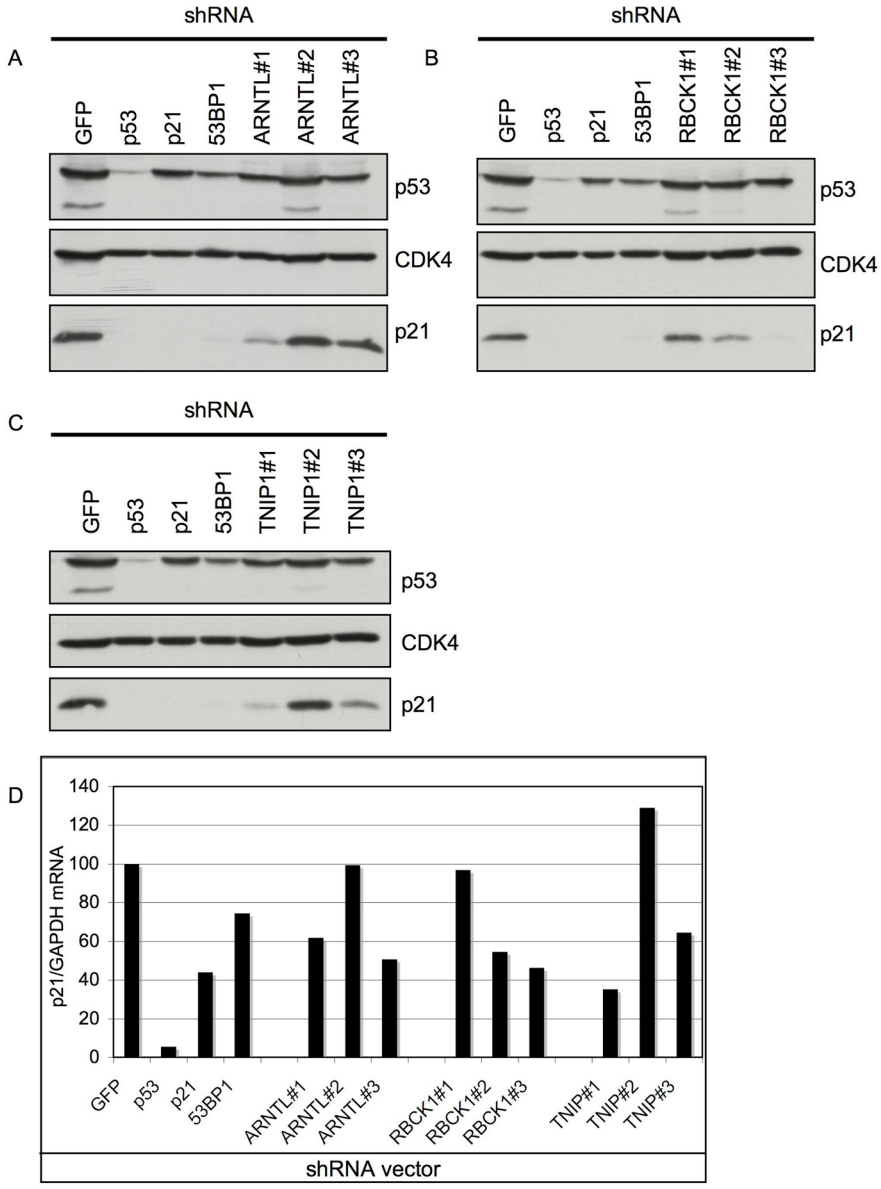


**Figure 4**

**Knockdown of ARNTL, TNIP1 and RBCK1 prevents $p21^{CIP1}$induction in BJtsLT cells**

*BJtsLT cells were infected at 32°C and shifted to 39°C for colony formation. After 14 days of culturing at 39°C cells were harvested, protein lysates were prepared and subjected to western blot for p53, CDK4 (control) and $p21^{CIP1}$ (Figure 4a-c). Additionally, total RNA was isolated and used for QRT-PCR for $p21^{CIP1}$ (Figure 4d).*

To be sure that the decrease in $p21^{CIP1}$ protein levels were caused by decreased $p21^{CIP1}$ transcription we also measured $p21^{CIP1}$ mRNA levels by QRT-PCR (Figure 4d). All shRNAs that could produce colonies at 39°C also showed a decrease in $p21^{CIP1}$ mRNA. This result suggests that the knockdown of ARNTL, RBCK1 and TNIP1 leads to a decreased transcriptional activity of p53 towards its target $p21^{CIP1}$. Recently multiple reports have discussed the relationship between cancer and circadian rhythm [24-26]. ARNTL is a core component of circadian rhythm transcriptional machinery [20,27]. ARNTL binds to CLOCK and together they regulate expression of 1,000s of genes in a circadian timing [28,29]. Genes regulated in a circadian fashion are involved in cell cycle, detoxification and other processes [30]. Therefore we decided to test if ARNTL is involved in the regulation of *$p21^{CIP1}$* expression in other cell systems.

### *Reduced $p21^{CIP1}$ activation after DNA damage in HCT116 cells with ARNTL knockdown*

Normal human cells arrest either in G1 or S phase of the cell cycle after encountering DNA damage to repair the DNA, thereby preventing accumulation of mutations in the genome of daughter cells. The G1 phase cell cycle arrest is p53 dependent and mainly executed by the CDK inhibitor $p21^{CIP1}$ [31,32].

To investigate if ARNTL is also required for the *$p21^{CIP1}$* activation after DNA damage, we infected U2OS osteosarcoma derived cells with different shRNAs targeting ARNTL. The cells were incubated to allow knockdown to take affect, after which cells were irradiated to inflict DNA damage and monitored for $p21^{CIP1}$ activation. When we compared cells that were infected with a shRNA vector targeting *p53* to cells infected with a control shRNA vector, we observed lower p53 and $p21^{CIP1}$ levels after γ-radiation. In the cells infected with *ARNTL* knockdown vectors we also observed lower $p21^{CIP1}$ protein levels, but p53 protein levels were unaffected (Figure 5a). This observation suggests that ARNTL can modulate the activity of p53 towards its target *$p21^{CIP1}$*. However, we cannot distinguish between a specific effect of ARNTL on *$p21^{CIP1}$* and a more general effect of ARNTL on p53 transcriptional activity.

### *ARNTL knockdown also allows bypass a $p19^{ARF}$ induced growth arrest*

As the BJtsLT cells are quite artificial due to the presence of the SV40 T viral oncogene, we also investigated if *ARNTL* knockdown could bypass a more physiological p53-induced cell cycle arrest. To address this, we used cells in which we can activate p53 by over-expression of *$p19^{ARF}$*. $p19^{ARF}$ inhibits MDM2 function thereby leading to an increase of p53 protein and activation of target genes [33]. Activation of *$p19^{ARF}$* leads to a stable p53-dependent cell cycle arrest [34]. To test if *ARNTL* knockdown can also rescue a $p19^{ARF}$-induced cell cycle arrest, we infected U2OS cells with the shRNAs targeting *ARNTL*. After knockdown had taken effect the cells were super-infected with a $p19^{ARF}$ encoding

retrovirus. We observed that cells with knockdown of *p53* or *p21$^{CIP1}$* continue proliferation after the forced expression of p19$^{ARF}$ (Figure 5b), knockdown of ARNTL also allows cells to proliferate after p53 activation by p19$^{ARF}$ (for knockdown see figure 5c). This result suggests that ARNTL expression is required for the anti-proliferative response of 19$^{ARF}$ activation. When ARNTL levels are low, the cells escape this arrest.

***p53 independent p21$^{CIP1}$ activation does not require ARNTL***

The results described above suggest a role for ARNTL in the regulation of p21$^{CIP1}$ expression by p53. However they do not rule out that ARNTL controls p21$^{CIP1}$ activation in a general fashion, independent of p53. To test this possibility we made use of small molecule HDAC inhibitors (HDACi). These HDACi cause induction of p21$^{CIP1}$ in both a p53 dependent and p53 independent manner [35-38]. In order to study the effect of ARNTL on p53 independent activation of p21$^{CIP1}$, we made use of a HCT116 p53 knockout cell-line (HCT116 p53-/- ) and the HDACi PXD101 (Belinostat®) [32]. When these HCT116 p53-/- cells are treated with PXD-101, a strong induction of p21$^{CIP1}$ is observed (Fig 5d and e). HCT116 p53-/- cells infected with a shRNA vector against p21$^{CIP1}$ show reduced p21$^{CIP1}$ protein levels after PXD-101 treatment. However, cells infected with a shRNA targeting ARNTL do not show any alteration in the induction of p21$^{CIP1}$ protein levels following HDACi treatment. Thus the p53-independent induction of p21$^{CIP1}$ by HDACi is not dependent on ARNTL. From this we conclude that ARNTL is not generally required for p21$^{CIP1}$ induction, but does affect the capacity of p53 to activate p21$^{CIP1}$ expression.

## Discussion

The screening of large-scale RNAi libraries has been used increasingly over the last years to identify the specific functions of genes in cellular pathways, networks and mechanisms. Here we describe the screening of a complex RNAi library to identify genes that were previously unknown to regulate a p53-dependent cell cycle arrest.

We have used the RNAi barcode technique to screen a human shRNA library containing ~24,000 vectors targeting ~8,000 genes. Using this approach, we were able to rapidly identify shRNAs that allow bypass of a p53 dependent cell cycle arrest. In total we confirmed that 32 out of the 37 genes that were identified by the barcode screen could indeed prevent cells from entering into a p53 dependent cell cycle arrest. However, only 5 of these 32 genes were targeted by two independent shRNAs. Two out of these five genes (*TP53BP1* and *p21$^{CIP1}$*) are well-known to be involved in p53 signaling. However the other three genes (*TNIP1*, *RBCK1* and *ARNTL*) were previously not known to be involved in the p53 pathway.

The three newly identified genes all affect the induction of the p53 target gene *p21$^{CIP1}$* but no change in p53 protein stability is observed after ARNTL, TNIP1 or RBCK1 knockdown. Importantly, *p21$^{CIP1}$* knockdown alone is sufficient to rescue cells from the p53 induced cell cycle arrest. This observation indicates that the rescue of the p53 induced cell cycle arrest by ARNTL, RBCK1 or TNIP1 knockdown is the result of a lack of p21$^{CIP1}$ induction by p53.

The activity of p53 has been mainly attributed to its role as transcription factor with tumor suppressive capacities. Therefore, we assessed if any of the genes identified in our screen had been linked to transcription before. TNIP1 was originally identified as an inhibitor of NF-κB signaling [22,39]. Although it was shown that TNIP1 over-expression inhibits the transcriptional activity of the NF-κB heterodimer it is believed that this is an indirect effect through an currently unknown mechanism. The ubiquitin E3 ligase RBCK1 has been reported to regulate and ubiquitinate several proteins [21,40-42]. Although experiments have been performed that suggest a role for RBCK1 in transcription [43] a clear role for RBCK1 in regulating transcription has not been reported up till now. This picture is different for ARNTL which is known to be the central transcription factor in regulating circadian rhythm. The critical role of ARTNL in circadian rhythm was demonstrated by the construction of the knockout mouse. Mice that are deficient for *ARNTL* are unable to maintain a circadian rhythm in constant darkness [20]. In addition, the *ARNTL* knockout mouse also suffers from premature aging [44]. In recent years, many other processes have been shown to be regulated in a circadian fashion. Most importantly it was shown that the mammalian cell cycle is controlled by circadian rhythm [45]. The possible involvement of circadian rhythm in cancer results from studies of the Period 2 knockout mouse.This mouse is prone to develop tumors after radiation. Later it was shown that also the Period 1 protein can regulate cell cycle checkpoints [24-26]. Interestingly both Period 1 and 2 are bona-fide transcriptional targets of ARNTL.

For the induction of target genes ARNTL must form a heterodimer with the CLOCK protein [28]. Target genes of the CLOCK/ARNTL heterodimer include the *Period 1, 2* and *3* and Cryptochromes (*Cry 1 & 2*) [46]. The increased abundance of Period and Cryptochrome proteins [47] induces a negative feedback loop that ultimately shuts down transcription by the CLOCK/ARTNL heterodimer. When the concentration of Period and Cryptochrome decreases due to proteasomal degradation the CLOCK/ARNTL complex can initiate another round of transcription thereby completing a cycle of circadian rhythm.
Another transcriptional target of the CLOCK/ARNTL is the CDK inhibitor *p21$^{CIP1}$* which is also regulated in a circadian manner [48]. We show here that *ARNTL* knockdown in

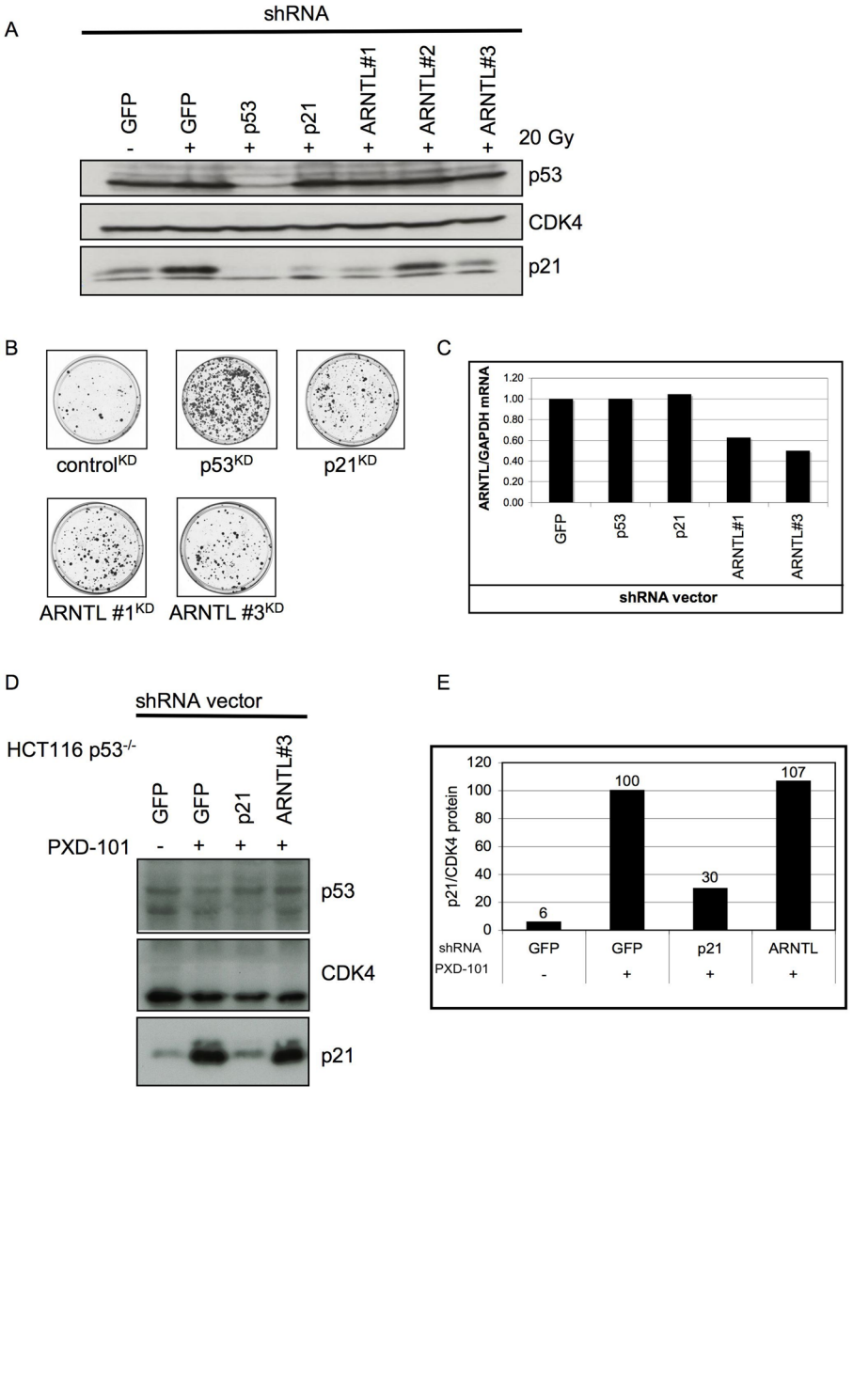
A
shRNA
GFP
- GFP
+ p53
+ p21
+ ARNTL#1
+ ARNTL#2
+ ARNTL#3
20 Gy
p53
CDK4
p21
B
control^KD
p53^KD
p21^KD
ARNTL #1^KD
ARNTL #3^KD
C
ARNTL/GAPDH mRNA
1.20
1.00
0.80
0.60
0.40
0.20
0.00
GFP
p53
p21
ARNTL#1
ARNTL#3
shRNA vector
D
shRNA vector
HCT116 p53-/-
GFP
GFP
p21
ARNTL#3
PXD-101 - + + +
p53
CDK4
p21
E
p21/CDK4 protein
120
100
80
60
40
20
0
6
100
30
107
shRNA GFP GFP p21 ARNTL
PXD-101 - + + +

human cells can abrogate induction of *p21$^{CIP1}$* after p53 activation and overrides a p53-dependent cell cycle arrest. The effect on the induction of *p21$^{CIP1}$* is in contrast with previous reports on the p21$^{CIP1}$ regulation in *ARNTL* knockout mice [48]. In these animals ARNTL is required for the circadian expression of p21$^{CIP1}$. This discrepancy might be explained by differential regulation of the p21$^{CIP1}$ promoter in mice or man. In particular, this difference may arise from stress signals differences from *in vitro* versus *in vivo* conditions. Nevertheless, our data clearly indicate that there is a link between the regulation of circadian rhythm and the control of p53 activity in human cells.

## Conclusions

By screening a large scale RNAi library in human cells we have identified three novel genes that can regulate p53 function. Loss of expression for each of three genes results in a decreased ability of p53 to activate *p21$^{CIP1}$* expression. Importantly, we showed that ARNTL is required for the p53-dependent induction of *p21$^{CIP1}$* in two additional cell types using different ways to activate p53: a p19$^{ARF}$-induced cell cycle arrest and a DNA damage mediated cell cycle arrest. We conclude that ARNTL suppression affects the ability of p53 to induce a cell cycle arrest upon cellular stress signals such as DNA damage.

**Figure 5**
**ARNTL regulates p21$^{CIP1}$ expression.**

a) *Knockdown of ARNTL inhibits radiation induced p21$^{CIP1}$ induction. U2OS cells were infected with the shRNA vectors as indicated. Cells were seeded and irradiated with 20 Gy of γ-radiation. After o/n incubation cells were lysed and lysates were subjected to western blot using antibodies for p53, CDK4 (control) and p21$^{CIP1}$.*

b) *Knockdown of ARNTL can also rescue a p19-induced cell cycle arrest. U2OS cells were infected with the indicated shRNA vectors followed by a super-infection with p19$^{ARF}$-RFP virus. Cells were seeded and incubated for three weeks. After three weeks the infected cells were fixed and stained.*

c) *Knockdown of ARNTL in U2OS cells (Fig 5b) was quantified by QRT-PCR.*

d) *ARNTL knockdown is not involved in p53 independent p21$^{CIP1}$ induction. HCT116 wt and p53-/- cells were infected with knockdown vectors targeting p53, p21$^{CIP1}$ and ARNTL. Cells were treated with 0.5 μM PXD101 for 16 hrs. Cells were then lysed and lysates were subjected to western analysis for p53, CDK4 (control) and p21$^{CIP1}$.*

e) *Quantification of p21 protein levels in the western blot in figure 5c using IMAGE J software.*

## Materials & methods

***Cell lines & culture conditions***
BJtsLT cells were cultured in medium that consisted of DMEM 75% / M199 25% supplemented with 10% FCS, Penicillin and Glutamine. BJtsLT cells were cultured at 32°C in 5% CO2. U2OS and Phoenix cells were cultured in DMEM supplemented with 10% FCS, Penicillin and Glutamine. U2OS and Phoenix cells were cultured at 37°C in 5% CO2.

***Plasmids and library***
Expression plasmid for ARNTL was generated by PCR from a cDNA library and subsequent cloning the PCR product into pCR3-Flag. The P19-RFP construct was described previously [11]. The construction of the library was described previously [11]. Briefly, the NKI shRNA library was designed to target 7914 human genes, using three shRNA vectors for every targeted gene, cumulating in a total of 23,742 shRNA vectors. The shRNAs are cloned into a retro-viral vector to enable infection of target cells.

***Retroviral infection***
Phoenix cells were transfected using calcium phosphate method. Viral supernatant was cleared through a 0.45 µM filter. Cells were infected with the viral supernatant in presence of polybrene (8 µg/ml). The infection was repeated twice.

***shRNA barcode screen***
To screen the NKI shRNA library we reasoned that we would need 100 fold coverage of the library to get a good representation of all 23,742 shRNA vectors present in the library. BJtsLT cells were infected with the NKI shRNA library. Two days after infection cells were plated at 150,000 cells/15 cm dish. In total 2 x 106 cells were shifted to 39°C, equal number of cells were kept at 32°C. Cells at 32°C were harvested after 5 days. Cells at 39°C were harvested at 21 days after shift. From both populations gDNA was isolated using DNAzol (Invitrogen). The shRNA cassettes were amplified by PCR. The PCR product was used for *in vitro* RNA synthesis. RNA was labeled with Cy3 or Cy5 (Kreatech) and hybridized on a microarray. Quantification of the resulting fluorescent images was performed with Imagene 5.6 (BioDiscovery), local background was subtracted, and the data were normalized and 2log transformed. Additional information on barcode screens can be found at http://www.screeninc.nl.

***Colony formation assay***
Cells were infected with retroviral supernatant. Two days after infection the cells were seeded at 50,000/10 cm dish and shifted to 39°C. Cells were cultured at 39°C for approx 21 days. When colonies appeared cells were fixed in MeOH/HAc (3:1) and subsequently stained (50% MeOH/10% HAc/0.1% Coomassie).

***Western blotting***
Cell lysates were separated using 10% SDS-PAAGE. Proteins were transferred to PVDF membrane and incubated with primary antibody as indicated. Primary antibodies were

detected using a secondary HRP-conjugated antibody. Antibodies used for these studies: Flag (M2; Sigma), TNIP1 (1A11E3; Zymed), CDK4 (C-22; Santa Cruz), p53 (DO-1; Santa Cruz) and p21CIP1 (C-19; Santa Cruz).

### *QRT-PCR*

Total RNA was isolated using TRIzol (Invitrogen). From the total RNA cDNA was generated using Superscript II (Invitrogen) using random primers (Invitrogen). cDNA was diluted and QRT reaction was performed using Taqman probes (Applied Biosystems). All QRT reactions were run in parallel for GAPDH to control of for input cDNA. The QRT reactions were run at a AB7500 Fast Real Time PCR system (Applied Biosystems). Results shown are a representative of three independent experiments.

### *$p21^{CIP1}$ induction by γ-radiation and PXD101*

For the $p21^{CIP1}$ induction by radiation 50,000 cells were seeded per 6-well. HCT116 p53-/- cells were irradiated with 20 Gy γ-radiation from a Cs-137 source. Cells were incubated for 16 hrs and lysed. For the $p21^{CIP1}$ induction by PXD101 50,000 cells were seeded/6-well and treated with 0.5 μM PXD101 for 16 hrs after which the cells were lysed and protein lysates were subjected to western analysis.

## References


[1] Vousden KH, Lane DP (2007) p53 in health and disease. Nat Rev Mol Cell Biol 8: 275-283.

[2] Toledo F, Wahl GM (2006) Regulating the p53 pathway: in vitro hypotheses, in vivo veritas. Nat Rev Cancer 6: 909-923.

[3] Chuikov S, Kurash JK, Wilson JR, Xiao B, Justin N et al. (2004) Regulation of p53 activity through lysine methylation. Nature 432: 353-360.

[4] Brooks CL, Gu W (2006) p53 ubiquitination: Mdm2 and beyond. Mol Cell 21: 307-315.

[5] Brooks CL, Gu W (2003) Ubiquitination, phosphorylation and acetylation: the molecular basis for p53 regulation. Curr Opin Cell Biol 15: 164-171.

[6] Gu W, Roeder RG (1997) Activation of p53 sequence-specific DNA binding by acetylation of the p53 C-terminal domain. Cell 90: 595-606.

[7] Momand J, Zambetti GP, Olson DC, George D, Levine AJ (1992) The mdm-2 oncogene product forms a complex with the p53 protein and inhibits p53-mediated transactivation. Cell 69: 1237-1245.

[8] Riley T, Sontag E, Chen P, Levine A (2008) Transcriptional control of human p53-regulated genes. Nat Rev Mol Cell Biol 9: 402-412.

[9] http://www-p53.iarc.fr/ IARC p53 Database.

[10] Oliner JD, Kinzler KW, Meltzer PS, George DL, Vogelstein B (1992) Amplification of a gene encoding a p53-associated protein in human sarcomas. Nature 358: 80-83.

[11] Berns K, Hijmans EM, Mullenders J, Brummelkamp TR, Velds A et al. (2004) A large-scale RNAi screen in human cells identifies new components of the p53 pathway. Nature 428: 431-437.

[12] Berns K, Horlings HM, Hennessy BT, Madiredjo M, Hijmans EM et al. (2007) A functional genetic approach identifies the PI3K pathway as a major determinant of trastuzumab resistance in breast cancer. Cancer Cell 12: 395-402.

[13] Brummelkamp TR, Fabius AW, Mullenders J, Madiredjo M, Velds A et al. (2006) An shRNA barcode screen provides insight into cancer cell

vulnerability to MDM2 inhibitors. Nat Chem Biol 2: 202-206.

[14] Bernards R, Brummelkamp TR, Beijersbergen RL (2006) shRNA libraries and their use in cancer genetics. Nat Methods 3: 701-706.

[15] Ngo VN, Davis RE, Lamy L, Yu X, Zhao H et al. (2006) A loss-of-function RNA interference screen for molecular targets in cancer. Nature 441: 106-110.

[16] Silva JM, Marran K, Parker JS, Silva J, Golding M et al. (2008) Profiling essential genes in human mammary cells by multiplex RNAi screening. Science 319: 617-620.

[17] Schlabach MR, Luo J, Solimini NL, Hu G, Xu Q et al. (2008) Cancer proliferation gene discovery through functional genomics. Science 319: 620-624.

[18] Birmingham A, Anderson EM, Reynolds A, Ilsley-Tyree D, Leake D et al. (2006) 3' UTR seed matches, but not overall identity, are associated with RNAi off-targets. Nat Methods 3: 199-204.

[19] Echeverri CJ, Beachy PA, Baum B, Boutros M, Buchholz F et al. (2006) Minimizing the risk of reporting false positives in large-scale RNAi screens. Nat Methods 3: 777-779.

[20] Bunger MK, Wilsbacher LD, Moran SM, Clendenin C, Radcliffe LA et al. (2000) Mop3 is an essential component of the master circadian pacemaker in mammals. Cell 103: 1009-1017.

[21] Yamanaka K, Ishikawa H, Megumi Y, Tokunaga F, Kanie M et al. (2003) Identification of the ubiquitin-protein ligase that recognizes oxidized IRP2. Nat Cell Biol 5: 336-340.

[22] Heyninck K, De Valck D, Vanden Berghe W, Van Criekinge W, Contreras R et al. (1999) The zinc finger protein A20 inhibits TNF-induced NF-kappaB-dependent gene expression by interfering with an RIP- or TRAF2-mediated transactivation signal and directly binds to a novel NF-kappaB-inhibiting protein ABIN. J Cell Biol 145: 1471-1482.

[23] el-Deiry WS, Tokino T, Velculescu VE, Levy DB, Parsons R et al. (1993) WAF1, a potential mediator of p53 tumor suppression. Cell 75: 817-825.

[24] Fu L, Pelicano H, Liu J, Huang P, Lee C (2002) The circadian gene Period2 plays an important role in tumor suppression and DNA damage response in vivo. Cell 111: 41-50.

[25] Fu L, Lee CC (2003) The circadian clock: pacemaker and tumour suppressor. Nat Rev Cancer 3: 350-361.

[26] Gery S, Komatsu N, Baldjyan L, Yu A, Koo D et al. (2006) The circadian gene per1 plays an important role in cell growth and DNA damage control in human cancer cells. Mol Cell 22: 375-382.

[27] Panda S, Hogenesch JB, Kay SA (2002) Circadian rhythms from flies to human. Nature 417: 329-335.

[28] Gekakis N, Staknis D, Nguyen HB, Davis FC, Wilsbacher LD et al. (1998) Role of the CLOCK protein in the mammalian circadian mechanism. Science 280: 1564-1569.

[29] Lowrey PL, Takahashi JS (2004) Mammalian circadian biology: elucidating genome-wide levels of temporal organization. Annu Rev Genomics Hum Genet 5: 407-441.

[30] Panda S, Antoch MP, Miller BH, Su AI, Schook AB et al. (2002) Coordinated transcription of key pathways in the mouse by the circadian clock. Cell 109: 307-320.

[31] Deng C, Zhang P, Harper JW, Elledge SJ, Leder P (1995) Mice lacking p21CIP1/WAF1 undergo normal development, but are defective in G1 checkpoint control. Cell 82: 675-684.

[32] Bunz F, Dutriaux A, Lengauer C, Waldman T, Zhou S et al. (1998) Requirement for p53 and p21 to sustain G2 arrest after DNA damage. Science 282: 1497-1501.

[33] Sherr CJ (2006) Divorcing ARF and p53: an unsettled case. Nat Rev Cancer 6: 663-673.

[34] Pomerantz J, Schreiber-Agus N, Liegeois NJ, Silverman A, Alland L et al. (1998) The Ink4a tumor suppressor gene product, p19Arf, interacts with MDM2 and neutralizes MDM2's inhibition of p53. Cell 92: 713-723.

[35] Qian X, Ara G, Mills E, LaRochelle WJ, Lichenstein HS et al. (2008) Activity of the histone deacetylase inhibitor belinostat (PXD101) in preclinical models of prostate cancer. Int J Cancer 122: 1400-1410.

[36] Ocker M, Schneider-Stock R (2007)

Histone deacetylase inhibitors: signalling towards p21cip1/waf1. Int J Biochem Cell Biol 39: 1367-1374.

[37] Lagger G, Doetzlhofer A, Schuettengruber B, Haidweger E, Simboeck E et al. (2003) The tumor suppressor p53 and histone deacetylase 1 are antagonistic regulators of the cyclin-dependent kinase inhibitor p21/WAF1/CIP1 gene. Mol Cell Biol 23: 2669-2679.

[38] Gartel AL, Ye X, Goufman E, Shianov P, Hay N et al. (2001) Myc represses the p21(WAF1/CIP1) promoter and interacts with Sp1/Sp3. Proc Natl Acad Sci U S A 98: 4510-4515.

[39] Heyninck K, Kreike MM, Beyaert R (2003) Structure-function analysis of the A20-binding inhibitor of NF-kappa B activation, ABIN-1. FEBS Lett 536: 135-140.

[40] Bayle J, Lopez S, Iwai K, Dubreuil P, De Sepulveda P (2006) The E3 ubiquitin ligase HOIL-1 induces the polyubiquitination and degradation of SOCS6 associated proteins. FEBS Lett 580: 2609-2614.

[41] Kirisako T, Kamei K, Murata S, Kato M, Fukumoto H et al. (2006) A ubiquitin ligase complex assembles linear polyubiquitin chains. Embo J 25: 4877-4887.

[42] Tian Y, Zhang Y, Zhong B, Wang YY, Diao FC et al. (2007) RBCK1 negatively regulates tumor necrosis factor- and interleukin-1-triggered NF-kappaB activation by targeting TAB2/3 for degradation. J Biol Chem 282: 16776-16782.

[43] Tatematsu K, Yoshimoto N, Koyanagi T, Tokunaga C, Tachibana T et al. (2005) Nuclear-cytoplasmic shuttling of a RING-IBR protein RBCK1 and its functional interaction with nuclear body proteins. J Biol Chem 280: 22937-22944.

[44] Kondratov RV, Kondratova AA, Gorbacheva VY, Vykhovanets OV, Antoch MP (2006) Early aging and age-related pathologies in mice deficient in BMAL1, the core componentof the circadian clock. Genes Dev 20: 1868-1873.

[45] Matsuo T, Yamaguchi S, Mitsui S, Emi A, Shimoda F et al. (2003) Control mechanism of the circadian clock for timing of cell division in vivo. Science 302: 255-259.

[46] Shearman LP, Sriram S, Weaver DR, Maywood ES, Chaves I et al. (2000) Interacting molecular loops in the mammalian circadian clock. Science 288: 1013-1019.

[47] Young MW, Kay SA (2001) Time zones: a comparative genetics of circadian clocks. Nat Rev Genet 2: 702-715.

[48] Grechez-Cassiau A, Rayet B, Guillaumond F, Teboul M, Delaunay F (2008) The circadian clock component BMAL1 is a critical regulator of p21WAF1/CIP1 expression and hepatocyte proliferation. J Biol Chem 283: 4535-4542.

**Author contributions**

JM and AWMF performed the experiments, wrote the manuscript. MM performed the microarray hybridizations. RB and RLB supervised the research and corrected the manuscript.

**Acknowledgements**

We thank K Berns and EM Heijmans for the BJtsLT cells. In addition, we thank all members of the Beijersbergen and Bernards labs for helpful discussions.

# CHAPTER V

# Candidate biomarkers of response to an experimental cancer drug identified through a large-scale RNA interference screen

Accepted for publication by *Clinical Cancer Research*

# Candidate biomarkers of response to an experimental cancer drug identified through a large-scale RNA interference genetic screen.

Jasper Mullenders[1], Wolfgang von der Saal[2], Miranda MW. van Dongen[1], Ulrike Reiff[2], Rogier van Willigen[1], Roderick L. Beijersbergen[1], Georg Tiefenthaler[2], Christian Klein[2, 3] and René Bernards[1, 3]

1. Division of Molecular Carcinogenesis, Center for Biomedical Genetics and Cancer Genomics Center, The Netherlands Cancer Institute, Plesmanlaan 121, 1066 CX Amsterdam, The Netherlands; 2. Pharma Research, Roche Diagnostics GmbH, Nonnenwald 2, 82372 Penzberg, Germany;
3. Corresponding authors

**Purpose:** A major impediment in the optimal selection of cancer patients for the most effective therapy is the lack of suitable biomarkers that foretell the patient's response to a given drug. In the present study, we have used large-scale RNA interference-based genetic screens to find candidate biomarkers of resistance to a new acyl sulfonamide derivative, R3200. This compound inhibits proliferation of tumor cells in vitro and in vivo, but its mechanism of action is unknown.

**Experimental Design:** We used a large scale RNA interference genetic screen to identify modulators of the efficacy of R3200. We searched for genes whose suppression in an in vitro cell system can cause resistance to the anti-cancer effects of R3200.

**Results:** We report here that knockdown of either RBX1 or DDB1 causes resistance to the anti cancer effects of R3200, raising the possibility that these two genes may have utility as biomarkers of response to this drug in a clinical setting. Interestingly, both RBX1 and DDB1 are part of an E3 ubiquitin ligase complex.

**Conclusions:** We propose that suppression of the activity of a RBX1 and DDB1-containing E3 ligase complex leads to the stabilization of certain proteins, whose increased abundance is in turn responsible for resistance to R3200. Moreover, our data suggest that RBX1 and DDB1 can potentially be developed into biomarkers of resistance to acyl sulfonamide-based cancer drugs. This will require clinical validation in a series of patients treated with R3200.

## Introduction

Effective cancer therapy has been hampered by the absence of drugs that selectively target cancer cells. The identification and characterization of new compounds that potentially specifically kill cancer cells is therefore of major interest. Recently a new class of compounds was shown to be effective in inhibiting growth of cancer cells *in vitro* and *in vivo*: the acyl sulfonamides [1-4]. However, the efficacy of these acyl sulfonamides varies greatly, depending on the cell models used. This is in line with clinical observations that patients with comparable diagnosis can often respond very differently to the same treatment. Knowledge of whether a patient will respond to a drug is obviously of major importance for the selection of the most appropriate therapy for the individual patient. Responses to some drugs can be predicted using biomarkers [5, 6]. Identifying such biomarkers is not a trivial process and it would be greatly facilitated when the mechanism of action of the drug is well-understood.

Many different approaches can be taken to establish the mode of action of a drug and to identify drug response biomarkers. Recently, RNA interference (RNAi)-based genetic screens have demonstrated utility in the identification of drug response biomarkers [7-9]. RNAi screens can be performed in several different ways [10]. Single-well siRNA screens often make use of synthetic siRNAs. This usually requires complex automation, executed in high throughput. Due to the short half life of siRNAs, this approach does not allow the selection of phenotypes in long-term assays. These drawbacks can be bypassed by using short hairpin RNAs (shRNA) to mediate stable gene knockdown. shRNA screening is efficient and requires minimal automation. Because shRNA screening makes use of retroviral shRNA vectors, both long- and short-term assays can be used for screening.

We have developed an shRNA library and have used this library to show that loss of PTEN confers resistance of *HER2*-amplified breast cancer cells to treatment with trastuzumab [9]. This observation suggested that the PI3K pathway, which is negatively regulated by PTEN, is a major determinant of trastuzumab efficacy, a notion that was validated in clinical samples from breast cancer patients treated with trastuzumab [9]. This observation shows that *in vitro* RNAi screens can yield biomarkers having clinical utility. Moreover, this information can then also be used to develop new drugs that target the pathways that cause drug resistance.

In this current approach we describe the anti cancer effects of a new acyl sulfonamide derivative, R3200. We show that this compound can actively block proliferation of tumor cells *in vitro* and *in vivo*. We describe here biochemical and genetic approaches to identify the molecular target(s) and potential biomarkers that predict responsiveness to this compound.

## Results

### *In vitro analysis of anti-proliferative effects of R3200*

It was shown previously that acyl sulfonamides have prominent anti proliferative effects in cancer cell lines [1-4]. We have synthesized a novel acyl sulfonamide, R3200 (Fig. 1A). To assess if R3200 can inhibit proliferation in cell lines derived from human cancers, we used 29 cell lines to determine the IC50 (Table S1). Included in this panel were cell lines generated from breast, colon, prostate and pancreas tumors. Fetal Calf Serum (FCS) can significantly modulate the response to drug treatment of cells *in vitro* due to binding of acyl sulfonamides to (bovine) serum albumine. Therefore, we determined the $IC_{50}$ value both in cells cultured in regular conditions (10% FCS) and low concentration of FCS (2.5%). In both conditions

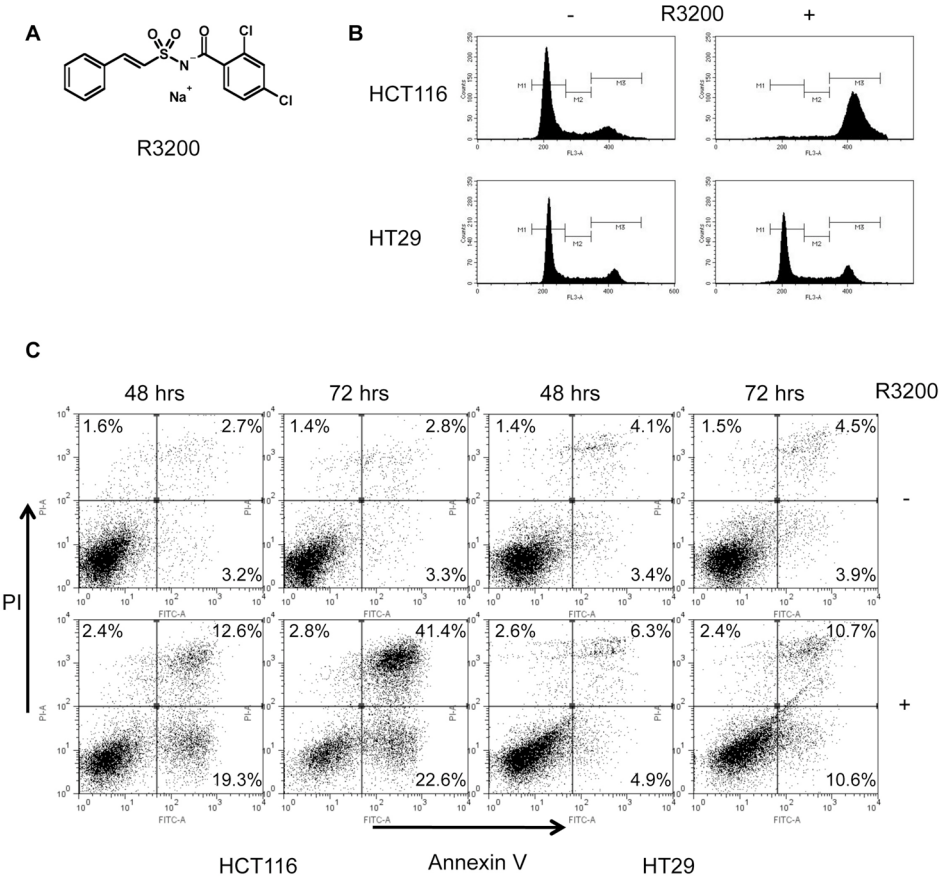


**Figure 1**

**In vitro analysis of R3200 anti-proliferative actions**.

*Cell cycle analysis of HCT116 and HT-29 cells treated with 30 μM R3200 (a) for 48 hrs. Cells were stained with PI and analyzed by FACS (b). Induction of apoptosis by R3200. FACS analysis of HCT116 and HT-29 cells treated with R3200 (30 μM) for 48 or 72 hrs. Cells were stained with Annexin V and PI (c).*

we observed a wide range of responses, which translated in $IC_{50}$ values ranging from 2.3 μM to > 100 μM in assays in medium with 2.5% FCS and 10.4 μM to > 100 μM in assays in medium with 10% FCS. For further *in vitro* studies we decided to use two colon cancer derived cell lines, a very sensitive cell line: HCT116 (IC50 = 4.9 μM in 2.5% FCS) and a relative resistant cell line HT-29 (IC50 = 71.6 μM in 2.5% FCS).

### *The anti-proliferative activity of the acyl sulfonamide R3200 is due to a cell cycle arrest followed by apoptosis*

The anti-proliferative effects described above, could be caused by various effects of the drug, most notably apoptosis and cell cycle arrest. To address these issues, a cell cycle analysis was performed following treatment of cells with R3200. When HCT116 cells were exposed to 30 μM R3200 for 48 hours, we observed an increase in the G2/M cell cycle phase (Fig. 1B). Quantification of the results from cell cycle profile show that more than 80% of the HCT116 cells have accumulated in the G2/M phase of the cell cycle (Supplementary Figure S1). The FACS profile obtained from the HCT116 cells suggests that the cells have arrested either in the G2- or M-phase of the cell cycle, we cannot exclude that the cells have undergone endo-reduplication of their genome and are arrested in the G1 phase of the next cell cycle with 4n DNA content. In the resistant HT-29 cell-line no cell cycle arrest was detected after treatment with R3200 (Fig. 1B) as expected.

### *R3200 induces apoptosis in human cancer cell lines*

Many anti cancer drugs induce a cell cycle arrest in short term assays, but can also induces apoptosis after prolonged drug exposure. We subjected HCT116 and HT-29 cells to R3200 for 48 and 72 hours and stained the cells with annexin V/PI to identify dead cells. Maximal effect was observed in HCT116 cells after 72 hrs of R3200 treatment (Fig. 1C). The amount of cells that was killed by the R3200 treatment was 64%. In HT-29 cells only a mild cell death was observed after 72 hours of treatment. The IC50 of apoptosis induction in HCT116 cells determined after 72 hours of drug exposure was 35 μM, while for HT-29 cells no IC50 could be determined.

### *Inhibitory activity in a drug-resistant cell line: Influence of P-glycoprotein*

Many drugs have limited efficacy because they are substrates for P-glycoprotein (P-gp) drug

| | P388 IC50 (μM) | P388/ADR IC50 (μM) | Difference n-fold |
|---|---|---|---|
| R3200 | 27.60 | 31.70 | 1.10 |
| Taxol | 0.08 | 4.40 | 55.00 |
| Etoposide | 0.14 | > 10 | > 71 |
| Cisplatin | 12.10 | 46.20 | 3.80 |
| Nocodazol | 0.01 | 0.03 | 2.80 |

**Table 1**
**R3200 is not a substrate for P-gp drug transporters.** *Table lists IC50 values for wt P388 and P-gp over expressing P388/ADR cells (as indicated) treated with R3200.*

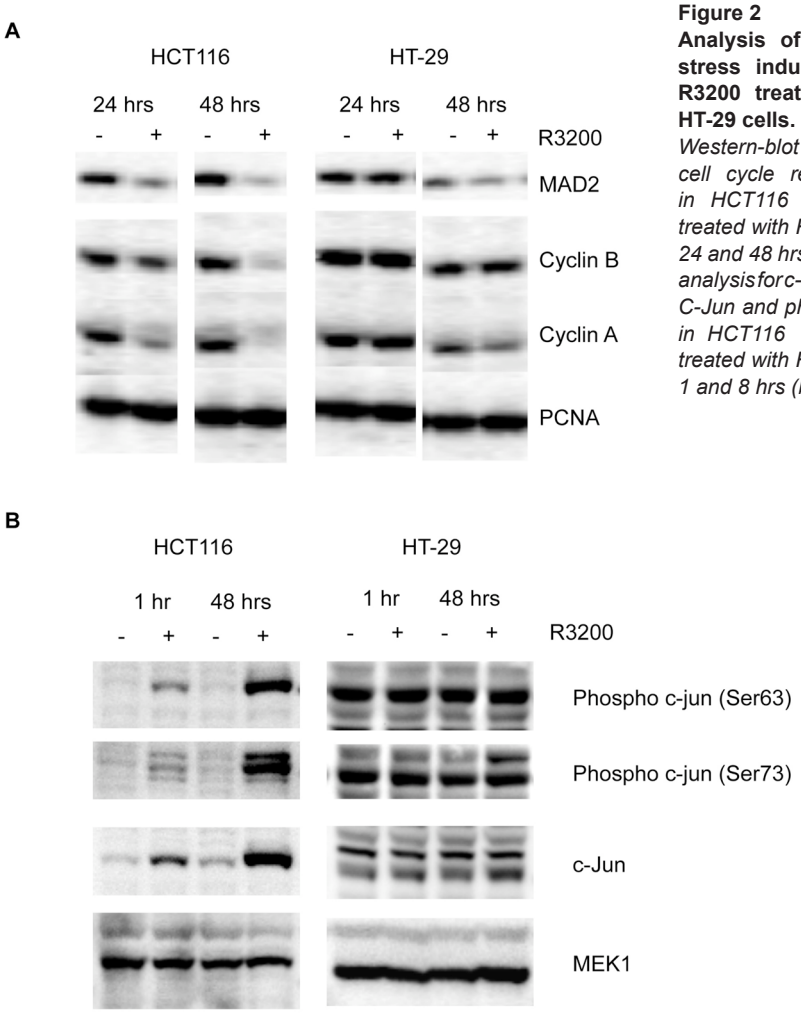


**Figure 2**
**Analysis of cell cycle and stress induced proteins in R3200 treated HCT116 and HT-29 cells.**
*Western-blot analysis for cell cycle regulated proteins in HCT116 and HT-29 cells treated with R3200 (30 μM) for 24 and 48 hrs (a). Western-blot analysis for c-Jun, phospho-S63 C-Jun and phospho-S73 c-Jun in HCT116 and HT-29 cells treated with R3200 (30 μM) for 1 and 8 hrs (b).*

resistance pumps [11, 12]. We therefore tested if R3200 is a substrate of P-gp ABC transporters. A mouse leukemia cell line P388 (parental, non/low expression of P-gp) and a derivative P388/ADR over-expressing the multidrug drug resistance pump P-gp encoded by the *ABCB1* gene were used to examine the influence of compounds on cell viability and proliferation. In these cells we determined the $IC_{50}$ for R3200, taxol, etoposide, nocodazole and cisplatin. In contrast to taxol and etoposide, which are P-gp substrates, R3200 showed nearly no difference in cell viability in both cell lines (Table 1). This suggests that R3200 is not transported by this P-gp drug pump.

### *R3200-induced changes in cell cycle proteins*

Next we tested if the observed G2/M cell cycle arrest was also

accompanied by altered levels of cell cycle regulated proteins. We treated HT-29 and HCT116 cells with R3200 (30 µM) for 24 and 48 hours and after lysis of the cells we detected the protein levels of cell cycle regulators by western blot analysis (Fig. 2A). In HCT116, but not in HT-29 cells, we observed a decrease in protein levels of Cyclin A, B and MAD2. This indicates that HCT116 cells are indeed inhibited in their proliferation while HT-29 cells are unaffected by R3200 treatment.

To investigate if R3200 treatment activates cellular stress response pathways we measured c-Jun activation. We treated HCT116 cells with R3200 (30 µM) for 1 and 8 hours. At both time points a clear induction of c-Jun protein was observed (Fig. 2B). A similar increase in levels of

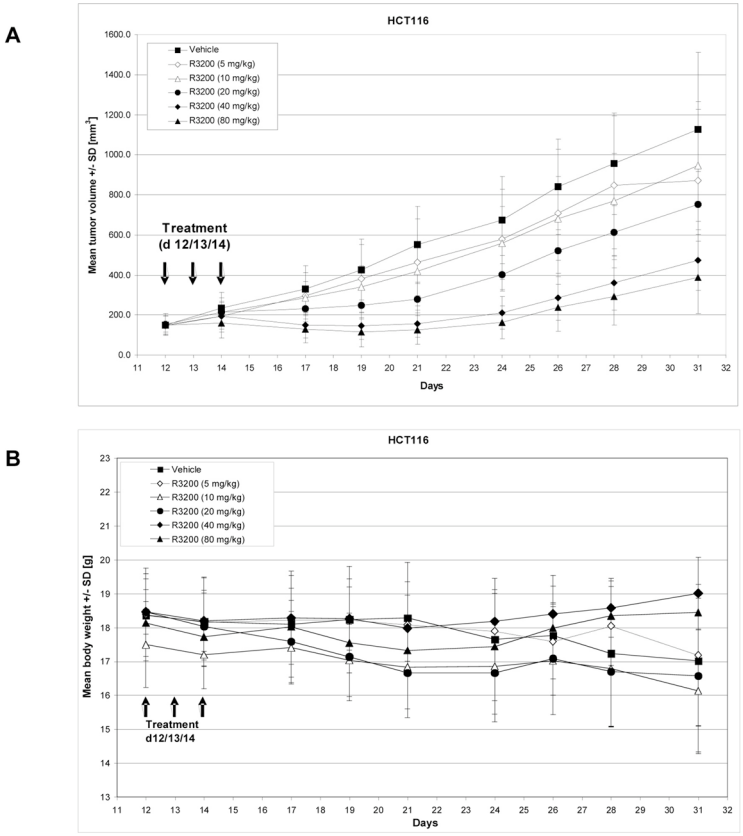


**Figure 3**

**In vivo analysis of R3200 anti-proliferative actions towards human cancer cells.**

*A, xenograft of HCT116 cells in SCID beige mice. Tumor growth was measured as an increase of tumor volume (Y-axis) in time (X-axis). Injections with R3200 (black arrows). B, Body weight monitoring during R3200 treatment. Body weight was measured (Y-axis) over time (X-axis). Injections with R3200 (black arrows) are indicated on the X-axis.*

phospho-c-Jun (pS63 and pS73) was seen, suggesting that c-Jun protein levels are induced rather than specific phosphorylation of the protein. This indicates that stress response pathways are activated by prolonged treatment of R3200 and this may explain some of the effects on cell cycle proteins seen after longer exposure to drug. In the HT-29 cells we did not observed any effect of R3200 on c-Jun or phospho-c-Jun protein levels (Fig. 2B).

***In vivo anti-proliferative effects of R3200***

To test whether the *in vitro* properties of R3200 translate into inhibition of tumor growth *in vivo*, the effect of R3200 on xenografts was assessed. R3200 induced acute toxicity in mice at doses exceeding 120 mg/kg (data not shown). Therefore, doses between 5 mg/kg and 80 mg/kg were chosen to assess the in vivo anti-cancer effects of R3200 in xenograft experiments using subcutaneously growing HCT116 tumors in immunodeficient SCID beige mice. The animals were randomized into 6 study groups containing 10 tumor-bearing mice each; treatment was started on day 12 after tumor cell injection, when the tumors had reached an average volume of ca. 150 $mm^3$. Treatment consisted of 3 i.v. administrations on three consecutive days (i.e. days 12, 13 and 14 after tumor cell implantation). The tumor volume (Fig. 3A) and body weight (Fig. 3B) was observed until day 31 after tumor cell implantation.

Treatment with R3200 caused a marked, and clearly dose-dependent, tumor growth inhibition which appeared to reach a plateau for the maximal anti-tumor effect at 40 mg/kg (Fig. 3A). In fact, R3200 treatment initially even led to tumor shrinkage, with the maximum occurring ca. 7 days after the first injection. At the same time, R3200 was tolerated well at all five doses and did not have a significant effect on body weight (Fig. 3B). Similarly, on day 31, the final day of the study, blood samples were taken from the animals and analyzed for hematological (red blood cell count, hemoglobin, packed cell volume, reticulocyte count, platelet count) and clinical chemistry (alanine-aminotransferase, creatinine, urea) parameters. In brief, no differences were found for any of the parameters when compared to the vehicle control animals; all values were in the range expected for SCID/beige mice (data not shown). To confirm the results obtained in the HCT116 model, the xenograft experiments were extended using 4 additional human xenograft models. Thus, in total, 3 of the models were originally derived from human colon carcinomas (HCT116, Colo-205 and SW620), and one each from an ovarian (IGROV-1) and a prostate (PC3) tumor. In all 5 xenografts significant tumor growth inhibition was observed in the mice treated with R3200 (Table S2). In addition, HCT116 tumors were also tested in a rat xenograft model. Similar to the mouse studies, also in this experiment a significant inhibition of tumor growth was observed (Table S2).

### *Biomarkers of R3200 resistance*

To find biomarkers of resistance to R3200, we infected HCT116 cells with the retroviral shRNA library targeting some 8,000 human genes for suppression by RNAi [13]. We have shown previously that this library can be used to identify biomarkers of drug resistance [9, 14]. To identify genes whose suppression allows cells to escape the cytotoxic effects of R3200, we treated infected cells with R3200. After two weeks, colonies of R3200 resistant cells were observed in cells infected with the library, but not in control cells treated with R3200 (Fig. 4A).

The screen was performed with a high multiplicity of infection (MOI), which leads to multiple shRNAs being present per cell. Consequently, each R3200-resistant cell colony has several "passenger" shRNA vectors that do not contribute to the resistance phenotype. To identify the active shRNA vectors in the population of resistant cells, we first recovered the shRNAs from the R3200-resistant colonies by isolating the genomic DNA. On this genomic DNA we performed a PCR reaction with primers that specifically amplify the shRNA cassette. These shRNA cassettes were cloned into the original retroviral shRNA vectors in a polyclonal format.

Next, we infected the recovered shRNA vectors from the initial screen into fresh HCT116 cells at low multiplicity of infection, leading to a single retroviral insertion per cell. Cells were again treated with R3200 and again (in this case more) colonies of resistant cells were observed. Sixteen colonies were picked and the shRNA cassettes were identified by sequencing, which revealed that 11 out of 16 R3200-resistant colonies contained a shRNA vector targeting *RBX1* (also known as *ROC1*). The 5 other colonies all contained a different shRNA vector, among which was a shRNA vector targeting *DDB1* (A list of all shRNAs identified in the colonies can be found in Supplementary Table S3). This is particularly interesting as it has been reported that RBX1 can bind DDB1 [15]. Together with CUL4A, RBX1 and DDB1 can form an ubiquitin E3 ligase complex. We therefore decided to study further the possible role of RBX1 and DDB1 in R3200-induced cytotoxicity.

### *Validation of the role of RBX1 and DDB1 in R3200-induced cytotoxicity*

Next, we set out to validate that knockdown of RBX1 and DDB1 indeed can give resistance to R3200 treatment. To address this, we infected HCT116 cells with the shRNA vectors targeting *RBX1* and *DDB1* that were identified in the rescued colonies from the screen (these vectors were named RBX1-Lib and DDB1-Lib). When the HCT116 cells with knockdown of RBX1 or DDB1 were exposed to R3200, these cells proved to be resistant to R3200 treatment (Fig. 4B). In addition, we tested if *RBX1* and *DDB1* knockdown can also protect cells from higher concentrations of R3200. A clear rescue was observed up to 35 μM in cells with knockdown of *RBX1* and

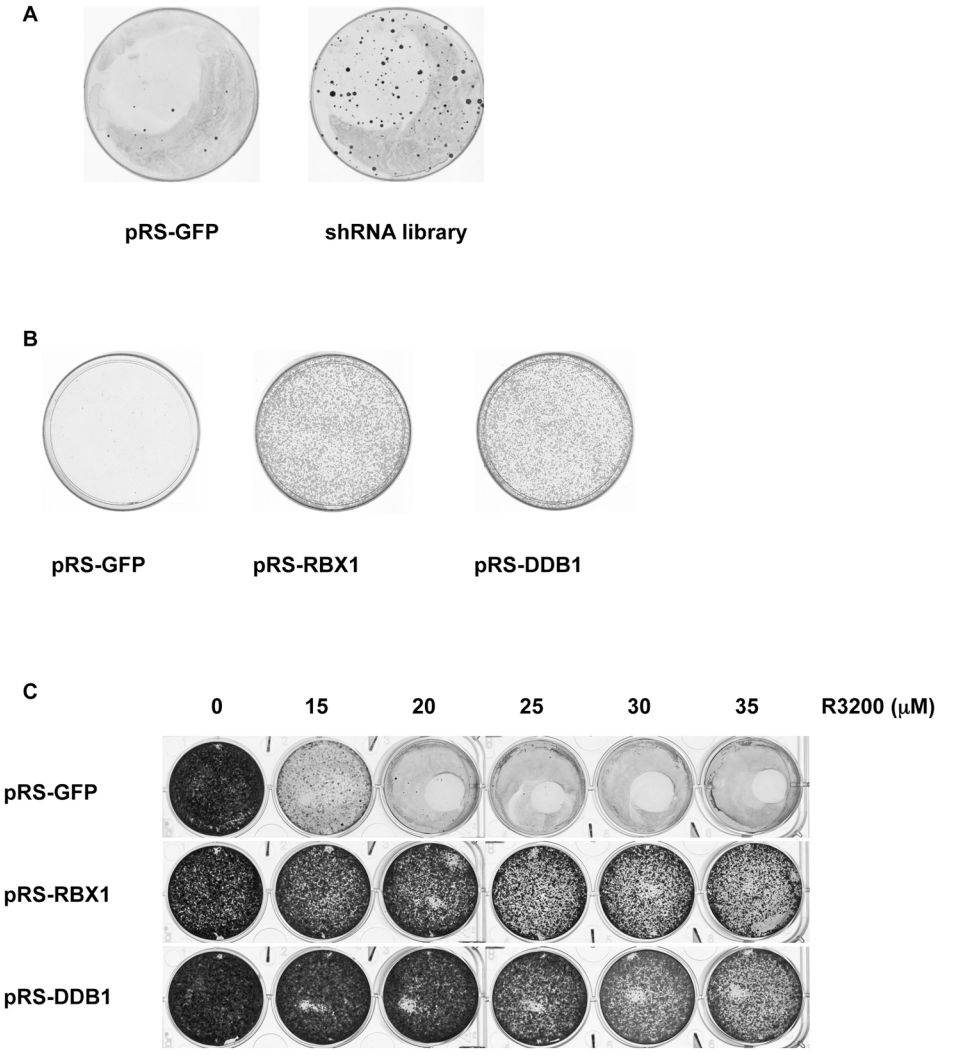


**Figure 4**
**Identification of putative biomarkers of R3200 treatment.**
*Cells were infected with shRNA library or control and selected with puromycin. 150,000 cells were seeded in a 15 cm dish and treated with R3200 (20 μM) for 21 days. Cells were fixed and stained with coomassie (a). RBX1 and DDB1 suppression rescues HCT116 from R3200 anti-proliferative effects. Cells were infected with indicated shRNA plasmids and selected with puromycin. 50,000 cells were seeded in a 10 cm dish and treated with 25 μM R3200 for 10 days. Cells were fixed and stained with coomassie (b). RBX1 or DDB1 suppression renders cells resistant to a range of concentrations of R3200. Cells were infected with indicated shRNA plasmids and selected with puromycin. 10,000 cells were seeded in a 6 well and treated with R3200 for 10 days. Cells were fixed and stained with coomassie (c).*

*DDB1* (Fig. 4C).

***Multiple shRNA vectors targeting RBX1 and DDB1 can produce resistance to R3200 treatment***

To find support for the notion that the knockdown vectors targeting *RBX1* and *DDB1* give rescue due to an 'on-target' effect, we designed four new shRNA vectors targeting both genes (For sequences see methods, vectors were named 1-4) and used these to infect HCT116 cells. We first assessed if the new shRNAs could suppress DDB1 and RBX1 mRNA. A clear reduction in mRNA levels as measured by QRT-PCR was observed in cells that were infected with shRNA vectors targeting *RBX1* and *DDB1* compared to control infected cells (Fig. 5A and 5B). Next we set out to investigate if we could find a correlation between the degree of knockdown and resistance to R3200. The first observation we made was that strong knockdown of RBX1 and DDB1 has an adverse effect on cell proliferation, even in the absence of R3200 (Fig. 5C), a phenotype that has been reported before [16, 17]. We also observed that cells infected with different shRNA vectors targeting *DDB1* (pRS-DDB1-2 and -3) and *RBX1* (pRS-RBX1-3 and -4) produced resistance to R3200 treatment. In addition these cells were also resistant to R3200 treatment in culture conditions with low levels of serum (2.5% FCS) (Supplementary Figure S2). Furthermore we decided to determine the IC50 of R3200 treated HCT116 cells with knockdown of RBX1 or DDB1. We observed an IC50 for RBX1-Lib infected cells of 75 μM and for DDB1-Lib infected cells of 68 μM, compared to an IC50 of 18 μM for control-infected cells (Supplementary Figure S3). From these data we conclude that suppression of both *RBX1* and *DDB1* can confer resistance to R3200 treatment *in vitro*.

***Suppression of RBX1 and DDB1 can abrogate the R3200 induced cell cycle arrest***

As shown above, treatment with R3200 leads to a G2/M arrest in cancer cell lines. Therefore we tested if knockdown of *RBX1* and *DDB1* can also lead to bypass of the G2/M arrest in HCT116 cells. Cells with a stable knockdown of *RBX1* or *DDB1* were treated with R3200 and subjected to cell cycle analysis (Fig. 5D). For *RBX1* we used pRS-Lib, -3 and -4 and for *DDB1* we used pRS-Lib, -2 and -3. These vectors induced no anti proliferative effects in untreated cells and in addition produced the best rescue after treatment with R3200 (Fig. 5C). The G2/M arrest in control cells is very efficient, meaning that 80% of treated cells are arrested. When we tested cells with knockdown of *RBX1* or *DDB1*, we observed that the G2/M peak was reduced accompanied by an increased G1 fraction (Fig. 5D). We therefore conclude that knockdown of *RBX1* and *DDB1* can also alleviate the cell cycle arrest in cells treated with R3200.

***RBX1 and DDB1 knockdown do not cause general drug resistance***

Next we performed some

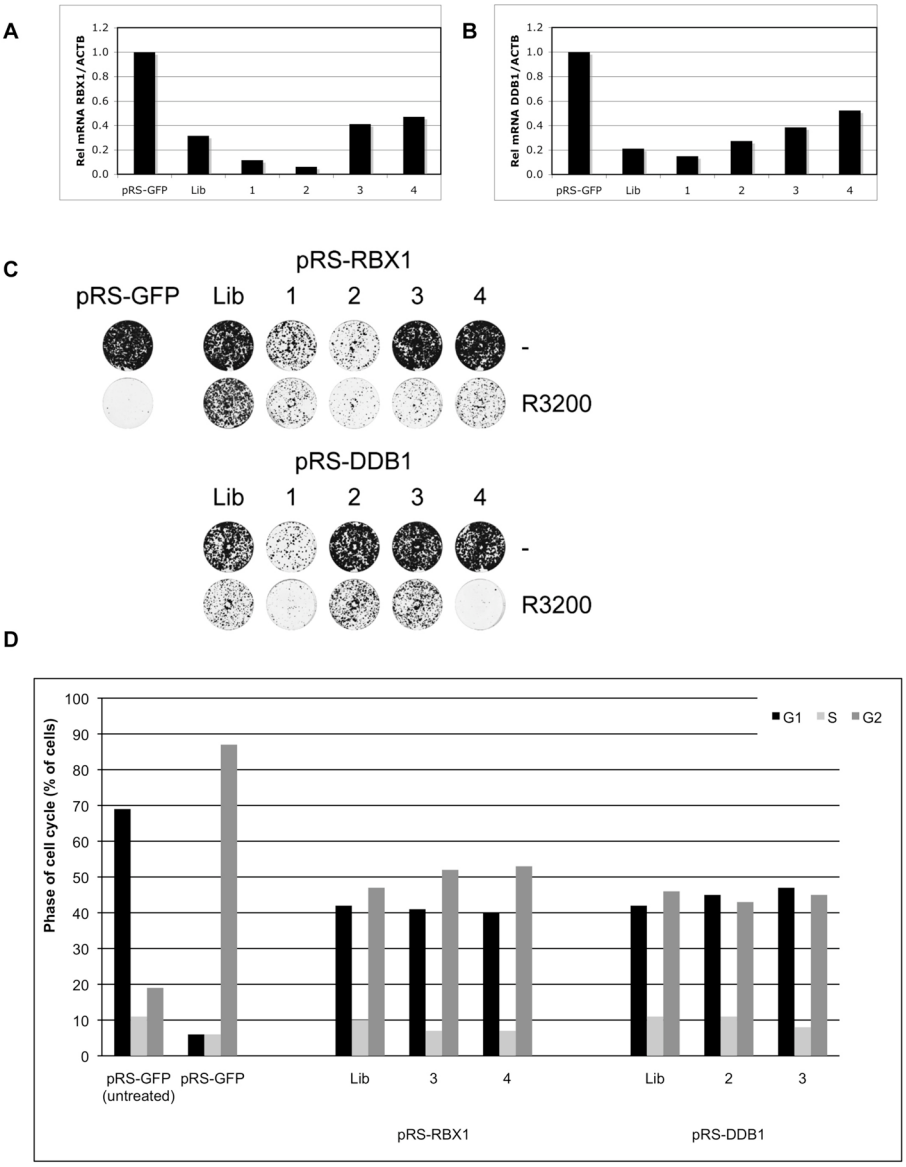


**Figure 5**

**Multiple shRNA vectors targeting RBX1 and DDB1 produce resistance against R3200 treatment.** *QRT-PCR to assess knockdown of RBX1 (a) and DDB1 (b) in HCT116 cells. Cells were infected with knockdown vectors targeting RBX1 or DDB1 and control knockdown vector (pRS-GFP). RBX1-Lib and DDB1-Lib are the shRNA plasmids identified from the library. Hit validation in HCT116 cells (c). Cells were infected with indicated plasmids and selected with puromycin. 10,000 cells were seeded in a 6 well and treated with R3200 for 10 days. Cells were fixed and stained with coomassie. Knockdown of RBX1 and DDB1 can rescue the R3200 induced G2/M cell cycle arrest in HCT116 cells (d). HCT116 cells were infected with pRS-GFP control vector or pRS vectors targeting RBX1 or DDB1 as indicated on the x-axes. Cells were treated with R3200 (30 μM for 48 hrs) and stained with PI. G1 phase is indicated in black bars, S-phase in hatched bars and G2/M phase in gray.*

experiments to ensure that the observed effects are not specific for both the cell type and drug used. To address the drug specificity issue we treated HCT116 cells with an unrelated drug, cisplatin in the presence or absence of *RBX1* or *DDB1* knockdown. As HCT116 cells are quite sensitive to low concentrations (5 μM) of cisplatin a strong decrease in proliferation can be observed (Supplementary Figure S4). The anti proliferative effects of cisplatin could not be overcome by knockdown of either *RBX1* or *DDB1*. This experiment shows that suppression of *RBX1* or *DDB1* confers resistance to R3200 treatment but not to anti-proliferative drugs in general.

***Suppression of RBX1 and DDB1 also confers resistance to R3200 treatment in U2OS cells***

To exclude that the observations we made are specific for HCT116 cells we decided to repeat some of the experiments in an unrelated cell type. For this we used U2OS cells, a cell line isolated from a human osteosarcoma. U2OS cells are equally sensitive to R3200 as HCT116 (U2OS (IC50 = 5.3 μM), HCT116 (IC50 = 4.9 μM). We used the active shRNA vectors to knockdown *RBX1* and *DDB1* in U2OS cells. When the mRNA levels of RBX1 and DDB1 were assessed we observed comparable results as in HCT116 cells (Supplementary Figure S5A and S5B). Subsequently we treated the U2OS cells in which we knocked down *RBX1* and *DDB1* with various concentrations of R3200. In cells that were suppressed for either RBX1 or DDB1 we saw a clear rescue from the anti-proliferative actions of R3200 as measured by colony formation assays (Supplementary Figure S5C).

## Discussion and conclusion

In this study we report biochemical and genetic studies using the new anti cancer acyl sulfonamide R3200. In previous studies it was shown that acyl sulfonamides can inhibit cell proliferation *in vitro* and *in vivo*. However no analysis was performed on the possible mode of action of acyl sulfonamides [1-4]. Here we show that R3200 has profound anti proliferative action in a series of cancer cell lines including a P-gp over-expressing cell line. This anti proliferative effect can be attributed to two different physiological responses. First, when we performed cell cycle analysis on R3200 treated cells we observed a cell cycle arrest. Second, R3200 treatment leads to substantial apoptosis when cells are exposed to drug for a longer time. After these promising *in vitro* results we tested the effects of R3200 in mouse and rat xenografts. In these experiments we observed a strong anti proliferative effect towards the grafted human cancer cells resulting in strong tumor growth inhibition.

To identify the mode of action of R3200 and to find biomarkers of resistance to this drug, we have performed a large-scale RNAi genetic screen. Two genes were

identified that, when suppressed, can bypass the cytostatic actions of R3200. Interestingly, these two genes, *RBX1* and *DDB1* can form a complex with CUL4A, leading to the formation of an active ubiquitin E3 ligase complex [18]. Suppression of components of this E3 ligase complex potentially leads to the stabilization of the target proteins. It is therefore possible that R3200 inhibits a protein, which is targeted for destruction by this ubiquitin ligase complex containing RBX1 and DDB1, as inhibition of this destruction complex may lead to increased concentrations of the putative protein target(s) of R3200, thereby conferring resistance to the drug. Many targets have been reported for the ubiquitin ligase complex containing RBX1 and DDB1, most striking targets are CDT1, c-Jun and Histone H3 and H4 [15, 19-21]. CDT1 is required for formation of the pre-RC complex and therefore essential for replication of the genome [22]. It has been described that CDT1, Histone H3 and H4 can be ubiquitinated by the complex containing RBX1 and DDB1 after DNA damage [7, 21].

Whatever the mechanism may be, our data indicate that the level of RBX1 and DDB1 may have clinical utility to predict the response of cancer cells to R3200. Therefore *RBX1* and *DDB1* should be evaluated as biomarkers for clinical response in the treatment of patients with R3200 and potentially also in clinical studies involving other acyl sulfonamides. If a tumor contains very low levels of transcripts encoding for either *RBX1* or *DDB1* it might be advisable not to use R3200 in this setting. One of these examples would be patients that suffer from a form of xeroderma pigmentosum (XP). XP patients that fall in complementation group XPE suffer from a defect in either the *DDB1* or *DDB2* gene [23, 24]. Therefore treatment of XP patients with a defect in *DDB1* or *DDB2* with R3200 might be less effective. Clinical studies involving these candidate biomarkers may substantiate these predictions in the future.

## Materials and Methods

***Cell lines & culture conditions***
Cell lines were derived from ATCC, NCI or DSMZ. The MTLn3 cell line is a mouse cell line, all other cell lines are human cell lines. All cell were cultivated in RPMI1640 medium supplemented with 10% FCS, 100 µg/ml Penicillin and 100 µg/ml Streptomycin at 37°C in 5% $CO_2$. For the RNAi barcode screen HCT116 and Phoenix cells were cultured at 37°C in 5% $CO_2$ in DMEM medium supplemented with 10% FCS, Penicillin and Glutamine.

***Reagents***
R3200 (2-Phenyl-ethenesulfonic acid 2,4-dichloro-benzoylamide sodium salt) was dissolved in DMSO to get a stock solution of 10 mM. Taxol (Paclitaxel), Cisplatin, Nocodazole (Oncodazole) and Etoposide were purchased from Sigma Aldrich and

dissolved following the instructions of the company.

***Cell titer glow assay***

The CellTiter-Glo™ Luminescent Cell Viability Assay (Promega) is used for determining the number of viable cells based on quantitation of the ATP present. Cells were seeded as 1000 – 3000 cells per well in 60 µl in a 384 well plate in the same medium supplemented with either 2.5% or 10% FCS. After 16-24 h at 37 °C and 5% $CO_2$ 10 µl of the serially diluted compound was added in triplicate wells. The final concentration in the assay was between 30 µM and 1.5 nM or between 100 µM and 4.5 nM (ten concentrations, dilution 1:3). The cells were incubated at 37 °C and 5% $CO_2$ for 5 days. At the end of the experiment, first the plate was equilibrated to room temperature for approximately 30 minutes and then the cells were treated with 30 µl of CellTiter-Glo reagent. After 45-60 minutes the luminescence was determined using a Victor$^2$ multi-probe plate reader from PerkinElmer.

***Annexin V apoptosis assay***

HCT116 cells were treated with R3200 for 24, 48 or 72 hours. After treatment cells were collected and stained with Annexin V and Propidium Iodide. Following staining cells were subjected to FACS analysis.

***Western blotting***

The following antibodies were used for Western blotting. Anti c-Jun (9162), c-Jun-pS63 (9262), c-Jun-pS73 (9164) were obtained from Cell Signaling Technologies. Anti Cyclin A (611269), Cyclin B (610220), MAD2 (610679) were obtained from BD Transduction Laboratories.

***HCT116 xenograft study***

SCID beige mice were purchased from Charles River Germany; HCT116 tumor cells were obtained from the NCI. To generate the primary tumors, $5x10^6$ HCT116 cells were injected subcutaneously into the flank of each mouse in a volume of 100 µL of phosphate buffered saline. Body weight and tumor volume were measured three times weekly. Tumors were measured in two dimensions (length and width), and the corresponding tumor volume was estimated using the formula: V [$mm^3$] = length [mm] x width [mm] x width/2 [mm]. Randomization (6 groups containing 10 animals each), and start of treatment was on day 12, when the tumors had reached an average volume of ca. 150 $mm^3$. Treatment was once daily for 3 days (on days 12, 13, and 14) by i.v. injection of vehicle or different doses of R3200. On day 31, the final day of the experiment, blood samples were taken from the animals and analyzed for hematological (red blood cell count, hemoglobin, packed cell volume, reticulocyte count, platelet count) and clinical chemistry (alanine-aminotransferase, creatinine, urea) parameters.

***NKI shRNA library***

The construction of the library was described previously [13]. Briefly, the NKI shRNA library was designed to target 7914 human genes, using

three shRNA vectors for every targeted gene, cumulating in a total of 23,742 shRNA vectors. The shRNAs are cloned into a retroviral vector (pRetroSUPER, pRS) to enable infection of target cells.

***Retroviral infection***

Phoenix cells were transfected using calcium phosphate method. Viral supernatant was cleared through a 0.45 μM filter. Cells were infected with the viral supernatant in presence of polybrene (8 μg/ml). The infection was repeated twice.

***shRNA screen***

To screen the NKI shRNA library we reasoned that we would need 100-fold coverage of the library to get a good representation of shRNA vectors present in the library. The screen was initiated by transduction of HCT116 cells with the shRNA library. After infection the cells were selected with puromycin (2 μg/ml). When the selection was completed 2 x $10^6$ HCT116 cells (100 fold library coverage) were seeded at a density of 150,000 cells/15 cm dish. Some 24 hours after seeding R3200 was added at a final concentration of 20 μM. Colonies of resistant cells appeared in the plates containing cells infected with the shRNA library, no colonies were observed in control infected cells treated with R3200. After 21 days of exposure to 20 μM R3200 the colonies were harvested. All colonies were pooled and the genomic DNA was isolated using DNAzol (Invitrogen). The shRNA cassettes were amplified by PCR, and re-cloned into the pRS shRNA vector. This polyclonal pool of shRNA vectors was infected into HCT116 cells at a low multiplicity of infection. The colony formation was repeated and 16 colonies were isolated. From these colonies genomic DNA was isolated and the shRNA cassettes were amplified by PCR. The PCR product was cloned into the pRS plasmid. To identify the shRNA cassette 5 re-cloned plasmids were sequenced for every re-cloned PCR product. The sequences of the shRNAs isolated from the colonies are listed in Table S3.

***Generation of additional shRNA vectors targeting RBX1 and DDB1***

19-mer sequences of shRNA plasmids targeting RBX1 and DDB1 used in this study.

RBX1 (NM_014248)

| | |
|---|---|
| Lib | GACTTCTTCCATCAAGCTT |
| 1 | GAAGCGCTTTGAAGTGAAA |
| 2 | GCATAGAATGTCAAGCTAA |
| 3 | GCAAGAAGCGCTTTGAAGT |
| 4 | CAACAGAGAGTGGGAATTC |

DDB1 (NM_ 001923)

| | |
|---|---|
| Lib | GAACCCAAAGCTCTGGTCA |
| 1 | GACAAGAGTTCTCATGTTA |
| 2 | GCAAGGACCTGCTGTTTAT |
| 3 | TGACATACCTTGATAATGG |
| 4 | CACTAGATCGCGATAATAA |

***Colony formation assay***

Cells were infected with retroviral supernatant and selected with puromycin. When the selection was completed cells were seeded at 150,000/15 cm dish, 50,000/10 cm dish or 10,000/6-well. The following day the R3200 was added. Cells were cultured in presence of R3200 for approx 10 days. When colonies appeared cells were fixed in MeOH/

HAc (3:1) and subsequently stained in staining solution (50% MeOH/10% HAc/0.1% Coomassie).

***QRT-PCR (quantitative real time PCR)***

Total RNA was isolated using TRIzol (Invitrogen) from cells that were infected with pRS plasmids and selected with puromycin. From the total RNA, cDNA was generated using Superscript II (Invitrogen) with random primers (Invitrogen). cDNA was diluted and QRT reaction was performed using SYBR green PCR master mix (Applied Biosystems). All QRT reactions were run in parallel for Actin B to control for amount of input cDNA. The QRT reaction was followed by a melting curve to confirm the formation of a single PCR product. The QRT reactions were run at an AB7500 Fast Real Time PCR system (Applied Biosystems). The PCR primer sequences were obtained from the qprimerdepot [25]

Primer sequences:
Actin B Forward:
CCTGGCACCCAGCACAA
Actin B Reverse:
GCCGATCCACACGGAGTACT
RBX1 Forward:
AGTGGAATGCAGTAGCCCTC
RBX1 Reverse:
ACGCCTGGTTAGCTTGACAT
DDB1 Forward:
GATCATCCGGAATGGAATTG
DDB1 Reverse:
ATTAGGGTCAGACCGCAGTG

***FACS cell cycle analysis***

Cells were infected with retroviral supernatant and selected with puromycin. When the selection was completed cells were seeded at 500,000/10 cm dish. One day after seeding R3200 (30 μM) was added for 48 hrs. Cells were harvested and fixed in 70% EtOH and subsequently stained with PI (propidium iodide). FACS analysis was performed by gating out the doublet cells.

## References


1. Corbett, T.H., et al., Discovery and preclinical antitumor efficacy evaluations of LY32262 and LY33169. Invest New Drugs, 2003. 21(1): p. 33-45.
2. Lobb, K.L., et al., Acyl sulfonamide anti-proliferatives: benzene substituent structure-activity relationships for a novel class of antitumor agents. J Med Chem, 2004. 47(22): p. 5367-80.
3. Mader, M.M., et al., Acyl sulfonamide anti-proliferatives. Part 2: activity of heterocyclic sulfonamide derivatives. Bioorg Med Chem Lett, 2005. 15(3): p. 617-20.
4. Haritunians, T., et al., Novel acyl sulfonamide LY573636-sodium: effect on hematopoietic malignant cells. Oncol Rep, 2008. 20(5): p. 1237-42.
5. Ludwig, J.A. and J.N. Weinstein, Biomarkers in cancer staging, prognosis and treatment selection. Nat Rev Cancer, 2005. 5(11): p. 845-56.
6. Sawyers, C.L., The cancer biomarker problem. Nature, 2008. 452(7187): p. 548-52.
7. Bartz, S.R., et al., Small interfering RNA screens reveal enhanced cisplatin cytotoxicity in tumor cells having both BRCA network and TP53 disruptions. Mol Cell Biol, 2006. 26(24): p. 9377-86.
8. Whitehurst, A.W., et al., Synthetic lethal screen identification of chemosensitizer loci in cancer cells.

Nature, 2007. 446(7137): p. 815-9.
9. Berns, K., et al., A functional genetic approach identifies the PI3K pathway as a major determinant of trastuzumab resistance in breast cancer. Cancer Cell, 2007. 12(4): p. 395-402.
10. Bernards, R., T.R. Brummelkamp, and R.L. Beijersbergen, shRNA libraries and their use in cancer genetics. Nat Methods, 2006. 3(9): p. 701-6.
11. Borst, P. and R.O. Elferink, Mammalian ABC transporters in health and disease. Annu Rev Biochem, 2002. 71: p. 537-92.
12. Gottesman, M.M., T. Fojo, and S.E. Bates, Multidrug resistance in cancer: role of ATP-dependent transporters. Nat Rev Cancer, 2002. 2(1): p. 48-58.
13. Berns, K., et al., A large-scale RNAi screen in human cells identifies new components of the p53 pathway. Nature, 2004. 428(6981): p. 431-7.
14. Brummelkamp, T.R., et al., An shRNA barcode screen provides insight into cancer cell vulnerability to MDM2 inhibitors. Nat Chem Biol, 2006. 2(4): p. 202-6.
15. Wertz, I.E., et al., Human De-etiolated-1 regulates c-Jun by assembling a CUL4A ubiquitin ligase. Science, 2004. 303(5662): p. 1371-4.
16. Schlabach, M.R., et al., Cancer proliferation gene discovery through functional genomics. Science, 2008. 319(5863): p. 620-4.
17. Tan, M., et al., RBX1/ROC1 disruption results in early embryonic lethality due to proliferation failure, partially rescued by simultaneous loss of p27. Proc Natl Acad Sci U S A, 2009. 106(15): p. 6203-8.
18. Groisman, R., et al., The ubiquitin ligase activity in the DDB2 and CSA complexes is differentially regulated by the COP9 signalosome in response to DNA damage. Cell, 2003. 113(3): p. 357-67.
19. Hu, J., et al., Targeted ubiquitination of CDT1 by the DDB1-CUL4A-ROC1 ligase in response to DNA damage. Nat Cell Biol, 2004. 6(10): p. 1003-9.
20. Higa, L.A., et al., Radiation-mediated proteolysis of CDT1 by CUL4-ROC1 and CSN complexes constitutes a new checkpoint. Nat Cell Biol, 2003. 5(11): p. 1008-15.
21. Wang, H., et al., Histone H3 and H4 ubiquitylation by the CUL4-DDB-ROC1 ubiquitin ligase facilitates cellular response to DNA damage. Mol Cell, 2006. 22(3): p. 383-94.
22. Nishitani, H., et al., The Cdt1 protein is required to license DNA for replication in fission yeast. Nature, 2000. 404(6778): p. 625-8.
23. Chu, G. and E. Chang, Xeroderma pigmentosum group E cells lack a nuclear factor that binds to damaged DNA. Science, 1988. 242(4878): p. 564-7.
24. Kapetanaki, M.G., et al., The DDB1-CUL4ADDB2 ubiquitin ligase is deficient in xeroderma pigmentosum group E and targets histone H2A at UV-damaged DNA sites. Proc Natl Acad Sci U S A, 2006. 103(8): p. 2588-93.
25. Cui, W., D.D. Taub, and K. Gardner, qPrimerDepot: a primer database for quantitative real time PCR. Nucleic Acids Res, 2007. 35(Database issue): p. D805-9.

## Acknowledgements

We would like to thank Diana Weininger for her contributions to this study.

## Supplementary tables and figures

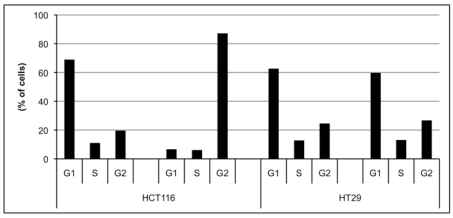


**Figure S1**
*Quantification of FACS analysis of PI stained HCT116 and HT-29 cells treated with 30 μM R3200 for 48 hrs.*

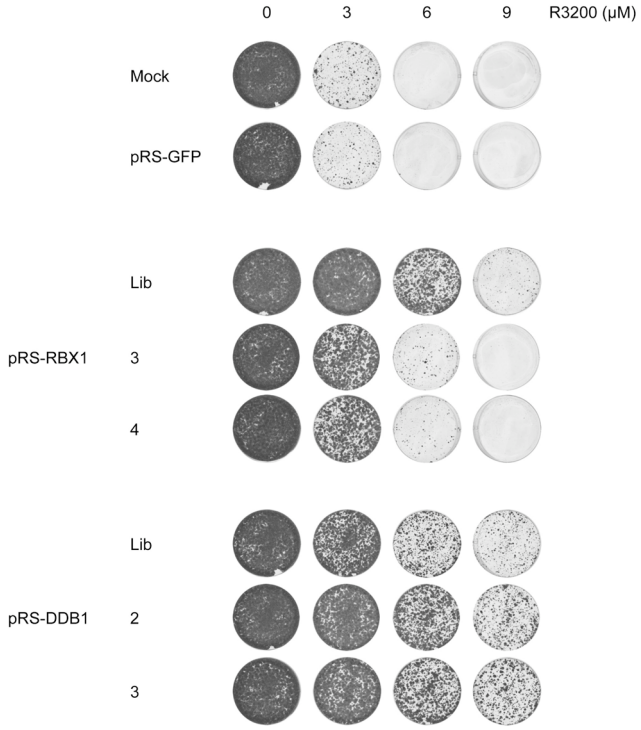


**Figure S2**
**RBX1 and DDB1 knockdown confer resistance to R3200 under low serum culture conditions.**
*10,000 cells were seeded per 6 well and cultured in presence of indicated concentrations of R3200 for 12 days.*

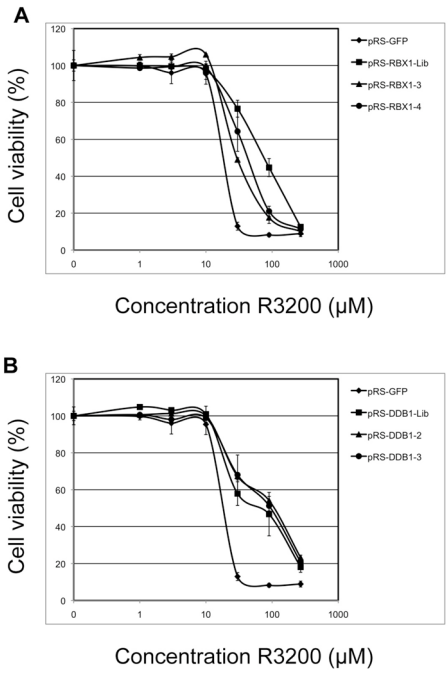


**Figure S3**
**RBX1 and DDB1 knockdown cause a shift in IC50 for R3200 treatment.**
*Dose response curves were measured using cell titer glow.*

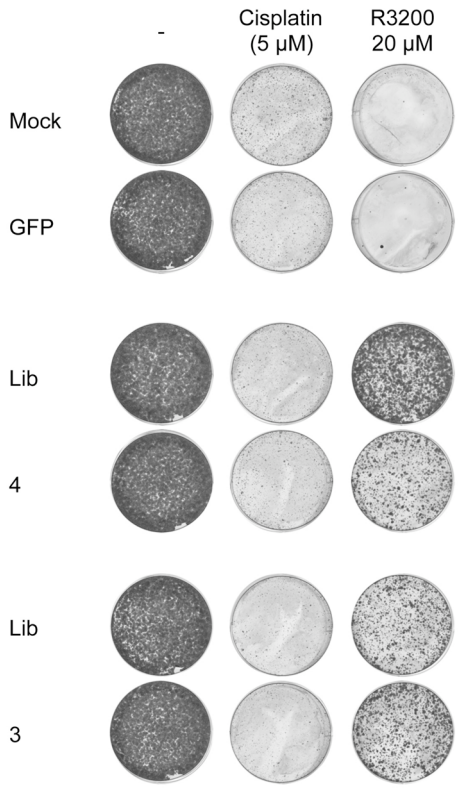


**Figure S4**
**Suppression of RBX1 or DDB1 does not cause general drug resistance.**
*HCT116 cells were seeded (10,000/6-well) and treated with either capsulation (5 μM) or R3200 (20 μM).*

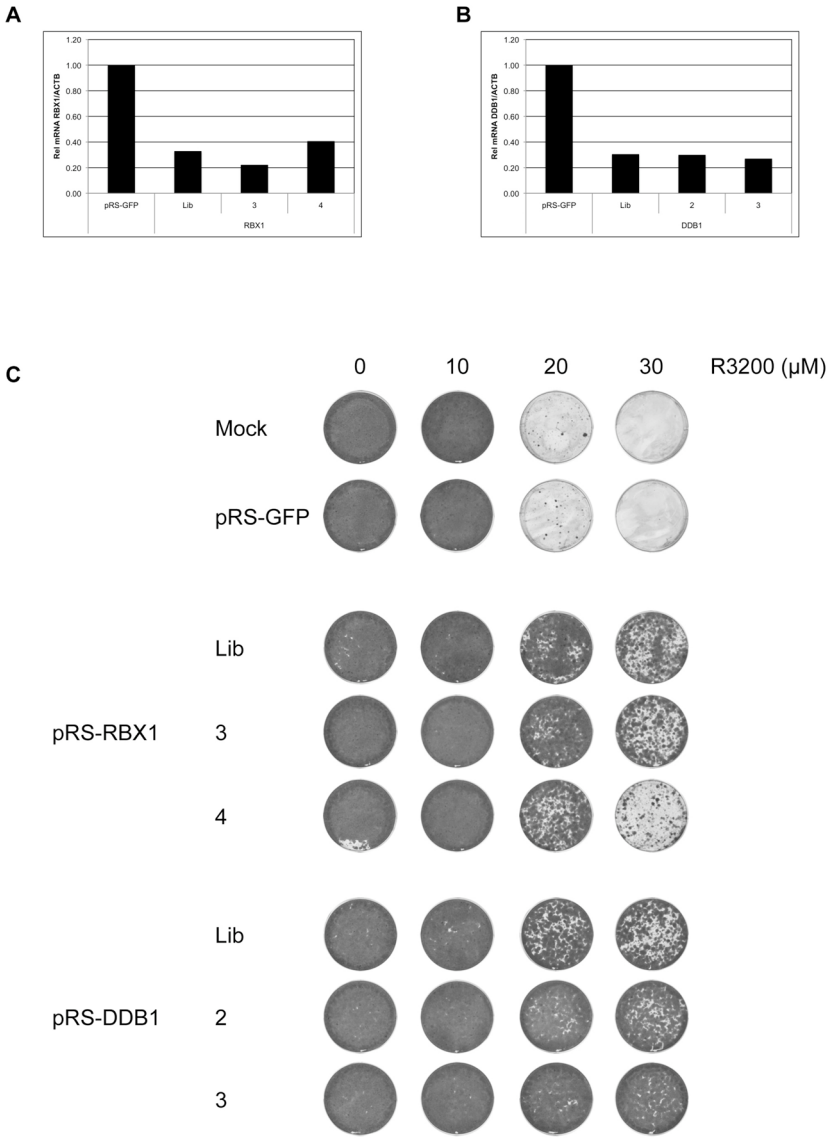


**Figure S5**
**Knockdown of RBX1 and DDB1 confers resistance to R3200 in U2OS cells.**
*QRT-PCR to assess knockdown of RBX1 (a) or DDB1 (b) in U2OS cells. Knockdown of RBX1 or DDB1 also confers resistance to R3200 treatment in U2OS cells (c). 10,000 U2OS cells were plated per 6-well and treated with R3200 for 14 days at the indicated concentrations.*

| Tumor Type | Cell line | Medium with 2.5 % FCS Mean values [µM] | Medium with 10 % FCS Mean values [µM] |
|---|---|---|---|
| Ovary | IGROV-1 | 2.3 | 10.4 |
| Breast | MDA-MB-468 | 4.8 | 13.7 |
| Colon | HCT-116 | 4.9 | 19 |
| Osteosarcoma | U2OS | 5.3 | 17.3 |
| Colon | SW-620 | 6.3 | 22.9 |
| Prostate | PC-3 | 6.6 | 24.1 |
| T-lymphocyte | Molt 4 | 9.9 | 26.3 |
| Colon | Colo 205 | 11 | 27.7 |
| Breast | MTLn3 | 11 | 26.4 |
| Burkitt Lymphoma | Raji | 11.2 | 27.8 |
| Breast | MDA-MB-435 | 11.3 | 28.3 |
| Pancreas | Panc Tu-1 | 11.3 | 28.7 |
| CNS | SF-295 | 12.9 | 29.2 |
| Ovary | SK-OV-3 | 13.2 | 29.5 |
| Colon | HCT-15 | 13.5 | 29.6 |
| Lung | A 549 | 14.3 | 30.4 |
| Ovary | OVCAR-5 | 14.8 | 32.9 |
| Prostate | DU-145 | 19.9 | 45.4 |
| Breast | MCF-7 | 21.8 | 58.6 |
| Breast | KPL-4 | 24.1 | 88.5 |
| Lung | H460-M2 | 24.3 | > 23.5 |
| Breast | MDA-MB-231 | 35.5 | > 27.9 |
| Colon | CX-1 | 42 | > 29.4 |
| Prostate | LNCaP | 65.5 | > 30 |
| Colon | HT-29 | 71.6 | > 30 |
| Lung | NCI-H441/Kam. | > 30 | > 100 |
| Pancreas | Panc-1 | > 30 | > 30 |
| Lung | QG-56 | > 30 | > 30 |
| Lung | Calu-3 | > 35.2 | > 100 |

**Table S1**
**R3200 has cytotoxic activities in a wide range of tumor cell lines.**
*IC50 values for cell lines (as indicated) treated with R3200 in 10% FCS and 2.5% FCS culture conditions.*

| Tumor growth inhibition at 80 mg/kg | | |
|---|---|---|
| Model | Tumor type | Tumor growth inhibition [%] |
| HCT116 | Colon | 90-98% |
| Colo-205 | Colon | 95-100% |
| SW620 | Colon | 45-50% |
| PC3 | Prostate | 90-100% |
| IGROV-1 | Ovarian | 70-75% |
| HCT116 **rat** | Colon | 80-85% |

**Table S2**
**Results of xenografts with six human cancer cell lines in SCID beige mice treated with R3200.**
*Growth inhibition was measured as described in materials and methods.*

| Colony # | shRNA Sequence | Genbank Acc | HUGO | Number identified |
|---|---|---|---|---|
| **Colony 1** | ACCTGGTGACTGATGAGGC | NM_152830 | Angiotensin I converting enzyme 1 (ACE) | 5 |
| | | | | |
| **Colony 2** | GACTTCTTCCATCAAGCTT | NM_014248 | Ring-box 1 (RBX1), mRNA | 3 |
| **Colony 2** | GCTATGTTAGCAACCATGT | NM_021907 | DTNB | 1 |
| | | | | |
| **Colony 3** | GTCACTACAGACAACAAAT | NM_006529 | GLRA3 | 2 |
| **Colony 3** | GACTTCTTCCATCAAGCTT | NM_014248 | Ring-box 1 (RBX1), mRNA | 2 |
| **Colony 3** | GCCATTCAAGTGCGCGGAC | NM_007249 | KLF12 | 1 |
| | | | | |
| **Colony 4** | GACTTCTTCCATCAAGCTT | NM_014248 | Ring-box 1 (RBX1), mRNA | 1 |
| **Colony 4** | CTTGGAAATCATTATTCTA | BC131822 | | 4 |
| | | | | |
| **Colony 5** | CTGTCCCAACATTAGAGTA | BC126338 | | 1 |
| **Colony 5** | GGCCGACACCTTGATATGG | NM_001079821 | NLRP3 | 1 |
| **Colony 5** | GACTTCTTCCATCAAGCTT | NM_014248 | Ring-box 1 (RBX1), mRNA | 1 |
| | | | | |
| **Colony 6** | CTAAATGGGGTACCTCGGC | NM_004572 | PKP2 | 1 |
| **Colony 6** | GACAATAATCGGCCTGGGA | NM_000901 | NR3C2 | 2 |
| **Colony 6** | TCTTCCTGCTGGGCACAGT | AY587582 | GALR3 | 2 |
| | | | | |
| **Colony 7** | GACTTCTTCCATCAAGCTT | NM_014248 | Ring-box 1 (RBX1), mRNA | 1 |
| **Colony 7** | GTCTGAAGTTGCAGCTGGA | not a 100% match | | 4 |
| | | | | |
| **Colony 8** | GACTTCTTCCATCAAGCTT | NM_014248 | Ring-box 1 (RBX1), mRNA | 5 |
| | | | | |
| **Colony 9** | GAAATGTCATTCTTGCTCC | NM_152896 | UHRF2 | 3 |
| | | | | |
| **Colony 10** | GAACCCAAAGCTCTGGTCA | NM_001923 | Damage-specific DNA binding protein 1 (DDB1) | 5 |
| | | | | |
| **Colony 11** | GACTTCTTCCATCAAGCTT | NM_014248 | Ring-box 1 (RBX1), mRNA | 4 |
| **Colony 11** | TTCAACTCCACGCGGGACT | NM_003412 | ZIC1 | 1 |
| | | | | |
| **Colony 12** | GACTTCTTCCATCAAGCTT | NM_014248 | Ring-box 1 (RBX1), mRNA | 4 |
| | | | | |
| **Colony 13** | ACTTCATTCCTTGATTGTG | not a 100% match | | 1 |
| **Colony 13** | GAATGATCGATTCAACTAT | NM_173500 | TTBK2 | 2 |
| **Colony 13** | GACTTCTTCCATCAAGCTT | NM_014248 | Ring-box 1 (RBX1), mRNA | 1 |
| **Colony 13** | CTTCATTCCTTGATTTGTG | BC093019 | | 1 |
| | | | | |
| **Colony 14** | CAGATTTACCCATTTGTGT | NM_004865 | TBPL1 | 5 |
| | | | | |
| **Colony 15** | GACTTCTTCCATCAAGCTT | NM_014248 | Ring-box 1 (RBX1), mRNA | 3 |
| | | | | |
| **Colony 16** | GACTTCTTCCATCAAGCTT | NM_014248 | Ring-box 1 (RBX1), mRNA | 4 |

**Table S3**

*Results from sequencing of 16 colonies obtained from the RNAi screen in HCT116 cells treated with R3200.*

# CHAPTER VI

# IRAK2 is a novel modulator of the TGF-beta signaling cascade

Submitted to *Molecular Cancer Research*

# IRAK2 is a novel modulator of the TGF-beta signaling cascade

Jasper Mullenders[1], Armida WM Fabius[1], Miranda MW van Dongen, Hendrik J Kuiken, Roderick L Beijersbergen and René Bernards

Division of Molecular Carcinogenesis, Center for Biomedical Genetics and Cancer Genomics Center, The Netherlands Cancer Institute, Plesmanlaan 121, 1066 CX Amsterdam, The Netherlands
1. These authors contributed equally to this work

**The TGFβ pathway orchestrates an extensive transcriptional program that is important for many processes in the cell. For example TGFβ regulates cell cycle, migration and epithelial-to-mesenchymal transition (EMT). The TGFβ pathway has a dual role in cancer: it is involved in early stage tumor suppression, but also contributes to tumor progression by in promoting invasion. To identify novel genes involved in TGFβ pathway signaling, we have performed a functional genetic loss-of-function screen. We screened 700 kinases and kinase related genes in a TGFβ responsive reporter assay. Several genes were identified that upon knockdown could repress the reporter signal; among these are the two cellular receptors for TGFβ. In addition to these two known components of the TGFβ pathway, several genes were identified that were previously not linked to the TGFβ signaling. Knockdown of one of these genes, the *IRAK2* kinase, resulted in not only in an impaired TGFβ target genes response but also in a reduction in nuclear translocation and phosphorylation of SMAD2. In addition, suppression of *IRAK2* expression led to a partial override of a TGFβ induced cell cycle arrest. Our data demonstrate that IRAK2 is a novel and critical component of TGFβ signaling.**

## Introduction

The TGFβ pathway is an important signaling pathway that regulates many different processes such as cell cycle, epithelial to mesenchymal transition (EMT), migration and angiogenesis [1, 2]. Stimulation of the TGFβ pathway is initiated by binding of the TGFβ ligand to the TGFβ receptors (TGFBR1 and TGFBR2). This leads to TGFβ receptor complex formation, which results in the phosphorylation of TGFBR1 by TGFBR2. Subsequently, SMAD2 and SMAD3 are phosphorylated by the TGFBR1, which leads to their translocation to the nucleus. In the nucleus the activated SMADs can form a complex with SMAD4. This activated SMAD complex recruits transcriptional co-factors which assist in the binding of SMAD responsive DNA elements in the promoters of TGFβ target genes, thereby regulating their transcription [3].

The TGFβ pathway plays a dual role in cancer pathogenesis. In normal epithelium and early stage tumors, the TGFβ pathway was reported to have an inhibitory effect on cell proliferation [4]. This is achieved mainly through induction of a G1 cell cycle arrest through up-regulation of the CDK inhibitors *CDKN1A* (encoding $p21^{CIP1}$) and *CDKN2B* (encoding p15) and downregulation of the *MYC* proto-oncogene [5-7]. However, cancer cells can become insensitive to this proliferation control by loss of expression of the TGFβ receptor or SMADs. The TGFβ pathway subsequently promotes cancer progression through induction of EMT, angiogenesis and evasion of immune surveillance [1, 2]. Furthermore, it was recently shown that tumors with an activated TGFβ pathway have a worse outcome than tumors without activation of the TGFβ pathway [8, 9]. For this reason different anti-cancer strategies are developed to inhibit the TGFβ pathway. Clinical trials have been performed with TGFβ antisense oligonucleotides, TGFβ antibodies and a TGFBR1 small molecule inhibitor [10].

Several approaches have been taken to identify new players in the TGFβ pathway. For example protein-protein interaction screens have been used to extend the knowledge about the TGFβ pathway [11, 12]. In addition, a functional genetic screen to identify new players in the mammalian TGFβ network has been performed by Levy and colleagues. They describe the screening of a siRNA library targeting the ubiquitin E3-ligase gene-family in a cell line with an integrated TGFβ responsive reporter. Through this approach they identified Arkadia as a positive regulator of the pathway [13].

We describe here a functional genetic screen aimed at the identification of novel kinases that function in the TGFβ pathway. We identify here an unexpected new kinase that contributes to TGFβ signaling.

## Results

***The screening of a TGFβ reporter cell line with a human kinome siRNA library***

To screen siRNA libraries in high throughput format for novel modulators of TGFβ signaling, we generated an U2OS osteosarcoma cell line with a stably integrated $pCAGA_{12}$-Luc TGFβ responsive reporter (this cell lines was named U2OS-CAGA) [14]. This reporter has been described to be primarily responsive to SMAD3/4 dependent transcription [14]. To test the responsiveness of the integrated reporter in the U2OS-CAGA cell line, we transfected siRNAs targeting a positive and a negative regulator of TGFβ signaling. As expected, ablation of the positive regulator TGFBR2 by RNAi led to complete abrogation of both based and TGFβ induced reporter activity (fig. 1a). Moreover, knockdown of a negative regulator of the TGFβ signaling cascade, SKIL caused the opposite effect, showing increased reporter activity. It is worth noting that in absence of exogenous TGFβ knockdown of SKIL still causes enhanced signal of the TGFβ responsive reporter (fig.1a). We also observed a slight induction of the TGFβ reporter upon addition of control siRNAs (fig. 1a).

These initial experiments showed that the integrated TGFβ reporter in the U2OS-CAGA cell line behaved as expected. Therefore we used this cell line to screen a siRNA library targeting 700 kinases and kinase related proteins. The siRNA library that we used consists of siRNA pools; each gene is targeted by 4 separate siRNA, which are used as a pool. The U2OS-CAGA cells were transfected in triplicate with siRNA pools of the human kinome library and the entire screen was performed in presence of TGFβ. To identify siRNAs that modulate the reporter, we measured both luciferase activity and cell viability. The cell viability was measured to exclude siRNAs that cause a decrease in cell viability as these might be identified as false positive repressors in the screen. Data was normalized and a hit list was generated by calculating a Z-score for every tested siRNA pool (fig. 1b).

Only siRNA pools that produced a Z-score greater than 2 (20 genes) or lower than -2 (17 genes) were selected for further analysis (Supplementary table 1). Among the genes targeted by siRNA pools that repressed the reporter were the positive controls: *TGFBR1* and *TGFBR2*. In addition, we identified the siRNA pool against *ALK1* (*ACVRL1*) as an activator of the TGFβ responsive reporter. ALK1 was previously identified as a TGFβ superfamily receptor type I protein that can complex with TGFBR2 and directly antagonizes TGFβ transcriptional activation mediated by TGFBR1 [15, 16]. The fact that the screen was able to identify these genes that are part of the canonical TGFβ signaling network support the notion that at least some of the other genes in the hit list are genuine players in the TGFβ pathway.

As a first step to validate

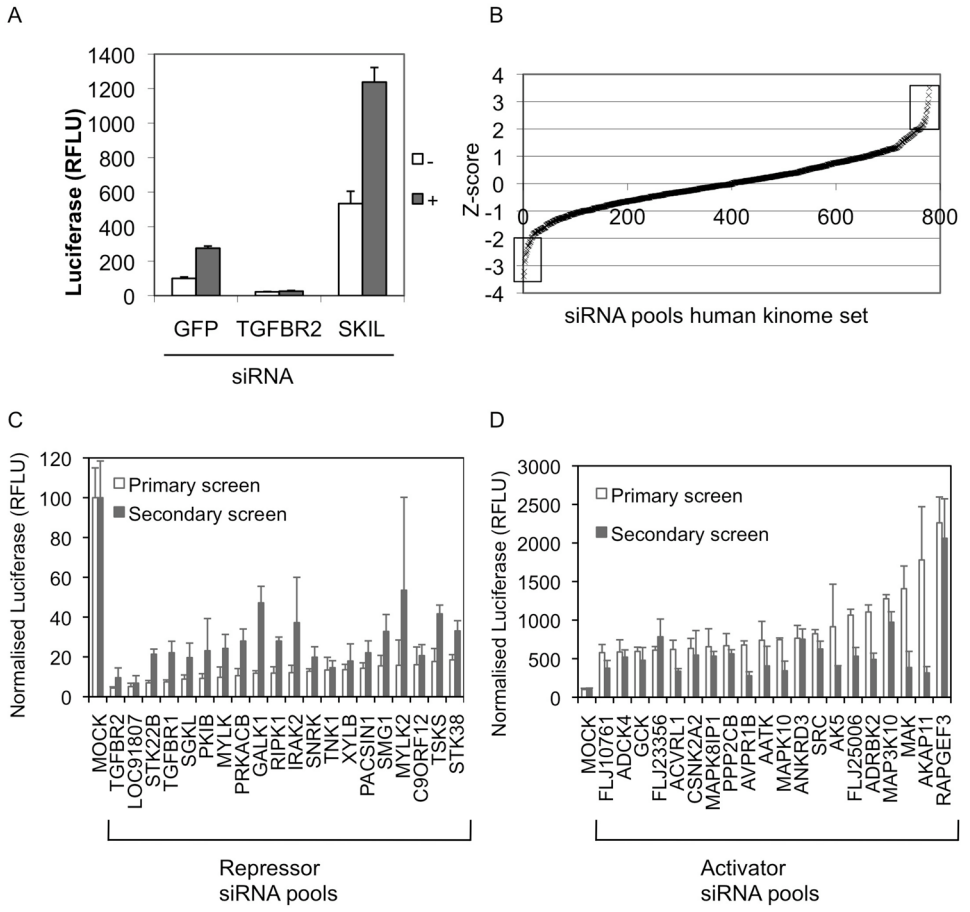


**Figure 1**

**Screen with TGFβ responsive reporter identifies modulators of the TGFβ pathway**

*U2OS-CAGA cells harboring a stable TGFβ responsive luciferase reporter were transfected with siRNAs against GFP, TGFBR2 or SKIL and treated with 200 pM TGFβ (+) for 14 hrs or left untreated (-) (a). Results from a kinase siRNA screen, Z-scores were calculated and plotted in ascending order. Boxed areas indicate the siRNA pools that were selected for follow-up which respectively repress or activate the TGFβ responsive reporter (b). Seventeen siRNA pools that repress the reporter (c) and twenty siRNAs that activate the reporter (d) were tested in a follow-up experiment. The normalized luciferase counts from the screen (white bars) and follow-up (black bars) are plotted.*

our screen we re-tested the same siRNA pools that were identified by the screen to verify that they could indeed reproduce the phenotype from the primary screen. Therefore, we transfected 37 siRNA pools into the U2OS-CAGA cell line and measured the luciferase signal. All 37 siRNA pools, selected by their Z-score, could significantly reproduce the phenotype that was measured in the primary screen, indicating that the initial screen with the siRNA pools was reproducible (fig. 1c and 1d).

One of the mayor drawbacks

of using RNAi as a screening tool is that some observed phenotypes can potentially be caused by 'off-target' effects [17, 18]. Therefore we performed a second round of validation for a subset of our hits. We selected hits based on the position in the primary hit list. In addition, protein-protein interaction databases were used to preferentially select hits that interact with known TGFβ pathway members. Sixteen hits (eight siRNA pools that could activate the reporter and eight that repressed) were selected for a second round of validation. In this second round validation the four siRNAs of each siRNA pool were tested separately, to test if they could reproduce the originally observed phenotype. For eleven of the sixteen hits tested we identified two or more individual siRNAs that could reproduce the original phenotype. The genes targeted by these siRNAs are considered to be 'on target' [19] (fig. 2, supplementary fig. S1a and S1b).

### *Effect of knockdown of 'on-target' hits on endogenous TGFβ signaling*

Since the reporter system used here is only an indirect measurement of TGFβ pathway activity, we set out to test if the validated hits could also affect TGFβ target gene expression. Many different genes are directly regulated by TGFβ; among these genes are *CDKN1A*, *SMAD7*, *PAI-1* and *MYC*. As a model for endogenous TGFβ signaling we used the prostate cancer cell line PC3, in these cells transcription of *CDKN1A, SMAD7, PAI-1* is upregulated while MYC is transcriptionally repressed after addition of TGFβ. Because we identified a relative large number (11) of hits that proved to be 'on-target', we decided to proceed with only the genes whose downregulation impaired activation of the TGFβ reporter (5 in total)

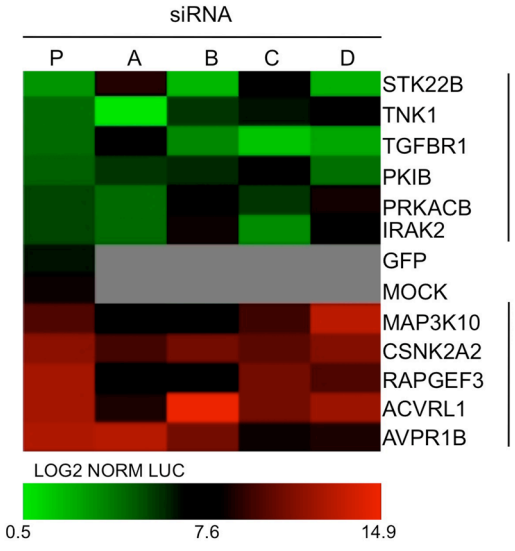


**Figure 2**
**Eleven hits from the screen are 'on-target'**
*The four separate siRNAs that form the siRNA pool (P) were tested separately (A,B, C, D) in the U2OS-CAGA cell line. MOCK (only transfection reagent) and a GFP siRNA were taken along as negative controls. LOG2 normalized luciferase counts of hits that validate with two or more separate siRNAs were plotted in a heatmap.*

as these genes are potential novel targets for therapy in cancer. These five hits, together with TGFBR2 used as a control, were tested for their ability to modulate endogenous TGFβ target gene expression. Indeed, all hits tested showed impaired target gene regulation for two or more endogenous TGFβ targets (fig. 3a-d).

### *Identified hits are involved in SMAD2/3 cytoplasmic to nuclear translocation*

TGFβ target gene activation is a downstream event in the TGFβ signaling cascade, which is preceded by the translocation of SMAD2/3 from the cytoplasm to the nucleus. For this reason we tested if the genes that could repress target gene activation also impaired SMAD2/3 translocation. As a control, we measured the effect of the knockdown of TGFBR2 on TGFβ induced SMAD2/3 nuclear translocation by immunohistochemistry. We quantified the effect by determining the ratio of SMAD2/3 in the nucleus versus the cytoplasm using Cellprofiler software [20] (fig. 4a). PC3 cells were transfected with siRNAs targeting the 'on

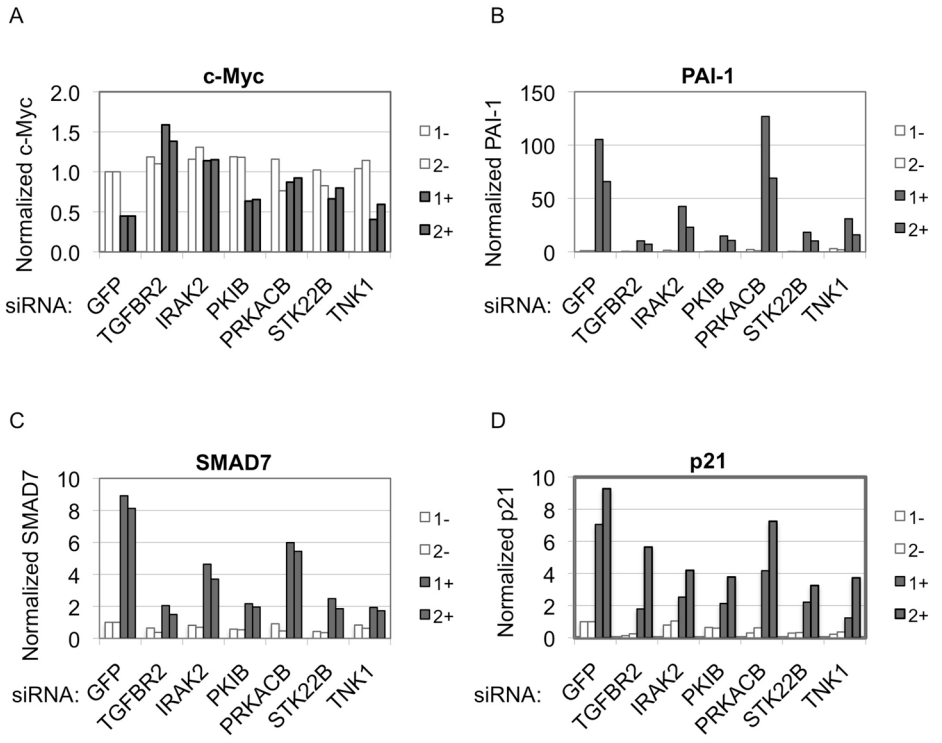


**Figure 3**
**Endogenous TGFβ target gene regulation**
*The siRNAs targeting 'on target' hits which repress the reporter were transfected in PC3 cells and target genes were not induced (in duplicate; 1- and 2-) or induced with TGFβ; 2 hrs for c-Myc (a) and p21$^{CIP1}$ (d) or 8 hrs for PAI-1 (b) and SMAD7 (c) (in duplicate; 1+ and 2+). The mRNA levels of the target genes were determined by quantitative PCR and were normalized to the reference gene RPL13.*

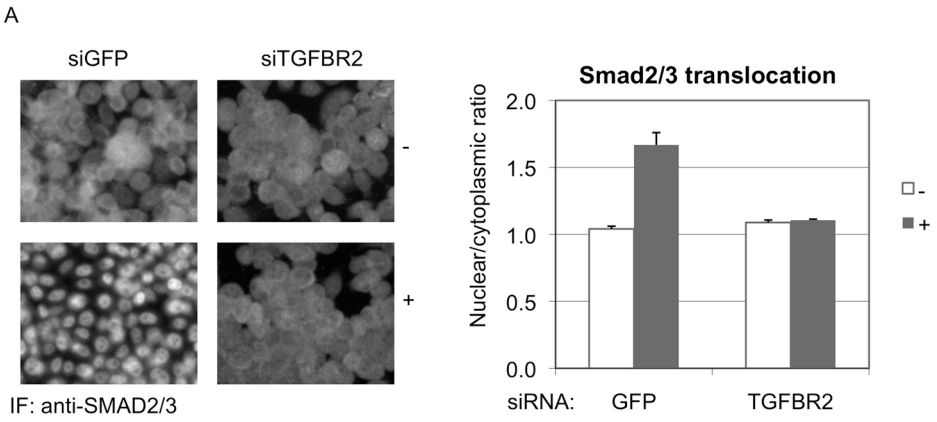


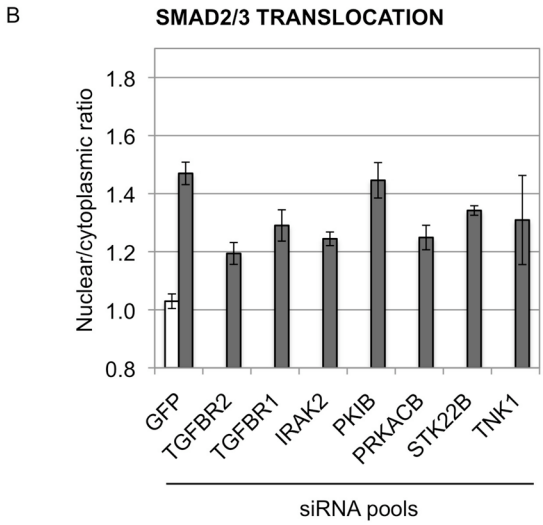


**Figure 4**
**Effect of knockdown of the hits on SMAD2/3 translocation**
*PC3 cells were transfected with siRNAs against GFP and TGFBR2, cells were treated with TGFβ (+) for 1 hr or left untreated (-). Immunohistochemistry was performed with an antibody specific for smad2/3 and cells were counterstained with DAPI to determine the position of the nuclei. The ratio of nuclear and cytoplasmic smad2/3 is determined with cell profiler (a). PC3 cells were transfected with siRNA pools and treated with TGFβ for 1 hr (+). The negative control siGFP was also tested in non-treated condition (-). Immunofluorescence for smad2/3 was performed and the images were quantified with Cellprofiler (b).*

target' hits in order to determine the nuclear/cytoplasmic ratio of SMAD2/3 in presence of TGFβ. A clear reduction in SMAD2/3 nuclear accumulation was measured in cells transfected with siRNAs against *TGFBR1* and *TGFBR2*. In addition, we measured a lower SMAD2/3 nuclear/cytoplasmic ratio for cells transfected with siRNA pools against *IRAK2*, *PRKACB*, *TNK1* and *STK22B* (fig. 4b). This suggests that IRAK2, PRKACB, TNK1 and STK22B function upstream or at the level of SMAD2/3 translocation in the TGFβ pathway. For PKIB the SMAD2/3 translocation seems to be intact suggesting that PKIB inactivates the TGFβ target gene activation at a lower level.

### *IRAK2 is a genuine player in the TGFβ signaling cascade*

As can be seen in figure 3, only knockdown of *IRAK2* expression affected all bona fide TGFβ target genes tested, which was accompanied by reduced nuclear

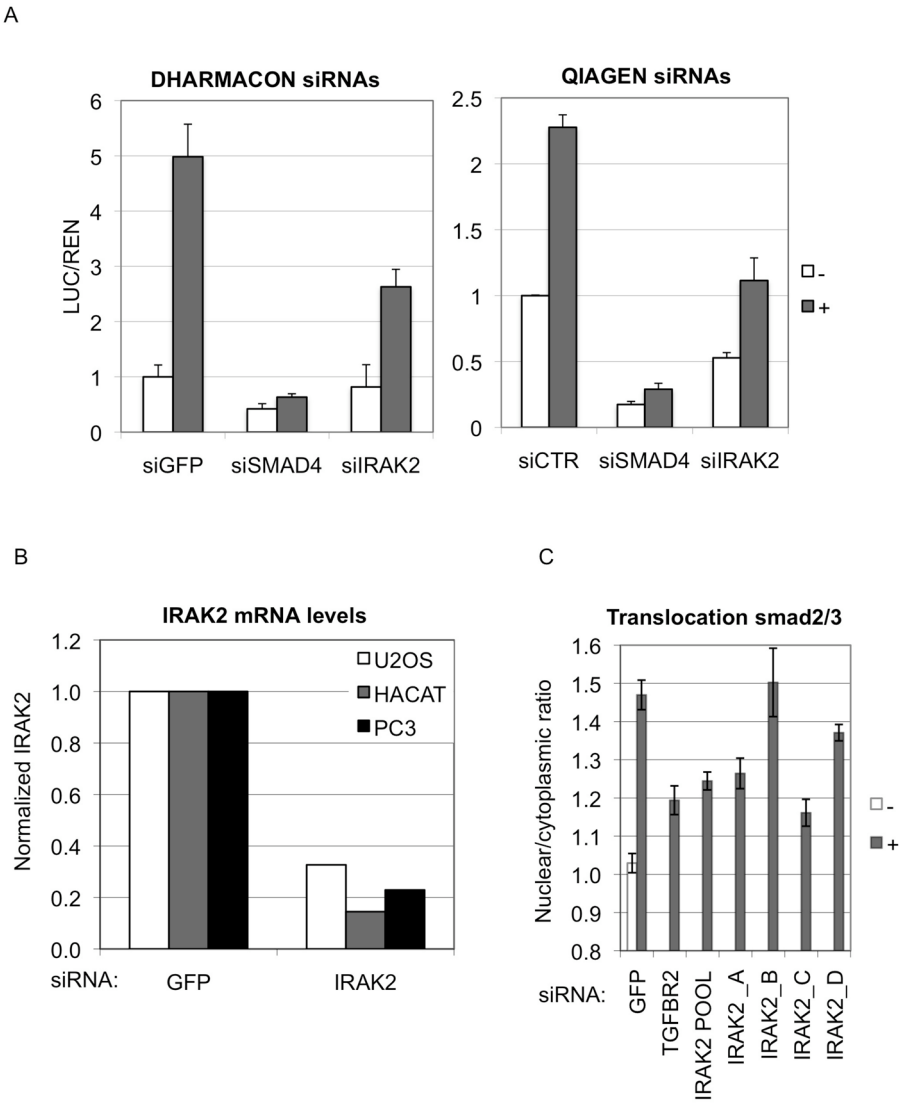


**Figure 5**
**IRAK2 is a genuine regulator of TGFβ signaling**
*U2OS cells were transfected with $CAGA_{12}$-Luc and TK-Renilla. Subsequently, Dharmacon and Qiagen siRNA pools were reverse transfected and the cells were treated with TGFβ (+) for 14 hrs or left untreated (-). Renilla normalized luciferase counts are plotted on the y-axis and siRNAs against GFP and SMAD4 were used as negative and positive controls respectively (a). U2OS, HaCaT and PC3 cells were transfected with a GFP siRNA or the Dharmacon siRNA pool against IRAK2. The mRNA levels of the IRAK2 were determined by quantitative PCR and were normalized against the reference genes RPL13 (U2OS) or GAPDH (HaCaT and PC3) (b). PC3 were transfected with the separate siRNAs and the siRNA pool (both from Dharmacon) against IRAK2 and treated with TGFβ for 1 hr (+). The negative control, siGFP was also tested in non-treated condition (-). Immunofluorescence for smad2/3 was performed and the images were quantified with Cellprofiler (c).*

translocation of SMAD2/3. Therefore, we decided to perform an additional validation round and a more in-depth analysis on the function of IRAK2 in the TGFβ signaling pathway. Previously, IRAK2 (IL-1R-associated kinase) was described to play a role in Toll like receptor signaling [21].

As an extra round of validation we tested if siRNAs targeting *IRAK2* obtained from a different vendor (QIAGEN) could also repress a TGFβ responsive reporter. The new pool of siRNAs contains siRNAs duplexes that target different sequences in the IRAK2 transcript. When we transfected these siRNAs we again observe repression of the TGFβ responsive reporter.

Furthermore we tested in different cell-lines if the *IRAK2* siRNA pool that was used in the primary screen confers knockdown of *IRAK2* mRNA. In all cell-lines used reduced *IRAK2* mRNA levels were measured in the cells transfected with IRAK2 siRNAs (fig. 5b). Subsequently we determined if separate siRNAs targeting *IRAK2* could also block the translocation of SMAD2/3. For the two siRNAs (A and C) that can repress the TGFβ responsive reporter we could also show a decrease off SMAD2/3 nuclear translocation (fig. 5c).

***IRAK2 knockdown affects SMAD2, but not SMAD3, translocation to the nucleus***

As shown earlier knockdown of the identified hits has a clear effect on the TGFβ induced translocation of SMAD2/3. However it must be noted the antibody used in the immunofluorescence assay (fig. 4) detects both the SMAD2 and SMAD3 proteins. This can potentially lead to misinterpretation of the results as the individual contributions of SMAD2 and SMAD3 cannot be determined. For this reason we measured the effect of *IRAK2* knockdown specifically on SMAD2 and SMAD3 individually. Therefore we transfected PC3 cells with either control or *IRAK2* siRNAs and after incubation treated the cells with TGFβ for 1 hour. Nuclear and cytoplasmic extracts were prepared and the lysates were analyzed by western blot using antibodies that can specifically detect either SMAD2 or SMAD3 (fig. 6a). In control transfected cells (siRNA GFP) a regular translocation of SMAD2 and SMAD3 can be observed after treatment with TGFβ. Strikingly in cells that were transfected with *IRAK2* siRNAs showed a normal translocation of SMAD3, but an impaired translocation of SMAD2. This points into a specific role for IRAK2 in the activation of SMAD2.

***IRAK2 knockdown impairs SMAD2 but not SMAD3 phosphorylation***

SMAD2/3 translocation is preceded by a phosphorylation by the TGFβ receptors [22-24]. For this reason we measured the level of phosporylation of both SMAD2 and SMAD3 upon *IRAK2* knockdown. PC3 cells were transfected with siRNAs targeting GFP and IRAK2 and incubated for 48 hours Transfected cells were subsequently treated with TGFβ for 1 hour. Protein lysates were prepared and analysed by western blot. No change in total

levels of either SMAD2 or SMAD3 could be detected while a reduction in phosphorylated SMAD2, but not SMAD3, was observed. This supports the notion that IRAK2 is specifically required for SMAD2 activation by TGFβ.

***IRAK2 knockdown abrogates the TGFβ induced cell cycle arrest***

Knockdown of *IRAK2* impaired the TGFβ target gene activation of *MYC*, *PAI-1*, $p21^{CIP1}$ and *SMAD7* (fig. 3). At least three of these genes are involved in cell cycle regulation (*MYC*, *PAI-1* and $p21^{CIP1}$) and it has been shown that $p21^{CIP1}$ and *PAI-1* are required for a TGFβ induced proliferative arrest [25, 26]. For this reason we setup an experiment to test if *IRAK2* is also required for a TGFβ induced cell cycle arrest. TGFβ is known to induce a G1 cell cycle arrest and consequently fewer cells will enter the DNA replication Phase (S phase). This arrest can be clearly measured in the HaCat cell-line which is derived from human keratinocytes. As expected a TGFBR2 targeting siRNA pool can block the proliferative arrest. Moreover, we also observed that knockdown of IRAK2 can also partly block the G1 cell cycle arrest (fig. 6c).

## Discussion

In this study we describe the identification of new modulators of the TGFβ pathway through the screening of a siRNA library targeting kinases and kinase related genes. Data analysis of the screen revealed a relatively large number of genes that could either repress or activate the TGFβ responsive reporter. Somewhat surprising was the fact that the data-distribution is exponential instead of linear. However, this was also observed in two previously performed reporter based RNAi screens [13, 27]. Some RNAi screening efforts have reported high levels of 'off-target' effects caused by aspecific suppression of mRNAs [28, 29]. Therefore we were pleased to find that about 70% (11 out of 16 genes) of the hits tested could be indicated as 'on target' [19]

Observations made in reporter assays can be are not necessarily reflecting endogenous pathway activation. Therefore we tested if the 5 'on target' hits that repressed the reporter also repress endogenous target gene induction. This experiment was performed in a different cell line than the original U2OS-CAGA to excluded cell type specificity of the identified hits. For all 5 'on target' hits impaired activation of two or more endogenous target genes was observed. The fact that not all 5 hits show a full repression on all TGFβ target genes can be explained by various previously reported observations. For instance the fact that the ratio of SMAD2, 3 and 4 dictates the selectivity for certain target genes [30-33]. In addition the availability of SMAD co-factors can also determine the specific regulation of subsets of TGFβ target

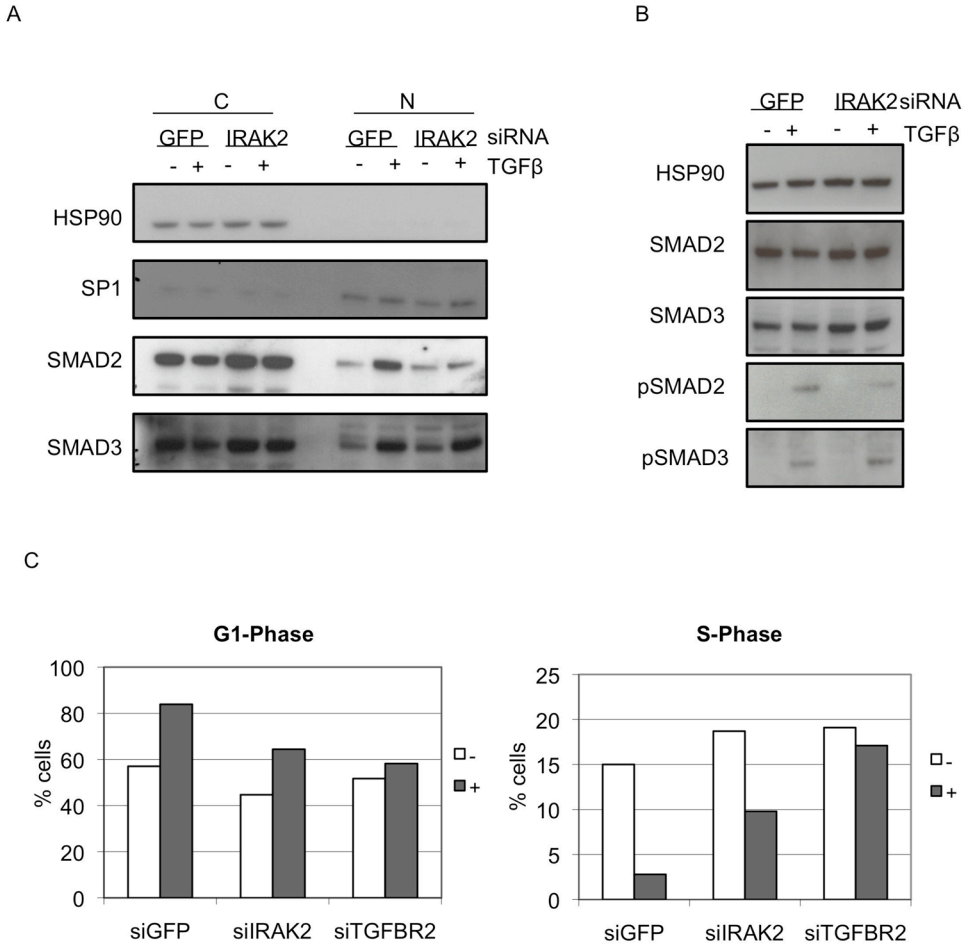


**Figure 6**
**IRAK2 knockdown impairs SMAD2 and SMAD3 translocation and phosphorylation**
*PC3 cells were transfected with siGFP and IRAK2 siRNAs (siRNA pool) and cells were treated with TGFβ (+) for 1 hr or left untreated (-). Nuclear and cytoplasmic fractions were immunoblotted for HSP90; cytosolic loading control, SP1; nuclear loading control and antibodies specific for SMAD2 and SMAD3 (a). To study the SMAD2 and 3 phosphorylation whole cell lysates were immunoblotted for HSP90 (loading control), total SMAD2 and SMAD3 protein and with phospo-SMAD2 (Ser465/476) and phospho-SMAD3 (Ser423/425) antibodies (b). HaCaT cells were transfected with siGFP, TGFBR2 or IRAK2 siRNAs (siRNA pool) and cells were treated with TGFβ (+) for 24 hrs or left untreated (-). The cells were fixed and stained with propidium iodide. Cell cycle profiles were measured and the amount of cells is G1 phase and S phase is plotted.*

genes [3]. The fact that our newly identified hits can regulate the TGFβ dependent transcription of certain TGFβ targets suggests that these genes indeed have a role in the TGFβ pathway.

The TGFβ/SMAD signaling pathway can be regulated at many different levels, co-factors that regulate SMAD dependent transcription, nucleopore proteins assist in SMAD nuclear accumulation and of course the phosphorylation by the TGFβ receptors. Strikingly for four out of five of the newly identified modulators of TGFβ signaling (IRAK2, PRKACB, STK22B and TNK1) we observed a defective SMAD2/3 translocation. This points into a direction for these genes to be function upstream of the SMAD translocation event.

***IRAK2 is specifically required for SMAD2 activation***

When we tested the effects of all newly identified genes on endogenous TGFβ target genes only *IRAK2* knockdown impaired the regulation of all tested TGFβ target genes. Further analysis showed that IRAK2 seems specifically required for the TGFβ dependent phosphorylation and subsequent translocation of SMAD2. Therefore it is expected that the observed effects of *IRAK2* knockdown at the $CAGA_{12}$-Luc reporter are also caused by an impaired activation of SMAD2. However several studies have reported that SMAD3 is responsible for the majority of the TGFβ induced phenotypes and that SMAD2 is often dispensable [32-34]. More recently it was reported that under some conditions SMAD2 indeed plays a critical role in transmitting TGFβ signals from the cell membrane to the nucleus [35]. More experiments are required to fully understand the mechanism of the loss of SMAD2-phosphorylation in cells with knockdown of IRAK2.

***IRAK2 and SMAD2: connecting IL-1 and TGFβ signaling***

IRAK2 is part of a family of four IL-1R-associated kinases (IRAKs) and it was previously predicted that IRAK2 does not contain an active kinase domain [36, 37]. As it's name suggest IRAK2 has been found downstream of the IL-1R in a complex with TRAF6 and MyD88 [38]. It was only recently, unveiled that IRAK2 also has a functional role in Toll like receptor signaling [21, 39]. Our observation that IRAK2 ablation leads to an impaired TGFβ response potentially suggests a possible interaction between TGFβ and IL-1/TLR signaling. This is supported by various previously performed studies. For example the fact that IRAK2 was found in a luminescence based interactome screen to interact with both SMAD2 and SMURF1 [12]. In addition it was recently shown that TRAF6, which interacts with IRAK2, mediates TGFβ dependent activation of JNK and p38. This effect was reported to be SMAD independent and which was proven by the fact that TRAF6 knockdown does not lead to activation of a TGFβ responsive reporter [40]. Finally it was shown that stimulation of cells with IL-1β leads in many cases to phosphorylation of SMAD2 and subsequent target gene activation [41]. Taken together our and others

observations indication cross talk between two important cellular signaling pathways involved in immunity and other processes.

## Methods

### *Cell lines & culture conditions*

U2OS, HaCaT and PC3 cells were cultured in DMEM supplemented with 10% FCS, penicillin, streptomycin and glutamine. All cells were cultured at 37°C in 5% $CO_2$.

### *Generation of stable reporter cell line*

U2OS cells were transfected using calcium phosphate with the TGFβ responsive reporter pGL3-$CAGA_{12}$-Luc and a puromycin resistant plasmid pBabe-puro in a ratio 10:1. Next the cells were sparsely and selected with 2 µg/ml puromycin. Subsequently, colonies were picked and tested these for TGFβ dependent induction of luciferase signal.

### *siRNA transfection*

Cells were reverse transfected with siRNAs according to manufacturers instructions (Dharmacon) (Day 1). Dharmafect 1 (Dharmacon) was used for U2OS cells and Dharmafect 2 (Dharmacon) for HaCaT and PC3 cells. At day two penicillin and streptomycin was added. TGFβ (200 pM) was added overnight on day 3 (U2OS) or for 24 hrs (HaCaT). For PC3 cells TGFβ (200 pM) was added on day 4 for 2 or 8 hrs in order to assay target gene activation or 1 hr for the SMAD2/3 translocation assay.

### *Human kinase siRNA screen*

Cells with stably integrated TGFβ responsive reporter were reverse transfected in 384 well plates in triplicate with the human kinome library of Dharmacon. Dharmafect 1 (0.1 µl per 384-well) was used as transfection reagent and the siRNA pools were transfected at a concentration of 50 nM. 3000 cells were seeded per well with a cell dispenser (Wellmate, Matrix). The transfection was performed in absence of antibiotics. Some 18 hrs after the transfection we added the penicillin and streptomycin. 48 hrs after transfection cells were stimulated with TGFβ (200pM is used in all experiments) for 14 hrs. Cell titer blue reagent (Promega) is used in order to determine the cell viability. After 1 hr incubation $560_{EX}/590_{EM}$ fluorescence is measured with a plate reader (Envision multilabel reader 2101, Perkin Elmer). Subsequently, medium was aspirated with a robot (STAR liquid handling workstation, Hamilton) and luminescence was measured with the same plate reader using Steady-Glo Luciferase (Promega).

The cell viability counts were used to calculate a viability score and siRNA pools that are less than 75% viable are not taken along in the further validation rounds. The luciferase counts were corrected for cell viability that gives the

normalized luciferase counts (NORM LUC). Subsequently, the NORM LUC counts are LOG2 transformed in order to get a normal distribution. The transformed NORM LUC counts are used to calculate the Z-score (Z = (luciferase measurement/ average luciferase of the population)/standard deviation of the population) per plate in order to be able to compare the different plates with each other. We did further validation on the siRNA siRNA pools that scored a Z<-2 or a Z >2.

***Validation of single siRNAs***

The four separate siRNAs and the siRNA pool were tested in the U2OS cell-line with stable TGFβ reporter. Two controls were taken along; GFP siRNA and MOCK (only transfection reagent). All experiments were performed three times in using quadruplicate transfection and one representative experiment is shown. For the heatmap representation data was normalized to GFP and the counts were LOG2 transformed. The heatmap was created with TM4 software [42].

***Immunohistochemistry to quantify SMAD 2/3 translocation***

Cells were cultured in 96 or 384 well plates. Formaldehyde was used for fixation of the cells and we permeabilized with 0.2% Triton X-100. Subsequently, samples were blocked with 5% BSA in PBST (0.05% Tween 20 in PBS). A SMAD2/3 (BD Transduction Laboratories, 610842) specific 1st antibody was used and subsequently a mouse FITC 488 conjugated (Alexa Fluor 488, Invitrogen) secondary antibody. The cells were counterstained with DAPI in order to define the position of the nuclei. Readout was performed with a high content imager (Pathway 855, BD biosciences) using a 20x objective (Olympus). CellProfiler software [20] has been used to quantify the nuclear/cytoplasmic SMAD2/3 ratio of all individual cells per well.

***Western blotting***

Cell lysates were separated using 4-12% Bis-Tris gels (Nupage, Invitrogen). Proteins were transferred to PVDF membrane and incubated with primary antibody as indicated. Primary antibodies were detected using a secondary HRP-conjugated antibody. Antibodies used for these studies: Hsp90 (Santa Cruz H-114, sc-7947), SP1 (Santa Cruz PEP 2, sc-59), SMAD2 (Cell Signaling (L16D3) #3103), SMAD3 (Cell Signaling (C67H9) #9523), p-SMAD2 ser465/467 (Cell Signaling #3101)
p-SMAD3 ser423/425 (Cell Signaling (C25A9) #9520).

***Quantitative PCR***

Total RNA was isolated using TRIzol (Invitrogen). From the total RNA cDNA was generated using Superscript II (Invitrogen) using random primers (Invitrogen). cDNA was diluted and QRT reaction was performed using FAST Cyber green (Invitrogen) with specific primers (Supplementary table 1). All QRT reactions were run in parallel for RPL13 or GAPDH to control of for input cDNA. The QRT reactions were run at a fast Real Time PCR system (AB7500, Applied Biosystems).

### *Cell-cycle analysis*

For fluorescence-activated cell sorting (FACS) analysis, siRNA transfected HaCaT cells that were TGFβ treated for 24 hrs are fixed, stained and assayed as described previously [43].

## References


1. Siegel, P.M. and J. Massague, Cytostatic and apoptotic actions of TGF-beta in homeostasis and cancer. Nat Rev Cancer, 2003. 3(11): p. 807-21.
2. Massague, J., TGFbeta in Cancer. Cell, 2008. 134(2): p. 215-30.
3. Massague, J., J. Seoane, and D. Wotton, Smad transcription factors. Genes Dev, 2005. 19(23): p. 2783-810.
4. Massague, J. and R.R. Gomis, The logic of TGFbeta signaling. FEBS Lett, 2006. 580(12): p. 2811-20.
5. Datto, M.B., et al., Transforming growth factor beta induces the cyclin-dependent kinase inhibitor p21 through a p53-independent mechanism. Proc Natl Acad Sci U S A, 1995. 92(12): p. 5545-9.
6. Hannon, G.J. and D. Beach, p15INK4B is a potential effector of TGF-beta-induced cell cycle arrest. Nature, 1994. 371(6494): p. 257-61.
7. Seoane, J., et al., TGFbeta influences Myc, Miz-1 and Smad to control the CDK inhibitor p15INK4b. Nat Cell Biol, 2001. 3(4): p. 400-8.
8. Bruna, A., et al., High TGFbeta-Smad activity confers poor prognosis in glioma patients and promotes cell proliferation depending on the methylation of the PDGF-B gene. Cancer Cell, 2007. 11(2): p. 147-60.
9. Penuelas, S., et al., TGF-beta increases glioma-initiating cell self-renewal through the induction of LIF in human glioblastoma. Cancer Cell, 2009. 15(4): p. 315-27.
10. Iyer, S., et al., Targeting TGFbeta signaling for cancer therapy. Cancer Biol Ther, 2005. 4(3): p. 261-6.
11. Colland, F., et al., Functional proteomics mapping of a human signaling pathway. Genome Res, 2004. 14(7): p. 1324-32.
12. Barrios-Rodiles, M., et al., High-throughput mapping of a dynamic signaling network in mammalian cells. Science, 2005. 307(5715): p. 1621-5.
13. Levy, L., et al., Arkadia activates Smad3/Smad4-dependent transcription by triggering signal-induced SnoN degradation. Mol Cell Biol, 2007. 27(17): p. 6068-83.
14. Dennler, S., et al., Direct binding of Smad3 and Smad4 to critical TGF beta-inducible elements in the promoter of human plasminogen activator inhibitor-type 1 gene. EMBO J, 1998. 17(11): p. 3091-100.
15. Oh, S.P., et al., Activin receptor-like kinase 1 modulates transforming growth factor-beta 1 signaling in the regulation of angiogenesis. Proc Natl Acad Sci U S A, 2000. 97(6): p. 2626-31.
16. Goumans, M.J., et al., Activin receptor-like kinase (ALK)1 is an antagonistic mediator of lateral TGFbeta/ALK5 signaling. Mol Cell, 2003. 12(4): p. 817-28.
17. Perrimon, N. and B. Mathey-Prevot, Matter arising: off-targets and genome-scale RNAi screens in Drosophila. Fly (Austin), 2007. 1(1): p. 1-5.
18. Svoboda, P., Off-targeting and other non-specific effects of RNAi experiments in mammalian cells. Curr Opin Mol Ther, 2007. 9(3): p.

248-57.
19. Echeverri, C.J., et al., Minimizing the risk of reporting false positives in large-scale RNAi screens. Nat Methods, 2006. 3(10): p. 777-9.
20. Carpenter, A.E., et al., CellProfiler: image analysis software for identifying and quantifying cell phenotypes. Genome Biol, 2006. 7(10): p. R100.
21. Kawagoe, T., et al., Sequential control of Toll-like receptor-dependent responses by IRAK1 and IRAK2. Nat Immunol, 2008. 9(6): p. 684-91.
22. Abdollah, S., et al., TbetaRI phosphorylation of Smad2 on Ser465 and Ser467 is required for Smad2-Smad4 complex formation and signaling. J Biol Chem, 1997. 272(44): p. 27678-85.
23. Liu, Q., S.S. Huang, and J.S. Huang, Function of the type V transforming growth factor beta receptor in transforming growth factor beta-induced growth inhibition of mink lung epithelial cells. J Biol Chem, 1997. 272(30): p. 18891-5.
24. Souchelnytskyi, S., et al., Phosphorylation of Ser465 and Ser467 in the C terminus of Smad2 mediates interaction with Smad4 and is required for transforming growth factor-beta signaling. J Biol Chem, 1997. 272(44): p. 28107-15.
25. Bachman, K.E., et al., p21(WAF1/CIP1) mediates the growth response to TGF-beta in human epithelial cells. Cancer Biol Ther, 2004. 3(2): p. 221-5.
26. Kortlever, R.M., J.H. Nijwening, and R. Bernards, Transforming growth factor-beta requires its target plasminogen activator inhibitor-1 for cytostatic activity. J Biol Chem, 2008. 283(36): p. 24308-13.
27. Firestein, R., et al., CDK8 is a colorectal cancer oncogene that regulates beta-catenin activity. Nature, 2008. 455(7212): p. 547-51.
28. Ma, Y., et al., Prevalence of off-target effects in Drosophila RNA interference screens. Nature, 2006. 443(7109): p. 359-63.
29. Tang, W., et al., A genome-wide RNAi screen for Wnt/beta-catenin pathway components identifies unexpected roles for TCF transcription factors in cancer. Proc Natl Acad Sci U S A, 2008. 105(28): p. 9697-702.
30. Kim, H.P., et al., Smad-dependent cooperative regulation of interleukin 2 receptor alpha chain gene expression by T cell receptor and transforming growth factor-beta. J Biol Chem, 2005. 280(40): p. 34042-7.
31. Levy, L. and C.S. Hill, Smad4 dependency defines two classes of transforming growth factor {beta} (TGF-{beta}) target genes and distinguishes TGF-{beta}-induced epithelial-mesenchymal transition from its antiproliferative and migratory responses. Mol Cell Biol, 2005. 25(18): p. 8108-25.
32. Piek, E., et al., Functional characterization of transforming growth factor beta signaling in Smad2- and Smad3-deficient fibroblasts. J Biol Chem, 2001. 276(23): p. 19945-53.
33. Yang, Y.C., et al., Hierarchical model of gene regulation by transforming growth factor beta. Proc Natl Acad Sci U S A, 2003. 100(18): p. 10269-74.
34. Brown, K.A., J.A. Pietenpol, and H.L. Moses, A tale of two proteins: differential roles and regulation of Smad2 and Smad3 in TGF-beta signaling. J Cell Biochem, 2007. 101(1): p. 9-33.
35. Yang, J., R. Wahdan-Alaswad, and D. Danielpour, Critical role of Smad2 in tumor suppression and transforming growth factor-beta-induced apoptosis of prostate epithelial cells. Cancer Res, 2009. 69(6): p. 2185-90.
36. Janssens, S. and R. Beyaert, Functional diversity and regulation of different interleukin-1 receptor-associated kinase (IRAK) family members. Mol Cell, 2003. 11(2): p. 293-302.
37. Hanks, S.K. and T. Hunter, Protein

kinases 6. The eukaryotic protein kinase superfamily: kinase (catalytic) domain structure and classification. FASEB J, 1995. 9(8): p. 576-96.
38. Muzio, M., et al., IRAK (Pelle) family member IRAK-2 and MyD88 as proximal mediators of IL-1 signaling. Science, 1997. 278(5343): p. 1612-5.
39. Keating, S.E., et al., IRAK-2 participates in multiple toll-like receptor signaling pathways to NFkappaB via activation of TRAF6 ubiquitination. J Biol Chem, 2007. 282(46): p. 33435-43.
40. Yamashita, M., et al., TRAF6 mediates Smad-independent activation of JNK and p38 by TGF-beta. Mol Cell, 2008. 31(6): p. 918-24.
41. Lu, T., et al., Dose-dependent cross-talk between the transforming growth factor-beta and interleukin-1 signaling pathways. Proc Natl Acad Sci U S A, 2007. 104(11): p. 4365-70.
42. Saeed, A.I., et al., TM4: a free, open-source system for microarray data management and analysis. Biotechniques, 2003. 34(2): p. 374-8.
43. Berns, K., et al., A large-scale RNAi screen in human cells identifies new components of the p53 pathway. Nature, 2004. 428(6981): p. 431-7.

## Acknowledgements
We thank C Lieftink and B Evers for technical assistance. In addition, we thank P ten Dijke and J Seoane for reagents and helpful discussion. Furthermore, we thank T Kuilman for providing the sequences for the QRT reference primers.

## Supplementary tables and figures

| siRNA POOL | NCBI RefSeq | AVG COUNTS | STDEV | Z score | Hitsort and number |
|---|---|---|---|---|---|
| TGFBR2 | NM_003242 | 445 | 64 | -3.4 | REPRESSOR REPORTER 1 |
| LOC91807 | NM_182493 | 570 | 195 | -3.2 | REPRESSOR REPORTER 2 |
| STK22B | NM_053006 | 714 | 122 | -2.9 | REPRESSOR REPORTER 3 |
| TGFBR1 | NM_004612 | 765 | 101 | -2.8 | REPRESSOR REPORTER 4 |
| SGKL | NM_013257 | 908 | 214 | -2.7 | REPRESSOR REPORTER 5 |
| PKIB | NM_032471 | 1037 | 267 | -2.5 | REPRESSOR REPORTER 6 |
| MYLK | NM_005965 | 1098 | 590 | -2.4 | REPRESSOR REPORTER 7 |
| PRKACB | NM_002731 | 1191 | 403 | -2.4 | REPRESSOR REPORTER 8 |
| RIPK1 | NM_003804 | 1219 | 329 | -2.3 | REPRESSOR REPORTER 9 |
| GALK1 | NM_000154 | 1233 | 123 | -2.3 | REPRESSOR REPORTER 10 |
| SNRK | NM_017719 | 1315 | 124 | -2.2 | REPRESSOR REPORTER 11 |
| IRAK2 | NM_001570 | 1359 | 418 | -2.2 | REPRESSOR REPORTER 12 |
| TNK1 | NM_003985 | 1379 | 660 | -2.2 | REPRESSOR REPORTER 13 |
| XYLB | NM_005108 | 1396 | 276 | -2.2 | REPRESSOR REPORTER 14 |
| SMG1 | NM_014006 | 1594 | 546 | -2.0 | REPRESSOR REPORTER 15 |
| PACSIN1 | NM_020804 | 1612 | 311 | -2.0 | REPRESSOR REPORTER 16 |
| C9ORF12 | NM_022755 | 1677 | 935 | -2.0 | REPRESSOR REPORTER 17 |
| RAPGEF3 | NM_006105 | 236250 | 35033 | 3.5 | ACTIVATOR REPORTER 1 |
| AKAP11 | NM_016248 | 185965 | 72124 | 3.2 | ACTIVATOR REPORTER 2 |
| MAK | NM_005906 | 158950 | 33275 | 3.0 | ACTIVATOR REPORTER 3 |
| MAP3K10 | NM_002446 | 144278 | 5978 | 2.9 | ACTIVATOR REPORTER 4 |
| ADRBK2 | NM_005160 | 115431 | 9590 | 2.7 | ACTIVATOR REPORTER 5 |
| FLJ25006 | NM_144610 | 111246 | 7961 | 2.6 | ACTIVATOR REPORTER 6 |
| AK5 | NM_012093 | 95504 | 57637 | 2.5 | ACTIVATOR REPORTER 7 |
| SRC | NM_005417 | 84798 | 5495 | 2.3 | ACTIVATOR REPORTER 8 |
| MAPK10 | NM_002753 | 84297 | 2516 | 2.3 | ACTIVATOR REPORTER 9 |
| ANKRD3 | NM_020639 | 79917 | 17361 | 2.3 | ACTIVATOR REPORTER 10 |
| AATK | XM_375495 | 77166 | 25618 | 2.2 | ACTIVATOR REPORTER 11 |
| PPP2CB | NM_004156 | 75428 | 17818 | 2.2 | ACTIVATOR REPORTER 12 |
| MAPK8IP1 | NM_005456 | 73987 | 26314 | 2.2 | ACTIVATOR REPORTER 13 |
| AVPR1B | NM_000707 | 70746 | 5557 | 2.1 | ACTIVATOR REPORTER 14 |
| CSNK2A2 | NM_001896 | 66154 | 13509 | 2.1 | ACTIVATOR REPORTER 15 |
| ACVRL1 | NM_000020 | 64707 | 12487 | 2.0 | ACTIVATOR REPORTER 16 |
| FLJ23356 | NM_032237 | 63775 | 4867 | 2.0 | ACTIVATOR REPORTER 17 |
| PRPS2 | NM_002765 | 63347 | 6626 | 2.0 | ACTIVATOR REPORTER 18 |
| PFKP | NM_002627 | 62607 | 4563 | 2.0 | ACTIVATOR REPORTER 19 |
| GCK | NM_000162 | 62005 | 5789 | 2.0 | ACTIVATOR REPORTER 20 |
| | | **10666** | **AVG all values** | | |

**Supplementary table 1**
*Overview of the top siRNA siRNA pools that repress and activate the TGFβ responsive reporter with a Z score respectively <-2 or >2.*

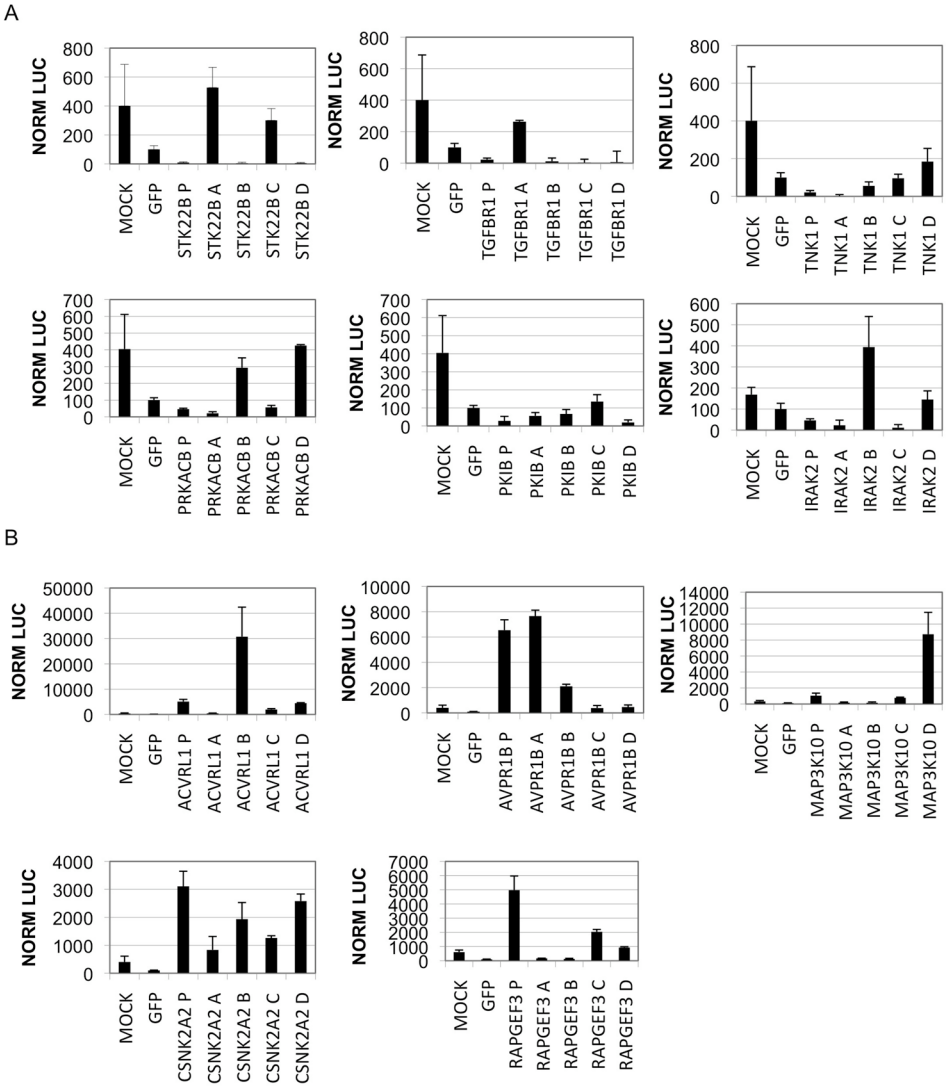


**Supplementary figure 1**

**Validation of four separate siRNAs targeting the outliers of the screen**

*The four separate siRNAs that form the siRNA pool (P) were tested separately (A,B, C, D) on the stable TGFβ responsive luciferase reporter like in the screen. MOCK and a GFP siRNA were taken along as negative controls. Normalized luciferase counts of hits that validate with two or more separate siRNAs as repressor (a) or activator (b) of the reporter are plotted.*

# CHAPTER VII

# General discussion

# General discussion

***The origin of functional genetics***

It was not until the 1940s that discoveries were made which established that genes are the carriers of genetic information [1]. Subsequently, it was shown that this genetic information can be transformed into a biochemical action through the synthesis of proteins [2]. Historically, functional genomics has been the study of gene function through the generation of mutant alleles. This can be a gain of function mutant allele by over-expression of the wildtype coding sequence or a cDNA containing an activating mutation. Loss of function phenotypes can be generated through inactivatig mutations or deletions.

Functional genomics were instrumental in the early searches for cancer genes. Many oncogenes were initially identified through cell fusion or chromosome transfer [3-5]. Improvements of gain of function genetic screens included the generation of retroviral cDNA libraries that can be used for the more specific over-expression of single cDNAs [6]. Many different screens have been performed using retroviral cDNA libraries. Some identified novel human oncogenes as *TBX2*, *TBX3*, *BCL6* and *TWIST* & *DERMO* [7-10]. However, also in other fields of research these libraries have proven their use, i.e. through the identification of the cellular receptor for the Ebola virus [11].

Loss of function can be brought about by different techniques to inactivate genes, i.e. chemical mutagenesis [12, 13], random insertional mutagenesis using retroviruses [14] and conventional knockout generation through homologous recombination [15, 16]. The discovery of RNAi has revolutionized the opportunities to perform loss of function screens in model organisms ranging from nematodes to mammals.

***Building RNAi collections***

Immediately after the discovery of vector-based RNAi, many efforts were started to create collections of shRNA vectors to perform genetic screens. Different methods have been established to build RNAi libraries. The most common method uses the annealing of a set of complementary oligonucleotides that contain the shRNA sequence. We were among the first labs to create a large shRNA library to be used in human cells [17-19]. This library has subsequently been used efficiently to identify genes in many different cancer related pathways [20-23]. Advantages of using the oligo-based construction of shRNA libraries are that the composition of the library is known and can be verified. On the other hand this requires substantial investment, not only financially, but also in labor and automation.

An alternative approach to shRNA library construction was developed independently by three labs [24-27]. Instead of designing shRNAs,

an enzymatic reaction is used to generate shRNA-expressing vectors. Both approaches make use of a restriction enzyme (Mme I) that cuts DNA 20 nt from its recognition site. Using this enzyme in combination with linker DNA fragments it is possible generate an shRNA cassette that can be cloned into a conventional shRNA producing plasmid. The major advantage of this approach is that shRNA libraries can be generated in an unbiased manner and at relatively low cost.

In addition, two individual efforts have been described that generated libraries consisting of shRNA plasmids that contain a random targeting sequence [28, 29]. Like the enzymatic-generated libraries this is a very cost effective approach. One mayor drawback is the complexity of the library, which can be as high as $1 \times 10^9$ for the case of a random 19-mer. This severely hampers the cell culture and shRNA identification processes of a screening effort. Even by today's standards of high throughput sequencing this is a formidable number.

In addition, many collections of siRNAs have been created. This is mainly done through commercial efforts, as it requires extensive infrastructure for production and storage. However siRNAs can also be also be obtained through the enzymatic cleavage of long dsRNAs. This esiRNA (for: endoribonuclease-prepared short interfering RNA) technology is a relative easy approach to constructing siRNA libraries at low cost en little automation required. EsiRNAs have subsequently been used for some elegant screens to find genes that function in the mammalian cell cycle [30, 31]

***Screening the p53 pathway***

In this thesis, three loss-of-function genetic screens using RNAi have been described to identify novel regulators of the p53 tumor suppressor protein. These screens were based on the bypass of a cell cycle arrest that is induced by p53. In the first approach we used a genetically modified cell line that was screened with an shRNA library. The active shRNAs were identified by sequencing of the shRNAs in the colonies that escaped p53-induced growth arrest (Chapter 1). In the second approach, we treated cells with a MDM2 inhibitor and performed an RNAi barcode screen to find shRNAs that mediated bypass of the arrest (Chapter 2). Finally, we used again the cell line from first screen, but now screened the entire library with the shRNA barcode technique. Together, these three genetic screens have led to the identification of 9 genes (table 1) that, when suppressed, allow proliferation under activated p53 conditions.

Many other approaches to perform genetic screens to study the p53 pathway have been reported. Some used antisense RNA libraries instead of RNAi libraries to screen for bypass of a p53-induced cell cycle arrest [32-34]. Other approaches were based on p53 reporter plasmids, these screens have been

performed in both gain- and loss-of-function settings including the use of microRNA libraries [34-36]. Although these screens have identified a number of genes that regulate p53 function, very little overlap between our screening efforts and other approaches can be seen. This can be attributed to differences between the screening systems used, including libraries and cell types. In addition most screens have not been performed till full saturation. In other words, no conclusion can be drawn from genes that were not positively identified. Nevertheless, it is striking that we and others have independently identified two genes of the family of s-adenosyl-homocysteine hydrolases to be essential for the p53 induced cell cycle arrest [18, 32]. It will be important to study the biochemical interaction of these enzymes with components of the p53 pathway in the future.

***Clinical relevance of the novel identified p53-modulating genes***

Although we have shown that the genes identified can override the function of p53 in *in vitro* assays, this does not directly mean that they are also involved *in vivo* carcinogenesis. Further analysis is required to investigate whether these genes are indeed functionally impaired in human cancer samples. This has been done for a number of the 9 genes identified through comparing the expression profiles of these genes between cancer and normal tissue samples [37]. From this study it can be concluded that the expression levels of *HDAC4*, *TIP60*, *KIAA0828* and *RPS6KA6* are significantly down regulated in colon tumor samples. Although it is not shown in this study that the specific tumors with low expression retain a wild type p53 protein, this could be a putative mechanism of functional inactivation of p53 in these tumors.

Besides the suggestion that some hits are lower expressed is encouraging, the case for 53BP1, another hit in our screens, is much stronger. We identified that knockdown of *53BP1* makes cells insensitive to activation of p53 through the inhibition of the MDM2-p53 interaction by small molecules. The 53BP1 protein, which has been shown to interact with p53, is a mediator of the DNA damage response [38, 39]. Therefore it is believed that at least one of the functions of 53BP1 is to transfer the DNA damage signal from the DNA lesion to p53. This is supported by several studies that show that abrogation of the *Trp53bp1* gene in mice can lead to chromosomal instability and tumorigenesis [40, 41]. In support of a true tumor suppressive function it was shown that protein levels of 53BP1 are lower in human tumors that surrounding healthy tissue [42, 43].

One surprising finding was the fact that two enzymes with potentially opposing functions were identified in the same setting. These two enzymes, *TIP60* a histone acetyl transferase and HDAC4 a histone deacetylase, are both involved in chromatin remodeling [44, 45]. For

both *HDAC4* and *TIP60* knockout mouse models have been created. Unfortunately in both cases the homozygous knockout presented a strong developmental phenotype, leading to death in the prenatal stage or shortly after birth, making it impossible to study tumor onset [46, 47]. Strikingly for TIP60 a tumor suppressive function was observed in the heterozygous knockout mouse [46]. In addition the TIP60 gene was also found to be essential to keep embryonic stem cells pluripotent [48].

The studies above show that genes identified through RNAi screening approaches can indeed have tumor suppressive functions. So far a true tumor suppressive phenotype has been observed for three out of the nine genes discovered by us. Obviously these propensities can only be fully uncovered by the use of mouse models. Although not pursued in the studies presented here, the use of shRNA plasmids *in vivo* can potentially speed up the validation of the genes identified in a screen [49]. Future studies are required to show if any of the other six genes also possesses a *bona fide* tumor suppressor function.

***ARNTL: A role for the circadian clock in cancer onset or progression?***

By screening a large shRNA library, we uncovered that the circadian clock regulator ARNTL (BMAL1) is essential for a p53-dependent cell cycle arrest (chapter 3). This observation points into the direction that circadian rhythm might be involved in p53 pathway regulation and therefore tumor suppression. Support for this can be found in studies that show a tumor suppressive function of the *Period 2* circadian target gene [50]. In addition it has been shown that the timing of the cell cycle is also regulated in circadian fashion [51-53].

As we identified nine hits in the p53 pathway, the possibility exists that some of these hits regulate other's hits function. A putative connection between two hits could be found in a study that reported the involvement of TIP60 in mediating cisplatin resistance [53]. Analysis of the promoter led to the identification of two E-boxes that were shown to be activated by the circadian regulators CLOCK and BMAL1 (ARNTL) [53]. This opens up the possibility that the effect measured by the ARNTL knockdown is in effect a result of lower TIP60 levels.

These biochemical findings are also reflected in some epidemiological and drugs response studies. For instance, it was reported that shift-workers have an increased risk of developing cancer [54, 55]. At this moment however, there is no consensus if the reported increase in cancer incidence can be attributed to disruption of circadian rhythm or other confounding factors. Another very interesting observation was the fact that efficacy and tolerability of chemotherapy depends on the time of the day administration [56]. This can at least partially be explained by circadian regulation of liver function [57]. It will be very interesting to see if this so called

chronotherapy can be expanded into a clinical setting.

***RNAi drug screens: insight into mode of action and clinical response***

Besides the identification of gene functions that were previously not associated with cancer, RNAi screen can also be used to give insight in drug responses. Two aspects of drug response can be studied namely, the identification of resistance factors and the investigation of mode of action of a given drug. We have applied RNAi barcode screening to identify genes that are essential for the cytotoxic effects of an acyl sulfonamide, a novel anti-cancer drug. When cells are treated with this drug they enter a G2 arrest and after some time will die through apoptosis. The screen yielded shRNA vectors targeting two genes, *RBX1* and *DDB1*. These two proteins can form a complex that has ubiquitin E3 ligase enzymatic activity [58, 59].

Some studies have previously shown that RBX1 and DDB1 are involved in the ubiquitination of cell cycle regulating proteins like CDT1 [60]. Loss of *RBX1/DDB1* could therefore lead to increase of CDT1 protein concentration. As CDT1 is required for DNA replication this could be a mechanism of resistance. Another intriguing observation was the fact that the knockdown of *DDB1* by itself can shift the cell cycle distribution to the G2 phase of the cell cycle while it can also cause abrogation of a viral induced G2 arrest [61-63]. This shows that at least in some cases the DDB1 protein is involved in regulating the G2 cell cycle checkpoint, although the exact mechanism is poorly understood.

Besides the fact that genes identified through RNAi-based screening approaches give insight in the mechanism of action of a drug, they can also be used as potential treatment response indicators. This has been successfully attempted for drugs currently used for the treatment of cancer patients [23, 64]. For RBX1 and DDB1 it remains to be seen if they can be used as biomarkers of clinical response in patients treated with acyl sulfonamide anti-cancer drugs. This depends on many factors, including whether a reliable method of detection of RBX1 and DDB1 can be developed.

As described above, the development of a diagnostic biomarker from a gene identified from a genetic screen requires sizeable amount of validation and optimization. Performing more specified phenotypic screens can circumvent some of this optimization process. Many currently-used biomarkers are based on the detection of the presence or absence of certain gene products by immuno staining, DNA FISH or RNA quantification. Designing screening techniques that make use of clinical detection modalities can potentially shortcut the development of clinical useful biomarkers.

***Reporter based screening to identify novel TGFβ pathway modulating factors***

Countless cellular processes can influence cell viability and proliferation. For this reason it can be difficult to assign a specific function to genes identified through functional genetic approaches using "proliferation" as a read out of such screens. More specific phenotypes on the other hand can be very difficult to screen using phenotypic read outs. This can be circumvented by the use of reporters systems that reflect the activity of a certain pathway. This has been performed in model organisms with great success (examples: [65, 66]).

By performing a genome wide siRNA screen (data only reported for kinase screen in this thesis) in a cell line with an integrated TGFβ responsive promoter, we have identified genes that were previously not known to be involved in the TGFβ pathway. One major point of concern is the fact that it has been reported that 'off-target' effects are potentially responsible for the majority of hits isolated from these types of screens [67]. However other reporter screening efforts have been able to isolate genes that are very important in signaling pathways involved in cancer [68, 69]. We have identified genes that are candidates to be genuine regulators of the TGFβ pathway. This is supported by the fact that we have also identified four *bona fide* players in the TGFβ pathway (SMAD3/SMAD4/TGFBR1 and TGFBR2).

We have focused on the IRAK2 kinase that was identified to be essential for the TGFβ response. This could be determined both by reporter based assays, but also through incomplete induction of genuine TGFβ target genes. The IRAK2 kinase was previously described to be involved in Interleukin-1 and Toll-like-receptor signaling [70, 71]. Some interplay between TGFβ and IL-1 receptor signaling has been reported like the inhibition of IL-1R effects by the SMAD6 protein [72]. Recently an inverse effect was described, namely the interaction of TRAF6 protein with the TGFBR1 which lead to SMAD independent TGFβ signals [73, 74]. As IRAK2 can bind to TRAF6, a mechanism can be envisioned in which IRAK2 is in proximity of the TGFBR1 facilitating SMAD phosphorylation.

***Off-target effects in RNAi screens***

As more RNAi screens are being performed and reported, some pitfalls also have become apparent. One of these pitfalls is characterized by a-specific phenotypes that can be associated with knockdown of genes through RNAi, the so-called 'off-target' effect [67, 75, 76]. Unfortunately the appearance of these adverse effects is very difficult to predict and usually can only be circumvented by creating large numbers of RNAi molecules targeting the same transcript.

Both the effectiveness of knock-down and degree of 'off-target' effects seem to be related directly to the sequence of the siRNA or shRNA. Currently-used design rules consider properties as thermodynamic stability and sequence identity to create effective siRNAs [77, 78].

One way to improve the use of RNAi is to increase the understanding about which sequences produce a very efficient knockdown without inducing 'off-target' effects. This can be done by improving design rules that dictate which bases are allowed at certain positions combined with target sites in the mRNA.

An easier approach to increase the efficacy of hit identification through RNAi screening is the use of the creation of RNAi libraries containing many different RNAi molecules targeting every transcript (some efforts are under way [79]). This will allow the parallel identification of several RNAi molecules targeting a single transcript lowering the possibility that this observation is caused by an 'off-target' effect. This requires the design and construction of RNAi libraries that consist of somewhere between 3 – 10 x $10^5$ RNAi molecules to cover a mammalian genome. The use of these types of libraries will need the development of novel screening technology to identify phenotype producing RNAi molecules from these libraries.

***Do RNAi-based loss-of-function screens live up to our expectations?***

The RNAi revolution [80] has changed the way researchers can design and perform experiments. As discussed previously, RNAi screens can be designed with the intention to identify drug targets. Up to now various screens have yielded a variety of genes that are involved in all types of processes contributing to cancer pathogenesis. Very few of these findings have been transformed into successful treatment options. However given the time clinical development paths usually take, this is too early to call. One exception is the very nice translation of the outcome of an RNAi screen into clinical application by Brummelkamp and colleagues [81, 82].

Many screens do not have the objective to identify drug targets directly, but rather try to elucidate molecular mechanisms. One example is a duo of screens that were aimed to find essential genes in human cells [83, 84]. This is an excellent example of screens that could not be performed without the use of RNAi. In addition RNAi screens have elucidated drug-gene interactions for some widely used anti-cancer drugs: cisplatin and paclitaxel [85, 86]. Finally some preliminary screening efforts to identify synthetic lethal interactions with the well-known RAS oncogene have been performed [87, 88].

Taken together, over the last 8 years over 100 RNAi screens have been performed ranging in scale from a dozen genes to genome wide efforts. Through these efforts functions were assigned to hundreds of genes many of which were not described before. This shows that RNAi can be used with significant success in mammalian cell systems.

***The future of RNAi screening in mammalian cells***

Much advancement has been made

since the introduction of RNAi libraries in the cancer research field. The majority of RNAi screens that have been published up to date were limited to the screening of relative simple assays like cell viability or reporter assays. Many of these assays do not properly reflect the situation that is seen in *in vivo* tumors. To be able to identify genes that have a true relevance for tumors in patients it might be advisable to use readouts that better reflect the clinical situation.

One technical innovation that might pave the way to the screening of more complex and clinical relevant phenotypes is the so-called living cell microarray. This technique is based on the reverse transfection of cells with either cDNA or RNAi molecules that are deposited on a glass slide [89, 90]. The use of very small siRNA containing spots allows the simultaneous screening of up to 10,000 individual siRNAs on a single glass slide. Because the cells are growing on a glass slide this method is ideal for assays based on immunohistochemical stainings with antibodies of interest. This allows the screening of endogenous processes like protein expression, localization and post-translational modifications. Furthermore it is possible to perform these screens in very high throughput with use of minimal amounts of reagents because of the small size of the glass slide. Another benefit is the fact that the cell microarray technique does not require extensive robotics and is relatively inexpensive.

Another way to screen more complex phenotypes is by limiting the number of genes to be screened. Especially the screening of *in vivo* phenotypes is very attractive, but this is limited to very small sets of shRNAs. Determining which selection of genes to be screened is most promising can be done in many ways. However, to increase the chance of making a clinical relevant observation this is best achieved by using datasets obtained of human tumor specimens. So far, two elegant approaches have shown that this is indeed a feasible method to find cancer relevant genes [91, 92]. Further developments of these types of screens will require the use of sophisticated mouse models that can truly mimic human pathologies. Generation of these mouse models can be assisted by the use of DNA constructs carrying combinations of cDNAs and shRNAs [93, 94]. The use of these constructs allows the simultaneous expression of i.e. oncogenes while inactivating a tumor suppressor by the shRNA in the very same cells.

Other future application could be the functional analysis of patient material by RNAi to assess which genes are essential for survival of an individual tumor. By regular DNA sequencing and gene expression profiling it is possible to determine which genes are mutated or aberrantly expressed. However this does not necessarily indicate the specific dependency of a tumor on a certain cell-signaling pathway. It was recently shown that in some cases cells with identical oncogenic mutations differentially depend on downstream effectors. An example

of this situation was reported for the *PIK3CA* oncogene that was shown to activate either the AKT and SGK3 pathway when mutated [95]. By transfecting isolated tumor cells from patient with a *PIK3CA* mutation with siRNAs targeting either *AKT* or *SGK3* the specific dependency can be determined. In the future these small-scale targeted RNAi based diagnostics could be very useful in guiding therapies in the right direction.

## References


1. Avery OT, M.C.a.M.M., Studies on the chemical nature of the substance inducing transformation of pneumococcal types. Journal of Experimental Medicine, 1944. 79: p. 137-158.
2. Beadle, G.W. and E.L. Tatum, Genetic Control of Biochemical Reactions in Neurospora. Proc Natl Acad Sci U S A, 1941. 27(11): p. 499-506.
3. Cooper, G.M., Cellular transforming genes. Science, 1982. 217(4562): p. 801-6.
4. Harris, H., et al., Suppression of malignancy by cell fusion. Nature, 1969. 223(5204): p. 363-8.
5. Anderson, M.J. and E.J. Stanbridge, Tumor suppressor genes studied by cell hybridization and chromosome transfer. Faseb J, 1993. 7(10): p. 826-33.
6. Kitamura, T., et al., Efficient screening of retroviral cDNA expression libraries. Proc Natl Acad Sci U S A, 1995. 92(20): p. 9146-50.
7. Jacobs, J.J., et al., The oncogene and Polycomb-group gene bmi-1 regulates cell proliferation and senescence through the ink4a locus. Nature, 1999. 397(6715): p. 164-8.
8. Brummelkamp, T.R., et al., TBX-3, the gene mutated in Ulnar-Mammary Syndrome, is a negative regulator of p19ARF and inhibits senescence. J Biol Chem, 2002. 277(8): p. 6567-72.
9. Shvarts, A., et al., A senescence rescue screen identifies BCL6 as an inhibitor of anti-proliferative p19(ARF)-p53 signaling. Genes Dev, 2002. 16(6): p. 681-6.
10. Maestro, R., et al., Twist is a potential oncogene that inhibits apoptosis. Genes Dev, 1999. 13(17): p. 2207-17.
11. Chan, S.Y., et al., Folate receptor-alpha is a cofactor for cellular entry by Marburg and Ebola viruses. Cell, 2001. 106(1): p. 117-26.
12. Schimenti, J. and M. Bucan, Functional genomics in the mouse: phenotype-based mutagenesis screens. Genome Res, 1998. 8(7): p. 698-710.
13. Keays, D.A. and P.M. Nolan, N-ethyl-N-nitrosourea mouse mutants in the dissection of behavioural and psychiatric disorders. Eur J Pharmacol, 2003. 480(1-3): p. 205-17.
14. Uren, A.G., et al., Retroviral insertional mutagenesis: past, present and future. Oncogene, 2005. 24(52): p. 7656-72.
15. Jonkers, J. and A. Berns, Conditional mouse models of sporadic cancer. Nat Rev Cancer, 2002. 2(4): p. 251-65.
16. Austin, C.P., et al., The knockout mouse project. Nat Genet, 2004. 36(9): p. 921-4.
17. Zheng, L., et al., An approach to genomewide screens of expressed small interfering RNAs in mammalian cells. Proc Natl Acad Sci U S A, 2004. 101(1): p. 135-40.
18. Berns, K., et al., A large-scale RNAi screen in human cells identifies new

components of the p53 pathway. Nature, 2004. 428(6981): p. 431-7.
19. Paddison, P.J., et al., A resource for large-scale RNA-interference-based screens in mammals. Nature, 2004. 428(6981): p. 427-31.
20. Kolfschoten, I.G., et al., A genetic screen identifies PITX1 as a suppressor of RAS activity and tumorigenicity. Cell, 2005. 121(6): p. 849-58.
21. Nicke, B., et al., Involvement of MINK, a Ste20 family kinase, in Ras oncogene-induced growth arrest in human ovarian surface epithelial cells. Mol Cell, 2005. 20(5): p. 673-85.
22. Brummelkamp, T.R., et al., An shRNA barcode screen provides insight into cancer cell vulnerability to MDM2 inhibitors. Nat Chem Biol, 2006. 2(4): p. 202-6.
23. Berns, K., et al., A functional genetic approach identifies the PI3K pathway as a major determinant of trastuzumab resistance in breast cancer. Cancer Cell, 2007. 12(4): p. 395-402.
24. Sen, G., et al., Restriction enzyme-generated siRNA (REGS) vectors and libraries. Nat Genet, 2004. 36(2): p. 183-9.
25. Shirane, D., et al., Enzymatic production of RNAi libraries from cDNAs. Nat Genet, 2004. 36(2): p. 190-6.
26. Luo, B., A.D. Heard, and H.F. Lodish, Small interfering RNA production by enzymatic engineering of DNA (SPEED). Proc Natl Acad Sci U S A, 2004. 101(15): p. 5494-9.
27. Buchholz, F., et al., Enzymatically prepared RNAi libraries. Nat Methods, 2006. 3(9): p. 696-700.
28. Chen, M., et al., A universal plasmid library encoding all permutations of small interfering RNA. Proc Natl Acad Sci U S A, 2005. 102(7): p. 2356-61.
29. Wang, Y., et al., A random shRNA-encoding library for phenotypic selection and hit-optimization. PLoS One, 2008. 3(9): p. e3171.
30. Kittler, R., et al., An endoribonuclease-prepared siRNA screen in human cells identifies genes essential for cell division. Nature, 2004. 432(7020): p. 1036-40.
31. Kittler, R., et al., Genome-scale RNAi profiling of cell division in human tissue culture cells. Nat Cell Biol, 2007. 9(12): p. 1401-12.
32. Leal, J.F., et al., Cellular senescence bypass screen identifies new putative tumor suppressor genes. Oncogene, 2008. 27(14): p. 1961-70.
33. Castro, M.E., et al., Loss-of-function genetic screening identifies a cluster of ribosomal proteins regulating p53 function. Carcinogenesis, 2008. 29(7): p. 1343-50.
34. Huang, Q., et al., Identification of p53 regulators by genome-wide functional analysis. Proc Natl Acad Sci U S A, 2004. 101(10): p. 3456-61.
35. Llanos, S., et al., A high-throughput loss-of-function screening identifies novel p53 regulators. Cell Cycle, 2006. 5(16): p. 1880-5.
36. Park, S.Y., et al., miR-29 miRNAs activate p53 by targeting p85 alpha and CDC42. Nat Struct Mol Biol, 2009. 16(1): p. 23-9.
37. ME, L.L., et al., New p53 related genes in human tumors: significant downregulation in colon and lung carcinomas. Oncol Rep, 2006. 16(3): p. 603-8.
38. Iwabuchi, K., et al., Two cellular proteins that bind to wild-type but not mutant p53. Proc Natl Acad Sci U S A, 1994. 91(13): p. 6098-102.
39. Wang, B., et al., 53BP1, a mediator of the DNA damage checkpoint. Science, 2002. 298(5597): p. 1435-8.
40. Morales, J.C., et al., Role for the BRCA1 C-terminal repeats (BRCT) protein 53BP1 in maintaining genomic stability. J Biol Chem, 2003. 278(17): p. 14971-7.
41. Ward, I.M., et al., p53 Binding protein 53BP1 is required for DNA damage responses and tumor suppression in mice. Mol Cell Biol, 2003. 23(7): p. 2556-63.

42. Bartkova, J., et al., DNA damage response mediators MDC1 and 53BP1: constitutive activation and aberrant loss in breast and lung cancer, but not in testicular germ cell tumours. Oncogene, 2007. 26(53): p. 7414-22.
43. Takeyama, K., et al., Integrative analysis reveals 53BP1 copy loss and decreased expression in a subset of human diffuse large B-cell lymphomas. Oncogene, 2008. 27(3): p. 318-22.
44. Squatrito, M., C. Gorrini, and B. Amati, Tip60 in DNA damage response and growth control: many tricks in one HAT. Trends Cell Biol, 2006. 16(9): p. 433-42.
45. Grozinger, C.M., C.A. Hassig, and S.L. Schreiber, Three proteins define a class of human histone deacetylases related to yeast Hda1p. Proc Natl Acad Sci U S A, 1999. 96(9): p. 4868-73.
46. Gorrini, C., et al., Tip60 is a haplo-insufficient tumour suppressor required for an oncogene-induced DNA damage response. Nature, 2007. 448(7157): p. 1063-7.
47. Vega, R.B., et al., Histone deacetylase 4 controls chondrocyte hypertrophy during skeletogenesis. Cell, 2004. 119(4): p. 555-66.
48. Fazzio, T.G., J.T. Huff, and B. Panning, An RNAi screen of chromatin proteins identifies Tip60-p400 as a regulator of embryonic stem cell identity. Cell, 2008. 134(1): p. 162-74.
49. Kunath, T., et al., Transgenic RNA interference in ES cell-derived embryos recapitulates a genetic null phenotype. Nat Biotechnol, 2003. 21(5): p. 559-61.
50. Fu, L., et al., The circadian gene Period2 plays an important role in tumor suppression and DNA damage response in vivo. Cell, 2002. 111(1): p. 41-50.
51. Matsuo, T., et al., Control mechanism of the circadian clock for timing of cell division in vivo. Science, 2003. 302(5643): p. 255-9.
52. Miller, B.H., et al., Circadian and CLOCK-controlled regulation of the mouse transcriptome and cell proliferation. Proc Natl Acad Sci U S A, 2007. 104(9): p. 3342-7.
53. Miyamoto, N., et al., Tip60 is regulated by circadian transcription factor clock and is involved in cisplatin resistance. J Biol Chem, 2008. 283(26): p. 18218-26.
54. Hansen, J., Light at night, shiftwork, and breast cancer risk. J Natl Cancer Inst, 2001. 93(20): p. 1513-5.
55. Viswanathan, A.N., S.E. Hankinson, and E.S. Schernhammer, Night shift work and the risk of endometrial cancer. Cancer Res, 2007. 67(21): p. 10618-22.
56. Levi, F. and U. Schibler, Circadian rhythms: mechanisms and therapeutic implications. Annu Rev Pharmacol Toxicol, 2007. 47: p. 593-628.
57. Gorbacheva, V.Y., et al., Circadian sensitivity to the chemotherapeutic agent cyclophosphamide depends on the functional status of the CLOCK/BMAL1 transactivation complex. Proc Natl Acad Sci U S A, 2005. 102(9): p. 3407-12.
58. Wertz, I.E., et al., Human De-etiolated-1 regulates c-Jun by assembling a CUL4A ubiquitin ligase. Science, 2004. 303(5662): p. 1371-4.
59. Wang, H., et al., Histone H3 and H4 ubiquitylation by the CUL4-DDB-ROC1 ubiquitin ligase facilitates cellular response to DNA damage. Mol Cell, 2006. 22(3): p. 383-94.
60. Hu, J., et al., Targeted ubiquitination of CDT1 by the DDB1-CUL4A-ROC1 ligase in response to DNA damage. Nat Cell Biol, 2004. 6(10): p. 1003-9.
61. Schrofelbauer, B., Y. Hakata, and N.R. Landau, HIV-1 Vpr function is mediated by interaction with the damage-specific DNA-binding protein DDB1. Proc Natl Acad Sci U S A, 2007. 104(10): p. 4130-5.
62. Tan, L., E. Ehrlich, and X.F. Yu, DDB1 and Cul4A are required for human immunodeficiency virus type 1 Vpr-induced G2 arrest. J

Virol, 2007. 81(19): p. 10822-30.
63. Wen, X., et al., The HIV1 protein Vpr acts to promote G2 cell cycle arrest by engaging a DDB1 and Cullin4A-containing ubiquitin ligase complex using VprBP/DCAF1 as an adaptor. J Biol Chem, 2007. 282(37): p. 27046-57.
64. Iorns, E., et al., Identification of CDK10 as an important determinant of resistance to endocrine therapy for breast cancer. Cancer Cell, 2008. 13(2): p. 91-104.
65. Longman, D., et al., Mechanistic insights and identification of two novel factors in the C. elegans NMD pathway. Genes Dev, 2007. 21(9): p. 1075-85.
66. Dorner, S., et al., A genomewide screen for components of the RNAi pathway in Drosophila cultured cells. Proc Natl Acad Sci U S A, 2006. 103(32): p. 11880-5.
67. Ma, Y., et al., Prevalence of off-target effects in Drosophila RNA interference screens. Nature, 2006. 443(7109): p. 359-63.
68. Tang, W., et al., A genome-wide RNAi screen for Wnt/beta-catenin pathway components identifies unexpected roles for TCF transcription factors in cancer. Proc Natl Acad Sci U S A, 2008. 105(28): p. 9697-702.
69. Firestein, R., et al., CDK8 is a colorectal cancer oncogene that regulates beta-catenin activity. Nature, 2008. 455(7212): p. 547-51.
70. Kawagoe, T., et al., Sequential control of Toll-like receptor-dependent responses by IRAK1 and IRAK2. Nat Immunol, 2008. 9(6): p. 684-91.
71. Wan, Y., et al., Interleukin-1 receptor-associated kinase 2 is critical for lipopolysaccharide-mediated post-transcriptional control. J Biol Chem, 2009. 284(16): p. 10367-75.
72. Choi, K.C., et al., Smad6 negatively regulates interleukin 1-receptor-Toll-like receptor signaling through direct interaction with the adaptor Pellino-1. Nat Immunol, 2006. 7(10): p. 1057-65.
73. Sorrentino, A., et al., The type I TGF-beta receptor engages TRAF6 to activate TAK1 in a receptor kinase-independent manner. Nat Cell Biol, 2008. 10(10): p. 1199-207.
74. Yamashita, M., et al., TRAF6 mediates Smad-independent activation of JNK and p38 by TGF-beta. Mol Cell, 2008. 31(6): p. 918-24.
75. Jackson, A.L., et al., Expression profiling reveals off-target gene regulation by RNAi. Nat Biotechnol, 2003. 21(6): p. 635-7.
76. Birmingham, A., et al., 3' UTR seed matches, but not overall identity, are associated with RNAi off-targets. Nat Methods, 2006. 3(3): p. 199-204.
77. Jagla, B., et al., Sequence characteristics of functional siRNAs. RNA, 2005. 11(6): p. 864-72.
78. Bramsen, J.B., et al., A large-scale chemical modification screen identifies design rules to generate siRNAs with high activity, high stability and low toxicity. Nucleic Acids Res, 2009. 37(9): p. 2867-81.
79. Moffat, J., et al., A lentiviral RNAi library for human and mouse genes applied to an arrayed viral high-content screen. Cell, 2006. 124(6): p. 1283-98.
80. Novina, C.D. and P.A. Sharp, The RNAi revolution. Nature, 2004. 430(6996): p. 161-4.
81. Brummelkamp, T.R., et al., Loss of the cylindromatosis tumour suppressor inhibits apoptosis by activating NF-kappaB. Nature, 2003. 424(6950): p. 797-801.
82. Oosterkamp, H.M., et al., An evaluation of the efficacy of topical application of salicylic acid for the treatment of familial cylindromatosis. Br J Dermatol, 2006. 155(1): p. 182-5.
83. Silva, J.M., et al., Profiling essential genes in human mammary cells by multiplex RNAi screening. Science, 2008. 319(5863): p. 617-20.
84. Schlabach, M.R., et al., Cancer

proliferation gene discovery through functional genomics. Science, 2008. 319(5863): p. 620-4.
85. Whitehurst, A.W., et al., Synthetic lethal screen identification of chemosensitizer loci in cancer cells. Nature, 2007. 446(7137): p. 815-9.
86. Bartz, S.R., et al., Small interfering RNA screens reveal enhanced cisplatin cytotoxicity in tumor cells having both BRCA network and TP53 disruptions. Mol Cell Biol, 2006. 26(24): p. 9377-86.
87. Luo, J., et al., A genome-wide RNAi screen identifies multiple synthetic lethal interactions with the Ras oncogene. Cell, 2009. 137(5): p. 835-48.
88. Scholl, C., et al., Synthetic lethal interaction between oncogenic KRAS dependency and STK33 suppression in human cancer cells. Cell, 2009. 137(5): p. 821-34.
89. Wheeler, D.B., A.E. Carpenter, and D.M. Sabatini, Cell microarrays and RNA interference chip away at gene function. Nat Genet, 2005. 37 Suppl: p. S25-30.
90. Ziauddin, J. and D.M. Sabatini, Microarrays of cells expressing defined cDNAs. Nature, 2001. 411(6833): p. 107-10.
91. Zender, L., et al., An oncogenomics-based in vivo RNAi screen identifies tumor suppressors in liver cancer. Cell, 2008. 135(5): p. 852-64.
92. Silva, J.M., et al., Cyfip1 is a putative invasion suppressor in epithelial cancers. Cell, 2009. 137(6): p. 1047-61.
93. Ma, H.T., et al., An inducible system for expression and validation of the specificity of short hairpin RNA in mammalian cells. Nucleic Acids Res, 2007. 35(4): p. e22.
94. Li, F. and R.I. Mahato, Bipartite vectors for co-expression of a growth factor cDNA and short hairpin RNA against an apoptotic gene. J Gene Med, 2009.
95. Vasudevan, K.M., et al., AKT-independent signaling downstream of oncogenic PIK3CA mutations in human cancer. Cancer Cell, 2009. 16(1): p. 21-32.

# APPENDICES

Summary

Samenvatting

Cirruculum Vitae

List of publications

Dankwoord

# Summary

One of the characteristics of cancer is the occurrence of aberrant gene products. Many mutations both activating and inactivating are found in genes controlling the cell cycle and other processes that regulate survival of cells. Some of these mutated genes have been used as targets for cancer therapy. For the majority of human cancers however not adequate treatment regimens are available. It is therefore of great importance to find other genes that are involved in cancer pathogenesis which can subsequently be inhibited by still to be developed drugs. RNA interference (RNAi) is a technique that was recently adapted for use in mammalian cells and can be used to very efficiently suppress expression of specific genes. RNAi can be used to identify genes that are essential for cancer proliferation. The genes identified can potentially be used as drug targets. In addition to finding new targets for drugs RNAi can also be used to identify markers for drug response in tumors. These markers can be used to predict clinical responses to therapies of individual tumors.

This thesis describes the construction and screening of one of the first human RNAi libraries. The screens are performed using conventional and high throughput techniques to find novel cancer relevant genes.

The application of large scale RNAi screens requires the construction of collections of RNAi molecules. This was made possible by the discovery that RNAi can be mediated through plasmid based techniques. In **chapter II** the construction of one of the first large scale collections of short hairpin RNAs (shRNAs) that targets 8000 human genes is described. This library is subsequently screened in a genetic cell model that recapitulates the function of the p53 tumor suppressor. Several genes are identified that when suppressed can abrogate the function of the p53 pathway. These genes are potentially themselves tumor suppressors in human cancer.

Besides screening genetic models RNAi can also be amended for the use of chemical induced phenotypes. Nutlin is an inhibitor of the MDM2 protein which is the protein that is responsible for the degradation of the p53 tumor suppressor protein. Inhibition of MDM2 leads to increase of p53 concentration which induces a cells cycle arrest. The RNAi library was used to find genes that are involved in this cell cycle arrest (**chapter III**). Through this screen it was shown that the 53BP1 protein was essential for this Nutlin induced cell cycle arrest. This was surprising as 53BP1 was previously reported to function upstream of p53.

RNAi screens can be performed in many different ways. Conventional screening options are often very labor intensive and time consuming. Innovative techniques that make use of microarray detection of shRNAs that produce a phenotype made the screening

of RNAi libraries much easier. By screening the same genetic cell system as in chapter 1 but now using the microarray technique a novel set of genes was identified (**chapter IV**). One of these genes is the circadian transcription factor ARNTL. This observation supports the notion that abrogation of the circadian clock might play a role in tumor suppression.

Another very interesting application of RNAi screening involves the testing of anti-cancer drugs. Many drugs currently used to treat cancer patients act through a mechanism that is poorly understood. Even more worrisome is the fact that many patients fail to respond to the administered drugs due to acquired or intrinsic resistance mechanisms. To increase the treatment efficacy of cancer patients it is therefore of great importance to be able to foretell if patient will or will not respond to a certain therapy. RNAi screens can be used to identify genes that mediate resistance and mode of action of cancer drugs. A novel cancer drug with unknown mechanism was tested through a shRNA barcode screen (**chapter V**). This led to the identification of two genes that are part of an ubiquitin E3 ligase complex that mediate resistance to the drug. These two genes can subsequently be developed as markers of response to this novel drug.

In addition to phenotypic assays based on cell proliferation RNAi screens can also be used to study cellular signaling pathways directly. The TGF-beta pathway is a pathway that has a very diverse role in cancer onset and progression. In the first stages of cancer TGF-beta is reported to have a tumor suppressive function while later it can promote the metastasis process. Through a large scale siRNA single-well screen we have attempted to identify novel genes that regulate TGF-beta signaling (**chapter VI**). One of the genes identified encodes the IRAK2 kinase which was previously reported to be involved in IL-1 signaling. This finding shows that RNAi screening can lead to insight in crosstalk between signaling pathways involved in cancer.

More insight in the genes that contribute to cancer onset and progression can lead to the development of novel cancer therapies. In this thesis a series of screens using RNAi is presented showing the potential of RNAi in human cells. Genes were identified in genetic- and drug-screening efforts giving insight in biochemical pathways and drug responses. These genes will have to be tested in more clinical relevant cancer models to show their true involvement in the carcinogenesis process.

# Nederlandse samenvatting

Een belangrijk kenmerk van kanker is het voorkomen van afwijkende genproducten. Zowel activerende als inactiverende mutaties zijn gevonden in genen die de cel-cylus en andere processen reguleren. De inactivatie van gemuteerde eiwitten kan gebruikt worden om de tumorgroei af te remmen. Helaas is voor de meerderheid van de tumoren echter nog geen effective therapie beschikbaar. Daarom is het van groot belang om nieuwe genen te vinden die betrokken zijn bij het ontstaan en in stand houden van tumoren.

De functie van genen kan door middel van verschillende methoden worden onderzocht. Het uitschakelen van genen is een effectieve manier om de functie te achterhalen. Dit was echter lange tijd onmogelijk in menselijke cellen. Een nieuwe techniek genaamd RNA interferentie (RNAi) heeft het mogelijk gemaakt om specifiek genen en hun eiwit producten te remmen. Zo kan RNAi onder meer worden gebruikt om genen te identificeren die essentieel zijn voor de proliferatie van kanker cellen. Deze genen kunnen vervolgens worden gebruikt voor de ontwikkeling van nieuwe medicijnen. Naast het vinden van nieuwe doelwitten van medicijnen is het ook mogelijk om RNAi te gebruiken om indicatoren van klinische respons te vinden in individuele tumoren. Door deze indicatoren kan worden voorspeld of een tumor wel of niet op een bepaalde behandeling zal reageren.

Dit proefschrift beschrijft de constructie en screening van een van de eerste grote RNAi collecties voor gebruik in humane cellen. De beschreven screens zijn uitgevoerd middels conventionele en nieuwe technieken met het doel om nieuwe kanker genen te vinden.

Het screenen van grote aantallen genen in humane cellen vereist de constructie van een collectie van RNAi inducerende moleculen. Dit werd pas mogelijk nadat was ontdekt dat RNAi kan worden toegepast door middel van een plasmide dat een kort haarspeld RNA maakt. In **hoofdstuk II** wordt de constructie van een RNAi collectie die 8000 humane genen kan onderdrukken beschreven. Deze collectie is vervolgens gebruikt in een genetisch celkweek model dat de activatie van het p53 tumor onderdrukkend eiwit simuleert. Een aantal verschillende genen die de activiteit van p53 kunnen blokkeren werd opgepikt door middel van deze screen. Het is mogelijk dat de opgepikte genen zelf een tumor onderdrukkende functie hebben.

Naast het gebruik van genetische cel systemen is het ook mogelijk om screens met chemische stoffen uit te voeren. Nutlin is een klein molecuul dat de functie van het MDM2 eiwit kan remmen. Het MDM2 eiwit is verantwoordelijk voor de afbraak van de p53 tumor suppressor. Onderdrukking van MDM2 functie leidt daarom tot een verhoogde concentratie van het p53 eiwit wat een remming

van cel cyclus tot gevolg heeft. De eerder beschreven RNAi collectie is vervolgens gebruikt om genen te vinden die betrokken zijn bij de remming van de cel cyclus onder invloed van Nutlin (**hoofdstuk III**). Middels deze screen werd aangetoond dat het 53BP1 eiwit noodzakelijk is voor Nutlin om de cel cyclus te kunnen stoppen. Deze observatie was enigszins verassend aangezien het 53BP1 eiwit voornamelijk een functie heeft in het activeren van het p53 eiwit na DNA schade.

Verschillende methoden kunnen worden gebruikt voor het screenen van RNAi collecties. Gebruikelijke technieken zijn vaak arbeids- en tijds-intensief. Een nieuwe methode die gebruik maakt van de hybridizatie van shRNAs die een fenotype genereren op microarrays maken het uitvoeren van RNAi screens veel eenvoudiger. Deze techniek is toegepast op het zelfde genetische model systeem als in hoofdstuk I en heeft geleid tot de identificatie van een aantal nieuwe genen (**hoofdstuk IV**). Een van deze genen is de transcriptie factor ARNTL die de circadiane klok reguleert. Deze observatie ondersteunt een model waarin de circadiane klok een rol speelt in het onderdrukken van tumor vorming.

Naast de toepassing van RNAi in de zoektocht naar nieuwe kanker genen is het ook mogelijk om deze techniek toe te passen in het onderzoek naar medicijnen. Een groot probleem bij de behandeling van kanker patiënten is dat veel gebruikte medicijnen een zeer beperkte effectiviteit hebben. Dit wordt veroorzaakt door intrinsieke of verworven resistentie van de tumor tegen een bepaald medicijn. Om de effectiviteit van kanker therapie the vergroten is het daarom van groot belang om the kunnen voorspellen welke patiënten wel of niet zullen reageren op een bepaalde therapie. RNAi screens kunnen worden toegepast om genen the identificeren die betrokken zijn bij resistentie en mechanisme van actie van een anti kanker medicijn. Deze aanpak is toegepast op een nieuw medicijn met een onbekend werkzaam mechanisme (**hoofdstuk V**). Door middel van deze screen hebben we gevonden dat de inactivatie van twee eiwitten resistentie tegen dit medicijn kan veroorzaken. Deze twee eiwitten kunnen mogelijk worden ontwikkeld tot functionele biomarkers om de effectiviteit van dit nieuwe medicijn te voorspellen.

Naast het onderzoeken van cell groei fenotypen door RNAi screens is het ook mogelijk om signaal transductie routes direct te bekijken. De TGF-beta signaal transductie route heeft een ambivalente invloed op het ontstaan en progressie van tumoren. Het is beschreven dat in de eerste fase van tumorgroei TGF-beta een remmende werking heeft terwijl het later de metastase van tumoren lijkt te versnellen. Door het gebruik van een grote RNAi screen hebben we geprobeerd om nieuwe genen te vinden die nog niet in de TGF-beta waren geplaatst (**hoofdstuk VI**). Een van de genen die gevonden is, is het IRAK2 kinase dat betrokken is bij de signalering

van interleukine-1. Deze observatie laat zien dat RNAi screening connecties kan blootleggen tussen verschillende cellulair signaal transductie routes.

Inzicht in de genen die het ontstaan en de progressie van kanker reguleren kan leiden tot de ontwikkeling van nieuwe therapieën. In dit proefschrift wordt beschreven hoe RNAi kan worden gebruikt om kanker-relevante genen te vinden. Zowel het screenen van genetische-modellen en modellen voor de werking van medicijnen worden beschreven. De genen die zijn gevonden zullen moeten worden getest in klinische relevante modellen om aan te tonen dat deze genen werkelijk functioneel betrokken zijn bij kanker.

# Curriculum Vitae

Jasper Mullenders was born on November 17th, 1977 in Nijmegen. He graduated from Teylingen College, Noordwijkerhout in 1996. In the same year he started as a chemistry major at Leiden University. During his studies he performed several research projects. The first project was aimed to identify antibodies against the FSHD associated gene product FRG1 through phage-display technology using llama antibodies. This study was performed as a joint-venture between Leiden University and Unilever Research Vlaardingen under supervision of Hans de Haard, Silvère van der Maarel and Arn van den Maagdenberg. Subsequently he performed his second internship at the University of Southern California, Los Angeles. In this study he tried to find chromatin binding sites of the WRN protein. In January 2003 he started his PhD in the lab of René Benards at the Netherlands Cancer Institute. During his PhD he was involved in the construction and screening of large scale RNAi collections to identify novel cancer genes.

# List of publications

IRAK2 is a novel modulator of the TGF-beta signaling cascade
**Mullenders J**, Fabius AW, Van Dongen MMW, Kuiken HJ, Beijersbergen RL and Bernards R
Submitted to Molecular Cancer Research

Loss of function genetic screens as a tool to improve the diagnosis and treatment of cancer
**Mullenders J** and Bernards R
Accepted for publication by Oncogene

Candidate biomarkers of response to an experimental cancer drug identified through a large-scale RNA interference genetic screen.
**Mullenders J**, Von der Saal W, Van Dongen MMW, Reiff U, Van Willigen R, Beijersbergen RL, Tiefenthaler G, Klein C and Bernards R
Accepted for publication by Clinical Cancer Research

A large scale shRNA barcode screen identifies the circadian clock component ARNTL as putative regulator of the p53 tumor suppressor pathway.
**Mullenders J**, Fabius AW, Madiredjo M, Bernards R, Beijersbergen RL.
PLoS One. 2009; 4 (3):e4798.

Miz1 and HectH9 regulate the stability of the checkpoint protein, TopBP1.
Herold S, Hock A, Herkert B, Berns K, **Mullenders J**, Beijersbergen R, Bernards R, Eilers M.
EMBO Journal. 2008 Nov 5; 27 (21):2851-61.

An shRNA barcode screen provides insight into cancer cell vulnerability to MDM2 inhibitors.
Brummelkamp TR, Fabius AW, **Mullenders J**, Madiredjo M, Velds A, Kerkhoven RM, Bernards R, Beijersbergen RL.
Nature Chemical Biology. 2006 Apr; 2 (4):202-6.

Involvement of MINK, a Ste20 family kinase, in Ras oncogene-induced growth arrest in human ovarian surface epithelial cells.
Nicke B, Bastien J, Khanna SJ, Warne PH, Cowling V, Cook SJ, Peters G, Delpuech O, Schulze A, Berns K, **Mullenders J**, Beijersbergen RL, Bernards R, Ganesan TS, Downward J, Hancock DC.
Molecular Cell. 2005 Dec 9; 20 (5):673-85.

Functional identification of cancer-relevant genes through large-scale RNA interference screens in mammalian cells.
Brummelkamp TR, Berns K, Hijmans EM, **Mullenders J**, Fabius A, Heimerikx M, Velds A, Kerkhoven RM, Madiredjo M, Bernards R, Beijersbergen RL.
Cold Spring Harb Symp Quant Biol. 2004; 69:439-45.

A genetic screen identifies PITX1 as a suppressor of RAS activity and tumorigenicity.
Kolfschoten IG, van Leeuwen B, Berns K, **Mullenders J**, Beijersbergen RL, Bernards R, Voorhoeve PM, Agami R.
Cell. 2005 Jun 17; 121 (6):849-58.

A large-scale RNAi screen in human cells identifies new components of the p53 pathway.
Berns K, Hijmans EM, **Mullenders J**, Brummelkamp TR, Velds A, Heimerikx M, Kerkhoven RM, Madiredjo M, Nijkamp W, Weigelt B, Agami R, Ge W, Cavet G, Linsley PS, Beijersbergen RL, Bernards R.
Nature. 2004 Mar 25; 428 (6981):431-7.

# Dankwoord

Om nu te gaan zeggen dat de afgelopen jaren voorbij zijn gevlogen is een beetje teveel van het goede, maar soms het lijkt nog steeds alsof ik pas net ben begonnen. In de afgelopen jaren heb ik de NKI familie goed leren kennen op alle werkbesprekingen, borrels, feestjes en al dan niet werkgerelateerde reisjes. Daarom wil ik hieronder al die mensen bedanken.

René, dank voor al je hulp bij mijn promotie. Het begon allemaal met jouw idee om 500 maxipreps van alle kinase pSUPERs te maken, die zijn nu nog steeds niet klaar, maar mijn boekje gelukkig wel. Jouw frisse kijk op de wetenschap kan projecten nog net even die twist geven die ze misten. Ook je pogingen om fundamentele vindingen in de kliniek toe te passen zijn zeer inspirerend.

En natuurlijk wil ik Roderick (Beijersbergen) bedanken voor alle tips en aanwijzigingen die ik als beginnend OiO, nieuw in het screenings veld, hard nodig had. Ook alle tijd die we samen in het robot-hok hebben doorgebracht niet snel vergeten, het ga je goed!

Oude gardes worden vervangen door nieuwe. Toch wil ik graag de 'oude garde' (Thijn, Menno en Sebastiaan) bedanken voor het bijbrengen van een lesje hoe je proeven moet doen. Piet ik zal nooit meer jouw harige rug uit mijn geheugen kunnen wissen. Kristina, I guess you did remember my name. Luis, good luck back home. Mandy, ik zal maar even inhouden..... Roderik (Kortlever) en Mirjam, veel succes in de VS en tot ziens!

Miranda, ik weet nog goed dat ik je op je eerste werkdag op ben gaan halen bij de receptie. Dank voor al je hulp bij de proeven, die zoals je ziet, toch een groot deel van dit boekje opvullen. Veel plezier en succes bij pathologie!

Zo, dan kunnen we nu eindelijk naar de huidige werknemers van Prof Bernards. Marielle en Katrien, jullie zijn een stabiele factor en ook een beetje het geheugen van het lab, dank voor alle hulp, vectoren en een luisterend oor. Rianne, volhouden nu! Sid, if I would have spent the time bullying you on my own labwork I would have finished much earlier, keep up the good work. Prashant, I am glad we can discuss all kinds of subjects like bleaching bodyparts etc. Ernst, dankzij jou is het geluidsniveau van het lab nooit meer onder de 100 dB gedaald, succes de komende tijd met het afmaken van je promotie. Guus en Michiel misschien dan screening jullie wel een pot goud opleverd.....we zullen zien.

De buren van het Beijersbergen lab wil ik natuurlijk niet vergeten. Johan en Jeroen, stug volhouden dan gaat het vanzelf een keer gebeuren. Ook Wouter, Helena, Pasi, Cor en Bram good luck!

Een speciale plek voor de studenten die ik tijdens hun stages heb begeleid. Het was erg leuk om

jullie te zien groeien vooral omdat jullie erg gemotiveerd waren. Esther, gelukkig ben ik toch nog net eerder klaar, al had ik een flinke voorsprong. Rogier (Van Willigen), LIVESTRONG FOREVER! Ik sta trouwens nog steeds 1,2 en 3 in de fotoquiz. Klaas, laten we de planeten nog een keer doornemen terwijl we naar Kate Ryan luisteren.

I would also like to thank the people from Roche in Penzberg, who were instrumental in making chapter V in this thesis.

Lieve Annette, onvergetelijke karaoke feestjes die de buren lang hebben wakkergehouden. Ik ben erg blij om je samen met Christine te zien, jullie zijn een leuk stel. Bedankt voor al je steun en relativeringsvermogen als ik het weer eens nodig had. Ik hoop je nog vaak tegen te komen, waar dan ook ter wereld!

Michael and Cornelia, unfortunately we couldn't keep your fish alive, I assure you it wasn't an experiment. Michael your effort and insight is very inspiring. In combination with the continous opportunity of German and Bavarian bashing it was great to have you as a colleague. I am looking forward to see the little Hölzeltje.

En dan zijn er natuurlijk nog de andere (tijdelijke) bewoners van B7. De Wolthuisjes, jullie zijn een mooie aanvulling op het screening werk, succes ermee! Natuurlijk ook de mensen van Schellens; bedankt voor de klinische invalshoek.

Ook wil ik graag het battaljon office-managers bedanken die ik de afgelopen jaren voorbij heb zien trekken: Marlijn, Francisca en natuurlijk Sue-Ellen!

Ook andere NKI-ers wil ik graag bedanken voor alle gezelligheid en hulp bij reagentie zijn. Ten eerste, de ex-H2ers, Francesca, Titia en Puck en natuurlijk ook de andere christalografen. Verder de B4 mensen, Eitan, Martijn, Marieke, Josyanne. En natuurlijk de co-organisatoren van de PhD Conference, Bernike, Floor en Daan. Ook de amuse-clan-leden Dieuwke en Marleen (de rest wordt al genoemd) bedankt voor de culinarie verdieping.

In het P-gebouw natuurlijk Thos, Thomas, Liesbeth en Joanna de groep van het Peeper Lab. Henri, zoveel lol heb ik nog nooit met een manager gehad. Henne, veel succes met de laatste loodjes. Sietske hou je taai, jij komt er wel.

Bastiaan, legendarische uitjes en verkleedpartijtjes. En natuurlijk ellenlange discussies over de wetenschap die onder genot van het nodige bier altijd wel een leuke wending kregen. Veel succes in Oxford en super dat je naast mij staat op mijn promotie.

Naast het labwerk was er gelukkig wel nog wat tijd over om iets leuks te doen. Guiseppe, de olympische spelen zullen we wel nooit halen, maar we zijn nu tenminste gemiddeld UD in de nachtwedstrijd.

Fab, ik ben blij dat je nu weer een stuk dichterbij woont. Roos en Martijn dank voor de etentjes en het kite-gebeuren. Natuurlijk wil ik ook Jan, Wim, Erica, Jimmy en Susanne bedanken voor de nodige afleiding tussen de proeven door. Karin, je woont nu weer vlakbij mijn favoriete dorp, Volkel, daar kom ik je graag één keer per jaar opzoeken. Bob en Ellen, bedankt voor alle gezelligheid en support!

Rogier (Pinkers), ik heb bewondering voor je doorzettingsvermogen, hou je taai, jochie.

Ook natuurlijk Dus, Bondien en Elise bedankt voor alle gastvrijheid. En het lekkere eten.

Rikkert, broertje, het is eigenlijk ook een beetje jouw boekje, dank daarvoor. Veel succes met je eigen carriere. Sebastian en Linda, fijn dat jullie ook van de partij zijn bij familiefeestjes.

Aukje, lieve zus, altijd sta je klaar voor iedereen. Nu maar hopen dat papa geen moeilijke vraag gaat stellen, want die pass ik meteen door naar jou! Heel fijn dat jij mijn paranimf wilt zijn.

Papa en mama, jullie hebben mij altijd gestimuleerd om het beste er uit te halen en door te zetten. Voor inspiratie heb ik nooit heel ver hoeven kijken natuurlijk. Ontzettend bedankt voor alle aandacht en gezelligheid.

Lieve Armida, samen met jou is het nooit saai. Gelukkig zijn we aan elkaar gewaagd. Succes met je laatste loodjes, het einde van je promotie is in zicht. Ik zie de toekomst met jou vol vertrouwen tegenmoet. Zolang de Suzuki rijdt gaan we vooruit!

**Jasper**